

3

**Coccoliths and oxygen isotope observations
from the sediment surface
of the southwest Indian Ocean.**

By Mark J. Fincham

**Thesis submitted in fulfillment of
the requirements for the degree of Master
of Science in the Faculty of Science at the
University of Cape Town.**

September 1986.

The University of Cape Town has been given
the right to reproduce this thesis in whole
or in part. Copyright is held by the author.

The copyright of this thesis vests in the author. No quotation from it or information derived from it is to be published without full acknowledgement of the source. The thesis is to be used for private study or non-commercial research purposes only.

Published by the University of Cape Town (UCT) in terms of the non-exclusive license granted to UCT by the author.

ABSTRACT

The interplay of three important parameters, dissolution, dilution and winnowing seem to be controlling the state in which sediment material is preserved in the study area though most samples examined under the SEM were generally well preserved.

The distribution of forty-four coccolithophore species in one hundred deep sea core-tops from the southwest Indian Ocean is described. Three coccolith assemblages have been recognised (Maputo, Agulhas Current and deep water) and are delineated by the relative abundances of four ecologically significant coccolithophore species (*Gephyrocapsa oceanica*, *Emiliana huxleyi*, *Calcidiscus leptoporus* and *Umbilicosphaera sibogae*). These four species are the most abundant in the study area and the major factors influencing their geographical distribution seem to be temperature, nutrient concentration and dissolution.

Coccolith and foraminifera preservations indicate that the carbonate lysocline lies somewhere between 3500 and 4000 meters, resulting in the concentration of dissolution resistant microfossils below this depth.

Stable oxygen isotope ratios in a planktonic foraminifera and percent abundances of *E. huxleyi* reveal that apart from cores taken in the Agulhas Passage, most of the core-top samples are probably less than 85,000 yrs BP. Lightest isotope ratios of -1.5 to -1.0 per mil PDB (equal to 22.8 to 25.1°C) occur in a narrow band on the sea floor beneath the "A" route of the Agulhas Current.

These values are about 0.5 per mil PDB lighter than samples analyzed on either side of this band and can be explained by the Agulhas Current's elevated temperature at the ocean surface of between 2 to 3°C. Thus an oxygen isotope imprint of the Agulhas Current exists beneath it on the sea floor.

The Agulhas Current is probably the major factor influencing sedimentation, sediment distribution patterns and geological features in the study area. At present it is voluminous and fast flowing, possibly eroding sediments 2500 meters below the surface.

The oxygen-isotope ratios and nannoplankton counts obtained in this study indicate however, that the majority of samples are most probably recent or at least not older than 85,000 years except for sediments found in the Agulhas Passage. This implies that sediments are accumulating on the ocean floor and that the current does not have a pronounced erosional influence, at least in areas from which cores were retrieved for this study.

ACKNOWLEDGEMENTS

Firstly, I should like to thank Professor Richard Dingle for inviting me out to South Africa and giving me the opportunity to participate in this project. The project was funded by SANCOR and the University of Cape Town Research Committee. In the course of this thesis I have enjoyed working closely with several departments of the University of Cape Town. The staffs of the Electron Microscope Unit, Archaeometry Department, and Computer Science Department are gratefully acknowledged for their professional advice and technical assistance. Thanks to Dr Grundlingh of NRIO for supplying satellite photos. Special thanks to Matthew Smith, Lesley Lowe, and Rob Noble for their assistance with sample preparations and analytical laboratory techniques. Discussions with Simon Robson, Dr Steve Goodlad, Dr Frances Westall, Dr Bill Siesser, Dr John Rogers, Prof Richard Dingle and especially Dr Keith Martin were much appreciated and proved fruitful. Dr Rich Johnson was a constant source of information and ideas, his assistance with the departmental computers was invaluable. Thanks to Rich and also Dr Charles Brownell for reding the manuscript. My wife Beverley deserves a big thankyou for helping out when and where she could and for putting up with attacks of thesis blues. Finally, a very special thankyou to my supervisor and mentor Dr Amos Winter for guiding me along the rocky road to a Masters degree.

CONTENTS

	Page
ABSTRACT	i
ACKNOWLEDGEMENTS	ii
CONTENTS	iii
LIST OF FIGURES	iv
LIST OF TABLES AND PLATES	v
1. INTRODUCTION	1
1.1 LIVING COCCOLITHOPHORES.	1
1.2 BIOLOGY OF COCCOLITHOPHORES.	1
1.3 SEDIMENTATION OF COCCOLITHS	1
1.4 REVIEW OF INDIAN OCEAN COCCOLITHOPHORES.	2
1.5 STUDY MOTIVATION	2
1.6 STUDY AREA	2
1.6.1 The Agulhas Current System	3
1.6.2 The Antarctic Bottom Water (AABW)	3
2. MATERIALS AND METHODS.	5
2.1 SAMPLES.	5
2.2 EXPERIMENTAL PROCEDURE	5
2.2.1 Smear slides preparation	5
2.2.2 Disaggregation and removal of organic material	5
2.2.3 Wet sieving into size fractions	5
2.2.4 Preparation for observation of coccoliths by SEM	5
2.2.5 Carbonate analysis	6
2.2.6 Foraminifera counts and sediment descriptions	6
2.2.7 Oxygen isotope analysis.	6
3. RESULTS.	7
3.1 SEDIMENT DESCRIPTION	7
3.2 CARBONATE PERCENTAGES	7
3.3 RELATIVE COCCOLITH ABUNDANCES AND ASSEMBLAGE COMPOSITION.	7
3.3.1 Taxonomic notes.	7
3.3.2 Assemblage composition	8
3.3.2.1 Major species; 3.3.2.2 Minor species	
3.4 FORAMINIFERAL COUNTS	8
3.5 OXYGEN ISOTOPE ANALYSIS	9
4. COMMUNITY STRUCTURE.	10
5. DISCUSSION	11
5.1 PRESERVATION OF CORE-TOP MATERIAL	11
5.2 REWORKED COCCOLITHS.	12
5.3 COCCOLITH CORE-TOP ASSEMBLAGE DISTRIBUTION	12
5.4 CORE-TOP AGE DETERMINATION	14
5.5 OXYGEN ISOTOPES	14
5.6 IMPLICATIONS FOR SEDIMENTOLOGY AND AGULHAS CURRENT STRENGTH.	15
6. CONCLUSIONS.	17
REFERENCES	18
APPENDIX	23

LIST OF FIGURES

	Title
Fig.1.1	Study Area: core positions and bathymetry.
Fig.1.2	Circulation patterns in the southwest Indian Ocean.
Fig.1.3	The path of the Agulhas Current determined from satellite imagery.
Fig.2.1	Sector divisions.
Fig.2.2	Flow chart of Experimental Procedure.
Fig.3.1	Percent finer than 63 microns.
Fig.3.2	Relative coccolith abundance.
Fig.3.3	Plot of carbonate percent vs. depth.
Fig.3.4	Relative coccolith abundance.
Fig.3.5	Distribution of coccolith preservasions.
Fig.3.6	Samples containing no coccliths.
Fig.3.7	Stacked bar graphs of sample composition.
Fig.3.8	Relative abundance of <i>Emiliana huxleyi</i> .
Fig.3.9	Relative abundance of <i>Gephyrocapsa oceanica</i> .
Fig.3.10	Relative abundance of <i>Calcidiscus leptoporus</i> .
Fig.3.11	Relative abundance of <i>Umbilicosphaera sibogae</i> .
Fig.3.12	Percent foraminifera fragments.
Fig.3.13	Plot of depth vs. percent foraminifera fragments.
Fig.3.14	Samples without Isotope data.
Fig.3.15	Isotope data.
Fig.5.1	Plot of sample depth vs. percent <i>Emiliana huxleyi</i> .
Fig.5.2	Plot of sample depth vs. percent <i>Calcidiscus leptoporus</i> .
Fig.5.3	Reworked coccoliths.
Fig.5.4	Samples containig unidentified coccoliths.
Fig.5.5	Coccolith assemblage distributions.

LIST OF TABLES AND PLATES

Title

- Table 1. Smear slide coccolith abundance indices.
- Table 2. Preservation index characteristics.
- Table 3. Core data.
- Table 4. Sample data.
- Table 5. Species list.
- Table 6. Relative percent abundances of Major coccolith species.
- Table 7. Relative percent abundances of Minor coccolith species.
- Table 8. Foraminifera percentages, Carbonate percentages and isotope ratios.
- Table 9. Core-top assemblage characteristics.

- Plate I Fossil coccoliths.
- Plate II Fossil coccoliths.
- Plate III Fossil coccoliths.
- Plate IV Fossil coccoliths.
- Plate V Fossil coccoliths.
- Plate VI Fossil coccoliths.
- Plate VII Fossil coccoliths.

1. INTRODUCTION

1.1 LIVING COCCOLITHOPHORES

Coccolithophores are minute (2-25 microns diameter), unicellular marine phytoplankton ubiquitously distributed throughout the photic and upper aphotic zones of the world's oceans, except in polar water masses (McIntyre et al 1970; Okada and Honjo 1973; and Okada and McIntyre 1977), and together with diatoms and dinoflagellates, constitute a major part of the marine phytoplankton. Production is greatest in high latitudes where they often dominate the phytoplankton assemblages (Braarud 1945), but have been reported to contribute up to 25% of total production in mid latitudes (Hutchings et al 1984). Living coccolithophores are frequently stratified in the water column and show a preference for subtropical-tropical waters where highest diversities have been recorded (McIntyre and Be, 1967; Okada and Honjo, 1973; Honjo and Okada, 1974; Honjo 1977). Their distribution in the water column appears to be influenced by current systems, temperature, light intensity and the depth of the mixed layer (Okada and Honjo 1973) and thus they are sensitive environmental indicators. A number of biogeographical floral zones have been erected (McIntyre and Be 1967) on the basis of their distribution in water masses.

1.2 BIOLOGY OF COCCOLITHOPHORES

Coccolithophores are sub-cylindrical in shape, tapering to one or both ends (Gaarder 1971). They usually contain two golden brown chromatophores (Webber-van Bosse 1901), a central nucleus (Ostenfield 1900), two acronematic flagella of about the same length and a coiled haptonema (Parke and Adams 1960). Some coccolithophores pass through two phases in their life cycle: a motile phase during which they possess the flagellar apparatus, alternating with a nonmotile phase. The cell in the non-motile phase normally bears a more or less rigid calcite skeleton consisting of minute (1-10 microns) interlocking platelets known as coccoliths, which are generally constructed of radial arrays of calcite crystallites. The motile phase is either naked or bears a type of coccolith that differs from that of the non-motile phase (Haq 1980). Reproduction is by fission, or sexual fusion, suggesting heterophasic life cycles; however, deviation from these modes of reproduction has been observed in culture. Two distinct types of pla-

telet are formed: 1) Holococcoliths form outside the cytoplasmic membrane (Manton and Leedale 1963). They are delicate and consist of many identical calcite crystallites. 2) Heterococcoliths form on a perforated organic template within the protoplasm, and then migrate to the surface of the cell where they are extruded to form an interlocking external skeleton (Wilbur and Watabe 1963, 1967). The calcite crystallites of this form have varied architecture and are more solution resistant than holococcoliths. They can be subdivided according to morphology into five major groups: placoliths, cyrtoliths, caneo-liths, scapholiths and rhabdoliths.

1.3 SEDIMENTATION OF COCCOLITHS

Coccoliths have been accumulating in the deep sea since the Jurassic and have contributed between 30 and 60% to calcareous oozes (Berger and Roth 1975; Honjo 1977). Coccolithophores as well as individual coccoliths have little chance of surviving the long journey through calcite undersaturated waters to the ocean floor. Instead it is thought that coccoliths are transported to the sea floor in faecal pellets of small, herbivorous zooplankton (usually copepods). The impermeable, chitinous organic membrane of these faecal pellets increase sinking velocity by providing a smooth surface and protect their contents from dissolution in this manner (Honjo 1976). One estimate in the Equatorial Pacific is that 92% of coccoliths produced in the euphotic layer reach the underlying deep sea floor in fecal pellets (Honjo 1976).

Isolated coccoliths shed from ruptured fecal pellets are quantitatively unimportant in the process of accumulation of deep sea sediments (Honjo and Roman 1978). The effects of preferential grazing and selective destruction during ingestion and digestion by zooplankton have received little study (Roth et al 1975) but may alter surface water coccolith biocoenoses during their transfer from the photic zone to the sea floor.

Patterns of coccolith accumulation in the sediments do, however, reflect environments of production in the overlying surface waters (Roth and Berger 1975; Guitzenhauer et al 1976, 1977) and maps of species distribution in the sediment correspond to plankton maps (Honjo and Okada 1975) and to the location of major water masses. Owing to their

rapid evolutionary rates coccoliths have proved to be useful biostratigraphic indicators (Haq 1973).

1.4 REVIEW OF INDIAN OCEAN COCCOLITHOPHORES

Few studies have been carried out on the distribution of living coccolithophores in the Indian Ocean (Gaarder 1971). Surface water phytoplankton including coccolithophores from the coast of Mozambique were studied quantitatively by Silva (1960) who found that coccolithophores as a group were closest to diatoms in numbers. Lecal (in Bernard and Lecal 1960) and Taylor (1966) described new species from the west Indian Ocean and South African coast respectively, while Travers and Travers (1965) studied the flora from coastal waters off west Madagascar. More recently Friedinger and Winter (1985) examined coccolithophores in the surface waters of the southwest Indian Ocean. Their distribution was found to be controlled by two different oceanographic regimes, the nearly stable region of the Agulhas Current and the sporadic Return Current where hydrographical and ecological conditions change frequently. While the distribution patterns of calcareous nannofossils in surface sediments of the Atlantic and Pacific have been the subject of extensive interest (McIntyre 1967; McIntyre and Be 1967; McIntyre et al 1970; Ushakova 1970; Roth and Berger 1975; Geitzenauer et al 1977; Roth and Coulbourne 1982), the Indian Ocean has been relatively neglected. Only four previous research papers have concentrated on nannofossils from S.Africa (Pienar, 1966 & 1968, Hart et al 1965 and Siesser 1975). The first three dealt with terrestrial occurrences while Siesser studied Quaternary nannofossils in sediment cores from the South African continental margin.

1.5 STUDY MOTIVATION

It is often difficult and impractical (due to patchiness, sampling limitations and expense) to correlate empirically the distribution of living coccolithophores with environmental factors. However, studying coccoliths from surface sediments on the ocean floor where biological and oceanographic fluctuations are integrated can overcome this limitation. This study is an attempt to describe the composition and distribution of core-top coccolithophore assemblages, and their correlation with ecological conditions

in the overlying water masses. This information should contribute to our understanding the ecological tolerances of southwest Indian Ocean coccolithophores, and help in palaeo-environmental interpretation of coccolith material from deep sea cores. This research project is part of a larger one aimed at reconstructing the palaeoceanography of the Agulhas Current region.

1.6 STUDY AREA

The study area extends approximately 2000 km in length from Maputo in the north to Cape Agulhas in the south and varies in width between 300 km in the north and 1500 km in the south. Fig. 1.1 shows the bathymetric relief of the region and identifies the most prominent features (see Goodlad 1978, Dingle 1978, Martin 1984 and Dingle and Robson 1985 for a more detailed description).

The Inharrime Terrace in the north is a smooth, shallow water, sedimentary feature, its eastern slope descending towards the northern end of the Mozambique Ridge. To the west the terrace merges with the Limpopo Cone forming a large triangular sediment wedge. The upper reaches of the Limpopo Cone, a smooth surfaced feature stretching 300 km south from the Limpopo river mouth, form a gently sloping terrace, with a smooth floored shallow valley on its western flank. The Almirante Leite Bank at 26°S is an outcrop of about eighty rocky volcanic sea-mounts which are relatively steep sided and break the otherwise smooth topography of the outer slopes of the Limpopo cone and the Inharrime Terrace. The Central Terrace is situated to the south of the Limpopo Cone and Almirante Bank extending east from the continental shelf and drops steeply into the Mozambique Basin at 36°E. Prominent valleys separate it from the continental slope and the Mozambique Ridge in the south. At around 29°S the Central Terrace steepens, forming the Natal Valley, which slopes NE-SW, becoming progressively deeper to the south. Its eastern margin, the Mozambique Ridge, is a large north-south running plateau. At around 35°S the Natal Valley merges into the abyssal Transkei Basin which is bordered to the southwest by the Agulhas Plateau. This feature, which is located about 500 km south-east of the Cape of Good Hope is an aseismic rise, nearly 700 km long and 400 km wide. The continental shelf off the east coast of

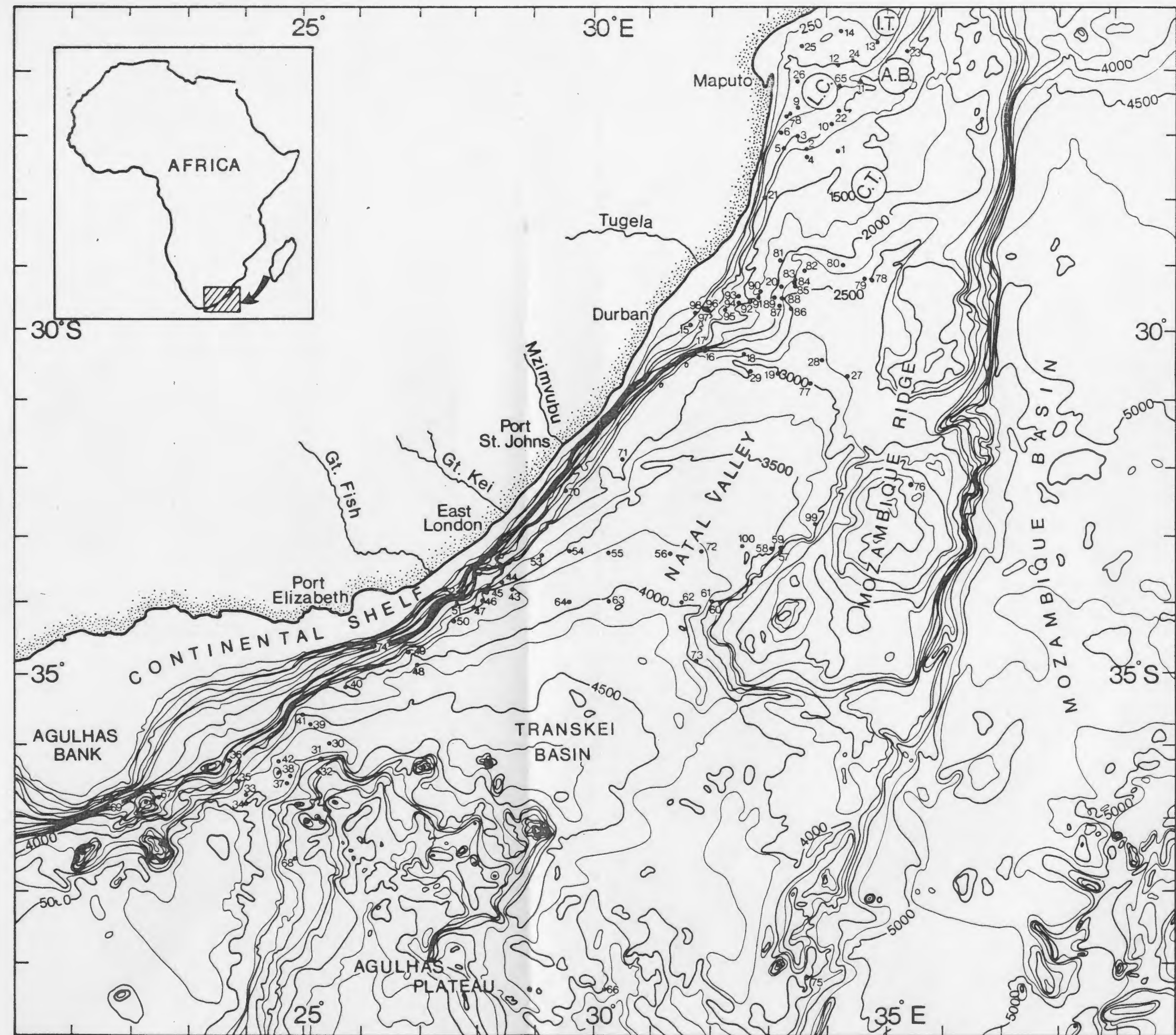


Figure 1.1 The study area. Bathymetric contours are in 250 meter intervals, core-top sample locations are numbered.

southern Africa is for most of its length steep and very narrow. There are however three exceptions. Sediment in-fill from the Limpopo River creates a bulge in the continental shelf off Maputo. Terrigenous input is also responsible for the widening of the continental shelf off Durban forming the Tuguela cone. The Agulhas Bank forms a triangular shaped continental margin at the southern tip of Africa, varying in E-W width from about 35-70 km, and with a maximum southerly extent off Cape Agulhas of about 250 km.

1.6.1 The Agulhas Current System

The Agulhas Current (Fig. 1.2) is the western boundary current of the South Indian Ocean subtropical gyre. It can be divided into four different oceanographic regimes which parallel the coast of southern Africa (Pearce 1977): 1) The inshore region which lies predominantly on the continental shelf and consists of relatively cool and low velocity water. 2) The current core, usually only a few tens of kilometers wide. It is warm (varying seasonally in temperature between 22 and 27°C), fast (velocity usually exceeds 1 meter per second though there is no pronounced seasonal variation in core velocity) and has a tendency to meander with a period of a few days. 3) Between the core and inshore region lies the western boundary of the current which is a region of intense horizontal shear. 4) The region beyond the eastern boundary of the current core is a region of weaker currents and cooler temperatures.

The core of the Agulhas Current divides into two major flow paths (commonly termed routes A and B: Fig. 1.2) at approximately 26°S (Harris and van-Foreest 1977). Route A, the inshore branch, travels from northeast to southwest following the edge of the continental shelf and is forced offshore by a widening of the continental shelf south of Port St. Johns. By the time it reaches Mossel Bay it is some 100 km offshore though it is deflected still further offshore by the Agulhas Bank and continues to flow southwest until it is south of the Cape Peninsula. Route B flows down the eastern Central Terrace following the Mozambique Ridge southward, until at approximately 32°S it takes a sharp westerly turn re-joining route A near the coast (Martin 1984). The main flow paths of the Agulhas Current are known to meander, and circulation may be alternately dominated by routes A and B.

The Agulhas Return Current is formed from Agulhas Current water that has turned eastward and meanders east into the South Indian Ocean gyre (Shannon et al 1973). Intermittent inshore counter-currents flowing in a northeasterly direction have been described by many authors (Grundlingh 1977; Pearce et al 1978; Harris 1978; and Malan and Schumann 1979) and are associated with the formation of cyclonic eddies near Durban and Maputo. Counter-currents cause dynamic upwelling which results in high nutrient and low oxygen values (Martin 1984). Evidence uncovered by satellite imagery and synoptic hydrographical data suggest that important changes occur in the system over periods of 3-4 weeks, rather than seasonally as was previously thought (Harris and van-Foreest 1977).

A selection of satellite photographs were taken by the European Space Agencies "Meteosat" satellite from the 3rd of Jan to the 16th of March 1984 and have been used to compile a composite map which roughly outlines the mean route of the Agulhas Current during this period (Fig. 1.3). For most of this time the Agulhas Current followed a constant route down the coast of southern Africa, its penetration south varying from week to week. The position of route B during this period is, however, not as clearly defined.

1.6.2 The Antarctic Bottom Water (AABW)

The Antarctic Bottom Water (Fig. 1.2) flows NE through the Agulhas Passage at depths greater than 4500 m, and may be represented in the Agulhas Basin by the 1°C isotherm (Westall 1984). Antarctic Bottom Water originates in the Weddell Sea and spreads from the Atlantic-Indian Basin in two directions: one path spreads easterly, through the Crotez Basin into the Madagascar, Mascarene, Somali and Arabian Basins (Kolla et al, 1976). The second branch flows north along the western boundary of the S. Atlantic and passes through the SW Indian Ocean ridge at about 25°E (Kolla et al, 1976, Westall 1984) into the East Agulhas Basin. This component then flows northwest into the West Agulhas Basin, and then northeast through the Agulhas Passage. After passing through the Agulhas Passage the current is deflected east in the Transkei Basin by the rising contours and loses its characteristics as it dissipates through mixing with warmer overlying waters. The Antarctic Bottom Water is rela-

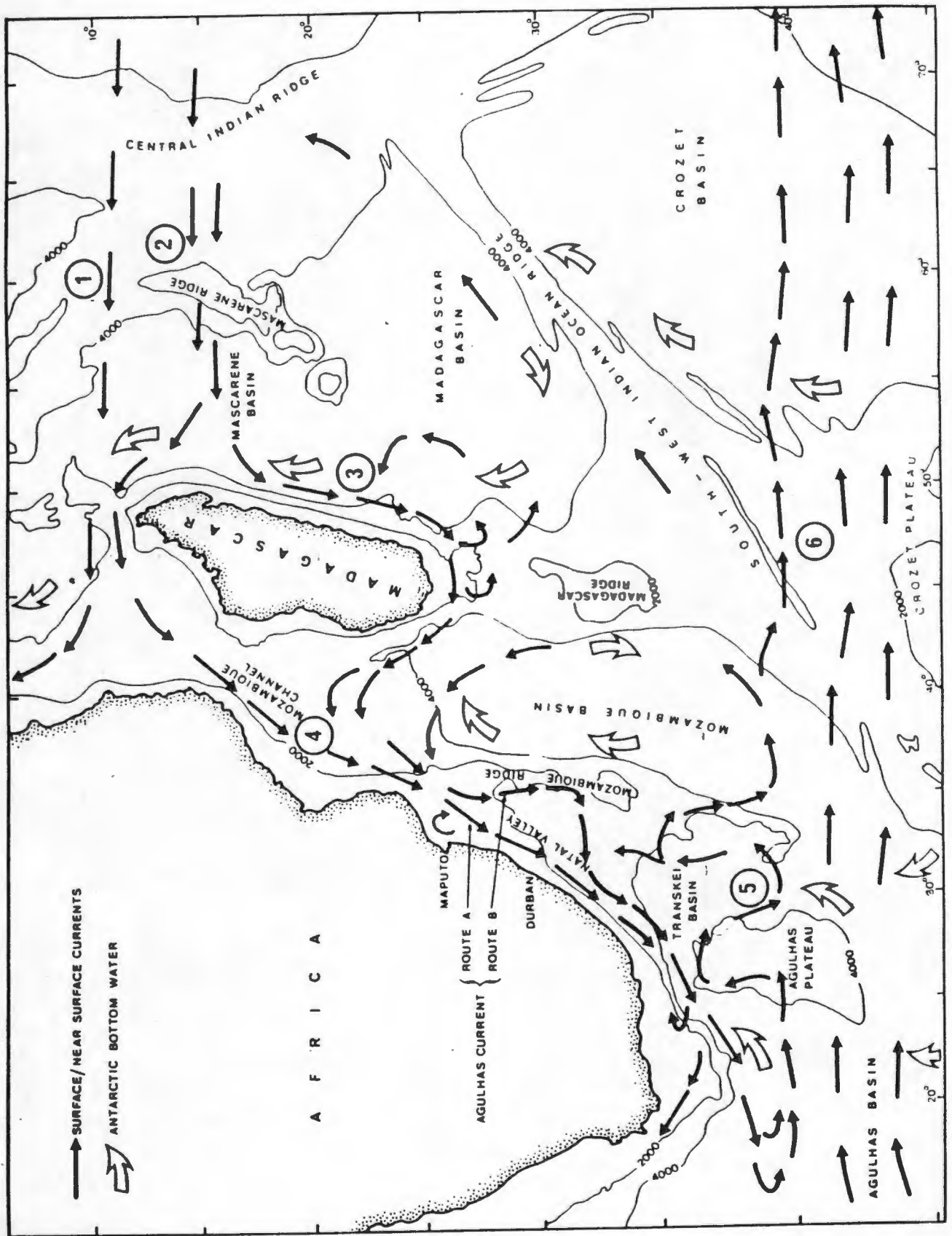


Figure 1.2 Circulation patterns in the southwest Indian Ocean. Surface/near-surface currents = black arrows. (1) North Equatorial Current (part of the North Indian Ocean subtropical gyre). (2) South Equatorial Current. (3) East Madagascar Current. (4) Mozambique Current. (5) Agulhas Current. (6) West Wind Drift at subtropical convergence (all sub units of the South Indian Ocean subtropical gyre). From Martin 1981.

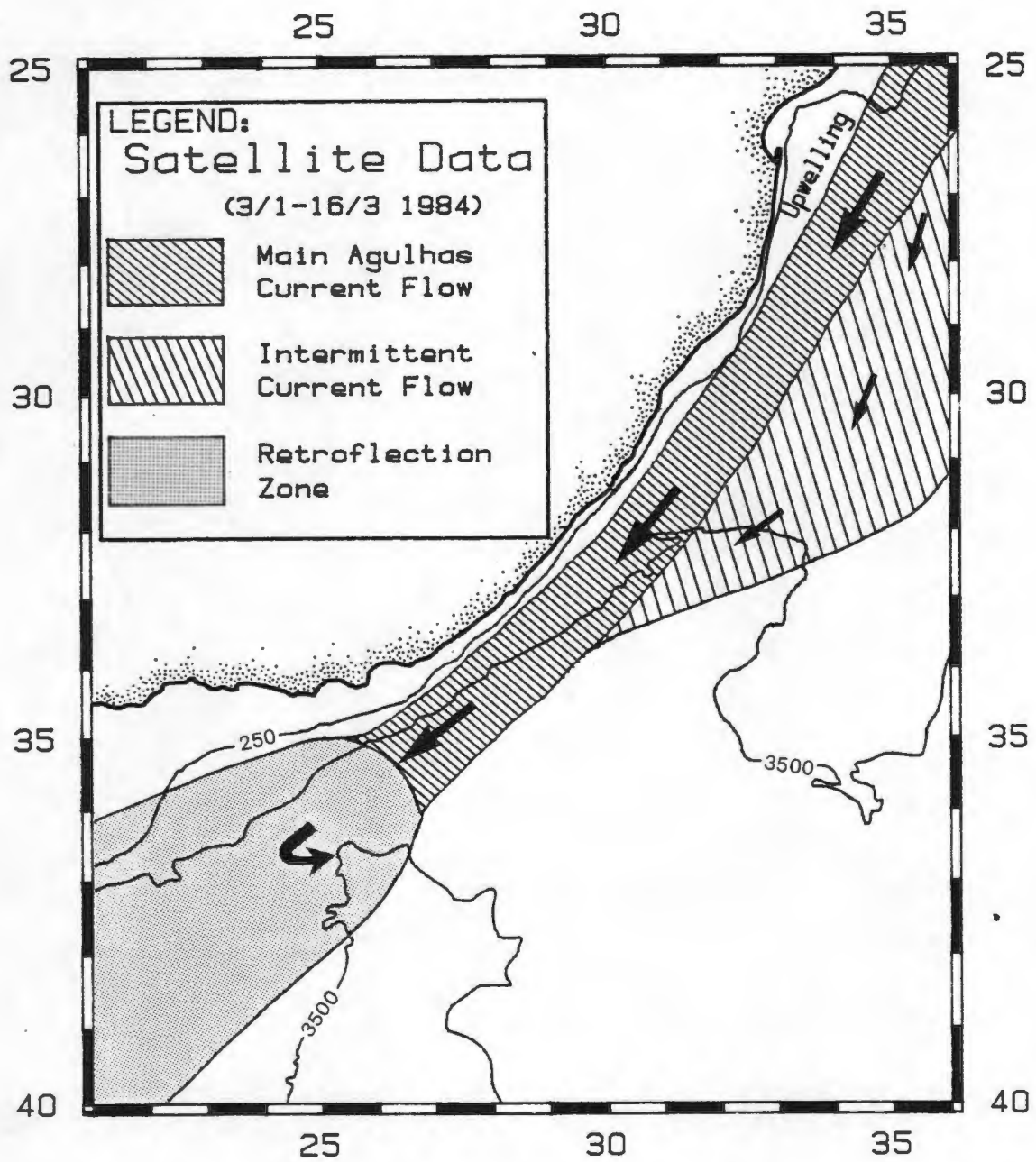


Figure 13 Mean Agulhas Current path and features over the period 3.1.84 to 16.3.84, as inferred from satellite imagery. Upwelling is marked off Maputo. Arrow size denotes current intensity.

tively rapid (19-26 cm/sec) and turbulent in its flow through the Agulhas Passage (Kolla et al, 1976) and bottom photographs showing well-developed ripples and a strong nephloid layer confirm the importance of Antarctic Bottom Water in sediment transport in the Agulhas Passage.

2. MATERIALS AND METHODS

2.1 SAMPLES

A total of one hundred core-top samples were investigated from water depths ranging between 248 m and 4845 m in the southwest Indian Ocean. Forty-four samples were obtained from piston cores, forty from trigger cores, and sixteen from gravity cores. Samples are distributed along the entire length and breadth of the Agulhas Current System, though some areas have a better sample coverage than others. This is because sample distribution is dependant on the cruise tracks of previous geological cruises in the study area. Because samples often tended to cluster in certain areas, for convenience the study area has been divided into four sample sectors: 1: Maputo (M); 2: Durban (D); 3: East London (EL); 4: Port Elizabeth (PE) (Fig. 2.1).

2.2 EXPERIMENTAL PROCEDURE

Between two and three grams of material from the top 2 cm of each core was removed and placed in sealed, labelled vials for analysis. The analytical procedure is illustrated by means of a flow chart (Fig. 2.2) and is described in detail below.

2.2.1 Smear slides preparation

Each sample was examined to determine whether it contained coccoliths and if so, the relative coccolith abundances. Smear slides were prepared by thoroughly mixing in a test tube a small amount of sample with 20 cm³ of distilled water and 2 cm³ of polyvinyl alcohol to aid adhesion. The mixture was allowed to settle for 5 minutes before a drop was placed on a coverslip, dried on a hot-plate at 40°C and then mounted on a slide with Canada balsam. Slides were observed under crossed nichols of polarizing light at high magnifications. The percentage cover of coccoliths per field of view at 1000X magnification was then categorized according to the index in Table 1.

2.2.2 Disaggregation and removal of organic material

Between 2 and 3 grams of dry sample material was placed in a 250 cm³ conical flask to which was added 15 cm³ of slightly alkaline distilled water (pH 8.0), 4 mls of 30% molar hydrogen peroxide and 2 cm³ of 5% Calgon solution. The mixture was placed in a water bath and heated to 40°C until effer-

vescing stopped. When large quantities of organic material were present, repeat doses of hydrogen peroxide were added. About one gram of organic free sample was removed and dried in preparation for carbonate determinations.

2.2.3 Wet sieving into size fractions

The organic free sample was washed with as little distilled water as possible, through a set of 10 cm diameter test sieves leaving three size fractions in aqueous suspension: Fine fraction (less than 63 microns), 63-150 microns, and coarse fraction (greater than 150 microns). Each size fraction was carefully washed onto a watch-glass and dried at 50°C in an oven. The dry fractions were weighed and sealed in individually labelled vials. The contribution by each size fraction was calculated as a percent of the original dry sample mass.

2.2.4 Preparation for observation of coccoliths by SEM

A small amount of the fine fraction material was placed in a glass centrifuge tube along with approximately 10 cm³ of distilled water. Test tubes of sediment suspension were centrifuged at 2,500 rpm for 45 seconds (Winter 1982). Afterwards the turbid supernatant (mainly silts and clays) was decanted, and the process repeated until the supernatant became clear. The final residue was once more mixed with distilled water and then allowed to settle for five minutes. Afterwards a few drops of the suspension were removed and placed on an SEM stub which was slowly dried on a hot plate at 50°C. Each stub was spattered with Gold-Palladium (AuPd) and viewed either by a Cambridge S200 or S180 Scanning Electron Microscope. Approximately 300 coccoliths from each stub were counted and identified under high magnification, the percent abundance of each species present was then calculated.

The preservation of coccoliths from the samples were described as they appeared on SEM using a preservation index (on a scale from one to five), see Table 2.

Indistinguishable calcite rings were found in a few highly dissolved samples, these were counted and grouped under the heading "calcite rings". Complete cocco-

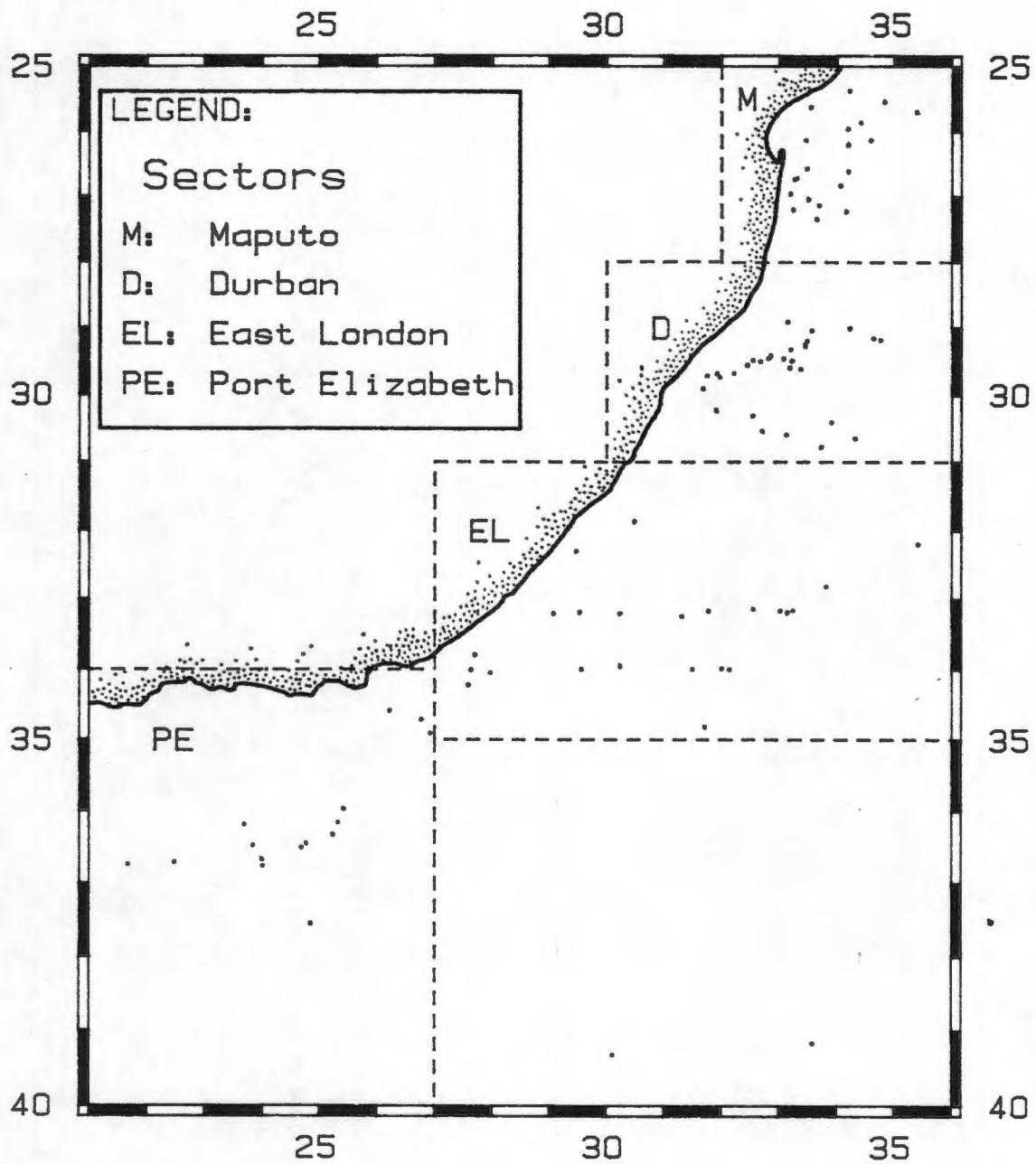


Figure 2.1 Sector divisions. Sample locations are marked with dots.

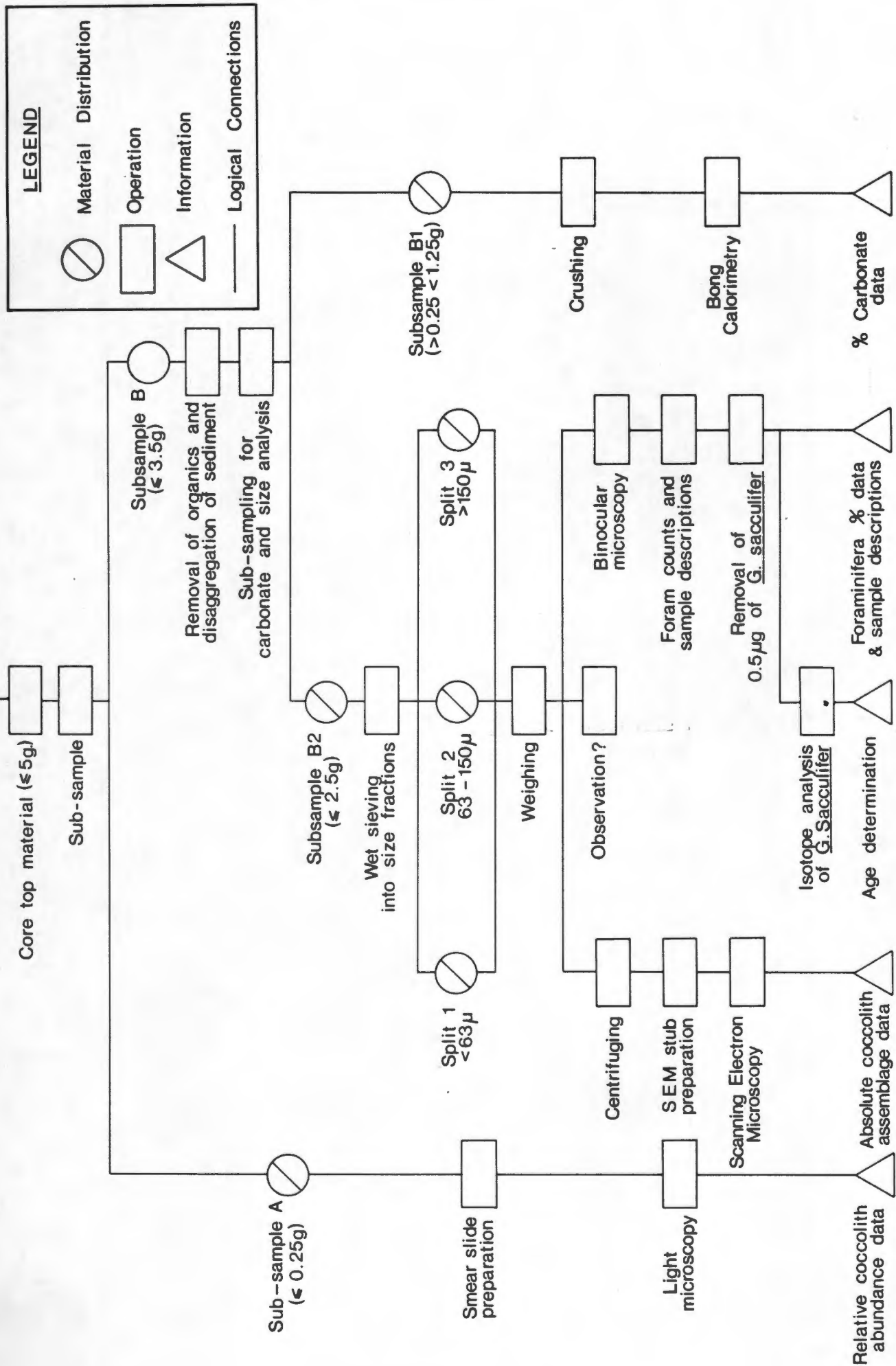


Figure 2.2 Flow chart describing experimental procedure.

TABLE 1.

Abundance Index	Approximate % cover
0 Absent	< 5
1 Rare	5-30
2 Common	30-60
3 Abundant	> 60

Table 1. Relative coccolith abundance indices estimated from percentage cover of microscope field of view.

TABLE 2.

Preservation Index	Features
1. Excellent	No evidence of dissolution or breakage.
2. Good	Few dissolution characteristics, some etching of the more solution susceptible species eg <u>Syracosphaerids</u> .
3. Fair	Etching and breakage of more fragile coccolith species.
4. Poor	Extensive etching; central grills and bridges often absent even on dissolution resistant species, eg <u>Emiliana huxleyi</u> , <u>Gephyrocapsa oceanica</u> and <u>Calcidiscus leptopus</u> .
5. Very poor	Extreme etching and breakage, some species become unrecognizable rings, large numbers of coccolith fragments.

Table 2. Coccolith preservation indices and their characteristic features as determined from Scanning Electron Microscopy.

spheres were extremely rare in sediment samples due to the fragility of the coccolithophore skeleton and the degree of mechanical pressure incurred by sediment material; however one specimen of *Gephyrocapsa oceanica* and one of *Gephyrocapsa ericsoni* were found.

2.2.5 Carbonate analysis

Whenever possible the percent of carbonate from each sample was determined from approximately one gram of crushed, dry, organic free material. Six samples (Nos. 26, 45, 73, 97, 99 and 100) consisted of less than 0.25 grams of sample and were not considered for carbonate analysis, since use of quantities of sample less than this resulted in large error in carbonate percentage calculations. A carbonate bombe was used and followed the procedure of Muller and Gastner (1971) and Birch (1981). Crushed samples were assigned soil colour codes using Munsell's (1975) soil colour chart.

2.2.6 Foraminifera counts and sediment descriptions

The greater than 150 micron size fraction was examined under a binocular microscope and some brief notes on the skeletal and mineral components were made for each sample. The fraction was then split using a dry sediment splitter. Between 300 and 600 foraminifera (both whole and incomplete specimens) were counted from the split and the relative abundance of foraminiferal fragments was estimated.

2.2.7 Oxygen isotope analysis

The coarse fraction was resieved and about 0.5 milligrams of well preserved *Globigerinoides sacculifer* were weighed from the 212-300 microns fraction (equivalent to about 45 specimens) and stored temporarily in labelled gelatin vials. *G. sacculifer* specimens were chosen for isotopic determination since they were abundant in most samples examined and since they have been shown by Erez and Luz (1983) to deposit their carbonate shells in isotopic equilibrium over a wide range of temperatures. Specimens were crushed in ethanol and dried for thirty minutes at 50°C. The calcium carbonate was dissolved in approximately 100% H₃PO₄ under vacuum at 50°C according to the method of Shackleton (1974), except that the samples were dropped into the acid and kept at constant temperature with a water jacket. Since there are no facilities at present available at the University of Cape Town to connect the extraction line

directly to the Micromass VG 602D mass spectrometer, samples had first to be isolated in 6 mm internal diameter glass tubing (break-seals) and sealed with a butane flame. Instrumental corrections of the results were calculated according to Craig (1957). The results are reported in per mil deviations relative to PDB and calibrated with standard NBS-20 according to the equation:

$$\delta^{18}\text{O} = \left(\frac{(^{18}\text{O}/^{16}\text{O})_{\text{sample}}}{(^{18}\text{O}/^{16}\text{O})_{\text{standard}}} - 1 \right) * 1000$$

Temperature estimates of oxygen isotope values were calculated from Vincent and Shackleton (1980):

$$T = 16.9 - 4.38(\delta^{18}\text{O}_{\text{C}} - \delta^{18}\text{O}_{\text{W}}) + 0.1(\delta^{18}\text{O}_{\text{C}} - \delta^{18}\text{O}_{\text{W}})^2$$

Where $\delta^{18}\text{O}_{\text{C}}$ is the oxygen isotope composition of the carbonate material, and $\delta^{18}\text{O}_{\text{W}}$ is the oxygen isotope composition of water (0.3 ppm) in which *G. sacculifer* lived.

3. RESULTS

3.1 SEDIMENT DESCRIPTION

The core-top material consisted mostly of nannoforaminiferal ooze (Kennett 1982) in the north of the study area (sectors one and two) and foram-nannofossil ooze in the south (sectors three and four). Glauconite, quartz and silica were found in sediment material, lying in a narrow band at the base of the continental slope and running down the length of the Natal Valley. Soil colours (Table 3) were found to be predominantly white and light grey hues (Munzell 1975), however, samples 13,15,17,44,71,96,97 and 98 displayed pale and very pale brown hues. Sediments ranged from muds to muddy sands with samples in the north being generally coarser than elsewhere. However, a particularly coarse group of samples was found in the Agulhas Passage. Fine material was concentrated off East London (sector three). Core numbers and locations are presented in Table 3 while finer than 63 microns percentages are plotted geographically in Fig. 3.1 and listed in Table 4.

3.2 CARBONATE PERCENTAGES

Carbonate results are presented as a percentage of the original sample (Table 8). Carbonate percentages in the core-top material varied greatly from sample to sample, ranging from 0% to 86% with an average of 46% (Fig 3.2). Lowest carbonate values (less than 30%) were found in the Agulhas Passage (sector four) at depths below four thousand meters and at the base of the continental slope off Durban (sector two). Slightly higher percentages were found in samples from beneath the Agulhas Current, while highest carbonate values were concentrated on the flanks and at the base of the Mozambique Ridge (sectors two and three) between two and four thousand meters. There is a sharp decline in the carbonate percentages of samples from water depths greater than 3500 m (Fig 3.3).

3.3 RELATIVE COCCOLITH ABUNDANCES AND ASSEMBLAGE COMPOSITION

Relative abundance of coccoliths generally increased in abundance with southerly latitude (Fig. 3.4). Highest abundances were recorded off East London (sector three), though low values were observed in the Agulhas Passage south of Port Elizabeth (sector four). Relative coccolith abundance indices are listed

in Table 1, while preservation indices are plotted in Fig. 3.5 and presented in Table 4.

Thirteen of the one hundred core-top samples studied by SEM contained very few or no coccoliths and were therefore excluded from further investigation (Fig. 3.6).

Forty-four identified and fifteen unidentified coccolithophore taxa were recognised from the Indian Ocean core-tops (Table 5). Thirty-four of the identifiable taxa are modern and ten extinct. Twenty six species of coccolithophores found in the water column of the southwest Indian Ocean by Friedinger and Winter (1985) are represented in the core-top samples by their coccoliths. Species recorded from the water column by Friedinger and Winter (1985) are indicated in Table 5 with an asterix. Six coccolithophore species known to live in the oceans at present (*Coccolithus pelagicus*, *Crenalithus cressilis*, *Gephyrocapsa protohuxleyi*, *Discolithina japonica* and *Calyptrorpha papilifera*) were found in core-top sediments but absent from water samples. Most of the species present in the water column but absent from the sediments were relatively fragile and probably dissolved on the journey to, or once at the sea floor.

3.3.1 Taxonomic notes

The two "ecophenotypic variants" of *Emiliania huxleyi*, a "cold-water" form with fused blade-like elements in the proximal shield and a "warm water" variety with T-shaped elements in both shields, have not been separated into two groups but placed together since it has been shown that there is little correlation between placolith type and temperature and their ecological affinities have not been confirmed (Winter 1985).

The orientation of the central bridge is a crucial factor in distinguishing between *Gephyrocapsa oceanica* and *Gephyrocapsa caribbeanica*. *G. oceanica*'s bridge is perpendicular to the long axis of the central area, while *G. caribbeanica* is obliquely aligned. Specimens which were similar in appearance to one of these two species, but which were lacking a central bridge or lying on the SEM stub proximal side upwards (bridge obscured) were probably mostly *G. oceanica* specimens since identifiable *G. caribbeanica*

TABLE 3.

Sample Number	Core Number	Core Type	Rock Colour	Lat. Degrees	Long. Degrees	Location
1	5088	G	10YR8/2	27°13'3	34°10'	SW of Al Liete Bank
2	5089	G	2.5Y7/2	27°07'8	33°41'5	St of Ponta do Ouro
3	5090	G	10YR8/1	27°02'2	33°30'5	Est of Ponta do Ouro
4	5091	G	2.5Y8/2	27°20'5	33°38'9	E of Lake Sibaya
5	5097	G	2.5Y8/2	27°11'5	33°14'3	E of Lake Sibaya
6	5098	G	10YR8/1	26°57'1	33°11'5	E of Kosi Bay
7	5104	G	2.5Y7/2	26°43'6	33°16'	ENE of Ponta do Ouro
8	5105	G	10YR8/2	26°42'6	33°18'8	ENE of Ponta do Ouro
9	5109	G	10YR7/2	26°34'1	33°29'1	NE of Ponta do Ouro
10	5110	T	2.5Y8/2	26°49'8	34°03'8	ENE of Ponta do Ouro
11	5111	T	2.5Y7/2	26°07'6	34°35'7	W of Al Liete Bank
12	5112	T	2.5Y8/2	25°57'2	34°11'7	E of Maputo
13	5113	T	5Y6/2	25°32'2	34°50'	NW of Al Liete Bank
14	5114	G	2.5Y7/2	25°22'1	34°13'3	NW of Al Liete Bank
15	5115	G	10YR6/4	29°54'7	31°40'5	E of Durban
16	5116	G	5Y7/2	30°14'7	31°54'9	SE of Durban
17	5117	G	10YR7/3	30°13'6	31°54'7	SE of Durban
18	5119	G	10YR8/1	30°18'9	32°32'7	ESE of Durban
19	5121	G	2.5Y7/2	30°35'8	33°07'6	ESE of Durban
20	5127	G	10YR8/1	29°19'1	33°12'	ENE of Durban
21	5729	P	5Y8/1	27°57'2	32°58'7	E of Lake St Lucia
22	5737	P	2.5Y7/2	26°36'4	34°12'1	SW of Al Liete Bank
23	5743	P	10YR8/1	25°41'6	35°24'	N of Al Liete Bank
24	5744	P	10YR8/2	25°51'9	34°25'	NW of Al Liete Bank
25	5745	T	10YR7/2	25°37'3	33°33'	S of Limpopo River
26	5746	P	2.5Y8/2	26°08'2	33°27'7	ESE of Maputo
27	5751	P	10YR7/1	30°39'1	34°19'3	ENE of Durban
28	5752	P	10YR8/2	30°24'23	33°54'4	ESE of Durban
29	5753	P	10YR8/2	30°32'5	32°42'5	ESE of Durban
30	5760	P	10YR8/1	35°58'3	25°25'3	S of Port Elizabeth
31	5761	P	5Y8/1	36°09'5	25°19'6	SSW of Port Elizabeth
32	5762	T	10YR8/1	36°19'8	25°14'	S of Gamtoos River
33	5764	P	2.5Y7/2	36°40'3	23°59'9	S of Storms River
34	5765	P	5Y8/2	36°45'8	24°00'7	S of Storms River
35	5766	P	10YR8/2	36°28'4	23°50'2	S of Plettenberg Bay
36	5767	P	10YR8/1	36°10'9	23°41'6	S of Plettenberg Bay
37	6326	P	10YR8/1	36°30'7	24°41'	S of Cape St Francis
38	6328	P	2.5Y8/2	36°26'6	24°46'1	S of Cape St Francis
39	6331	P	2.5Y7/2	35°42'6	25°04'1	S of Gamtoos River
40	6333	P	10YR8/1	35°11'5	25°42'6	S of Port Elizabeth
41	6334	T	10YR8/2	35°33'5	24°58'7	S of Cape St Francis
42	6336	T	2.5Y8/2	36°13'4	24°33'	S of Cape St Francis
43	6571	P	10YR8/2	33°45'4	28°34'4	SE of East London
44	6572	P	10YR7/3	33°41'	28°24'	SE of East London
45	6575	P	10YR8/2	33°50'9	28°08'3	SSE of East London
46	6576	P	10YR7/2	33°57'8	28°02'6	S of East London
47	6577	P	10YR7/2	34°02'8	27°58'5	S of East London
48	6671	T	10YR8/2	34°54'7	26°55'4	SE of Port Elizabeth
49	6672	P	2.5Y8/2	34°42'6	26°46'3	SE of Port Elizabeth
50	6673	P	10YR8/2	34°13'3	27°35'2	SSW of East London

Table 3. Core types indicated are as follows: P Piston, G Gravity and T Trigger. Rock colours 10YR8/1, 10YR8/2, 5Y8/1, 5Y8/2 and 2.5Y8/2 are White. 10YR7/2, 2.5Y7/2 and 5Y7/2 are Light Grey, 5Y6/2 is Light Olive Grey, 10YR6/4 Light Yellowish Brown and 10YR6/3 is Pale Brown.

TABLE 3. (cont.)

Sample Number	Core Number	Core Type	Rock Colour	Lat. Degrees	Long. Degrees	Location
51	6674	P	10YR7/2	34°00'3	27°38'2	SSW of East London
52	6675	P	2.5Y8/2	33°47'6	27°42'5	SSW of East London
53	6677	T	10YR8/2	33°12'	29°04'7	E of East London
54	6679	T	2.5Y8/2	33°10'9	29°32'5	E of East London
55	6680	T	10YR8/2	33°12'	30°14'3	E of East London
56	6681	T	10YR8/2	33°14'5	31°18'8	E of East London
57	6682	T	10YR8/2	33°10'8	33°09'1	E of East London
58	6683	P	10YR8/2	33°09'4	33°01'6	E of East London
59	6686	P	10YR8/2	33°09'5	33°14'7	E of East London
60	6689	T	10YR8/1	34°00'3	32°08'4	E of Port Elizabeth
61	6690	T	10YR8/2	33°59'3	32°00'3	E of East London
62	6691	T	10YR8/2	33°59'8	31°29'5	E of East London
63	6693	T	10YR8/2	33°57'	30°14'3	E of East London
64	6694	P	10YR8/2	34°00'1	29°33'9	E of East London
65	A1229	P	10YR8/1	26°12'	34°12'	W of Al Leite Bank
66	N10E15	P	10YR8/2	39°19'5	30°06'5	E of East London
67	N10E39	P	5Y8/1	36°42'2	22°29'	S of George
68	N10E40	P	10YR8/1	37°33'	24°51'	S of Cape St Francis
69	N10E45	P	10YR8/1	36°44'1	21°40'7	S of Gourits River
70	N10E49	P	10YR8/2	32°17'8	29°28'7	NE of East London
71	N10E50	P	10YR7/3	31°51'7	30°29'2	NE of East London
72	N10E51	P	10YR8/2	33°10'4	31°46'9	E of East London
73	N10E55	P	5Y8/2	34°49'1	31°42'9	SE of East London
74	N10E56	P	5Y8/2	34°35'1	26°13'	SSE of Port Elizabeth
75	N10E136	P	10YR8/1	39°10'	33°35'	SE of Port Elizabeth
76	N10E8	P	10YR8/1	32°11'8	35°25'1	ENE of East London
77	MN1	T	2.5Y8/2	30°46'1	33°43'6	E of Durban
78	MN4	T	10YR8/1	29°10'5	34°45'9	E of Durban
79	MN5	T	10YR8/2	29°08'8	34°38'4	E of Durban
80	MN9	T	5Y8/1	29°00'	34°13'8	E of Durban
81	MN12	T	10YR8/2	28°54'3	33°08'7	E of Durban
82	MN13	T	10YR8/2	29°02'3	33°34'1	E of Durban
83	MN14	T	10YR8/2	29°12'	33°29'	E of Durban
84	MN15	T	2.5Y7/2	29°15'2	33°26'8	E of Durban
85	MN16	T	10YR8/2	29°16'7	33°27'	E of Durban
86	MN18	T	10YR8/2	29°37'2	33°22'1	E of Durban
87	MN19	T	10YR8/2	29°36'	33°10'7	E of Durban
88	MN20	T	10YR8/2	29°29'7	33°13'	E of Durban
89	MN21	T	10YR8/1	29°27'4	33°04'6	E of Durban
90	MN23	T	2.5Y8/2	29°24'9	32°51'2	E of Durban
91	MN24	T	10YR8/1	29°27'2	32°48'9	E of Durban
92	MN25	T	10YR8/2	29°30'3	32°40'7	E of Durban
93	MN26	T	10YR8/1	29°28'8	32°32'8	E of Durban
94	MN27	T	10YR8/2	29°33'4	32°27'1	E of Durban
95	MN29	T	10YR8/2	29°40'9	32°13'	E of Durban
96	MN30	T	10YR8/3	29°44'2	31°58'2	E of Durban
97	MN1531	T	10YR7/4	29°40'9	31°55'6	E of Durban
98	MN32	T	10YR6/3	29°42'8	31°44'9	E of Durban
99	6759	P	10YR8/2	32°49'	33°49'25	E of East London
100	6761	T	10YR8/2	33°08'5	32°33'4	E of East London

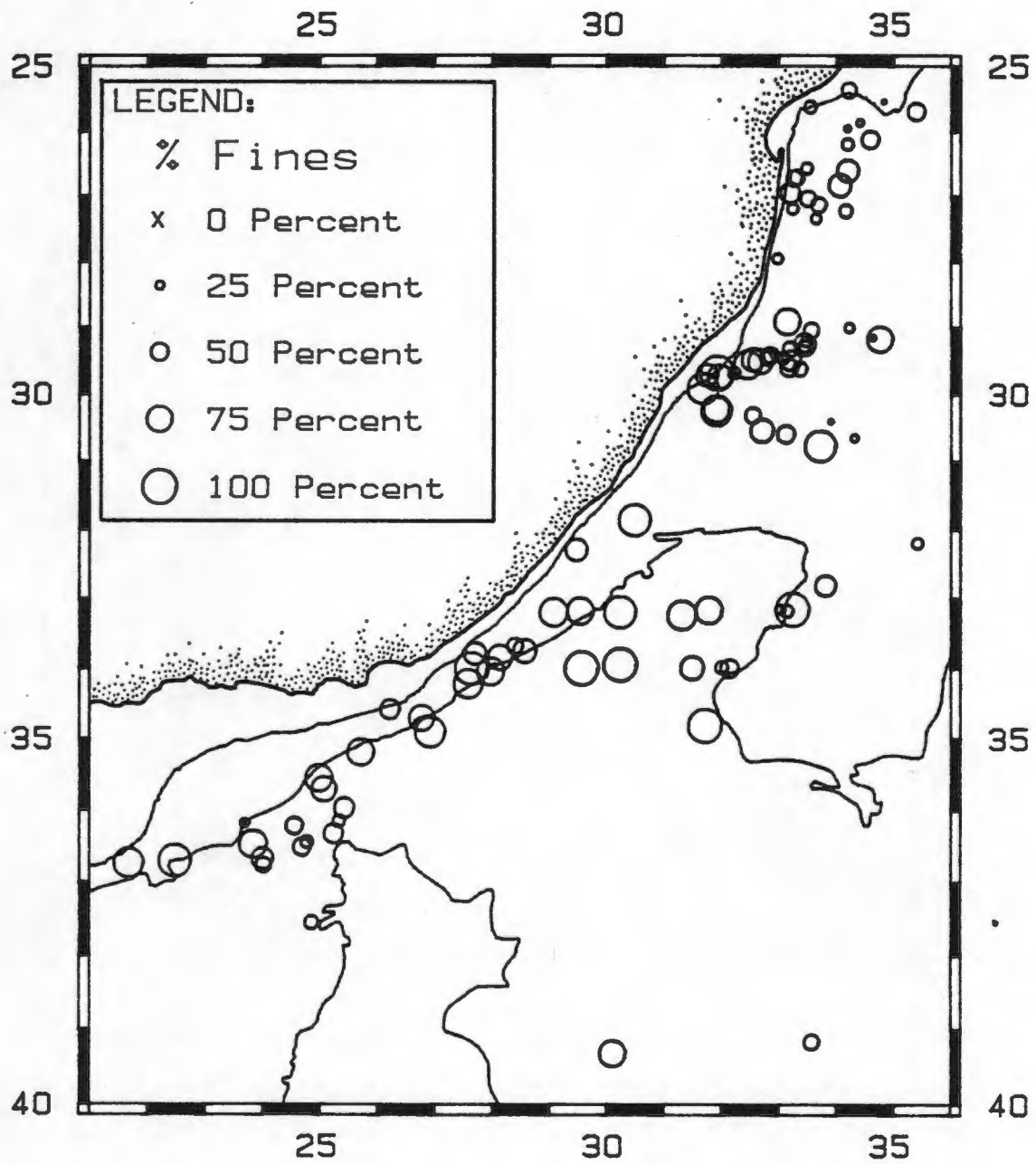


Figure 3.1 Percentage of material finer than 63 microns.

TABLE 4.

Sample Number	Sector	Depth (M)	Sample Wt. (g)	Percent <63microns	Coccolith Abundance Index	Preservation
1	1	1510	2.363	37.9	2	3
2	1	1229	1.677	44.3	0	2
3	1	1020	0.902	45.3	0	4
4	1	1320	1.181	30.1	0	4
5	1	1063	1.347	31.1	0	3
6	1	828	1.477	57.8	1	3
7	1	708	1.254	46.3	1	4
8	1	699	1.343	43.2	0	4
9	1	673	0.855	34.1	2	3
10	1	1000	1.182	65.3	2	4
11	1	900	1.631	49.3	1	3
12	1	527	0.732	17.8	1	4
13	1	248	2.463	12.0	1	4
14	1	365	1.287	43.0	1	4
15	2	765	0.035	90.0	NA	NA
16	2	2010	0.456	87.9	2	5
17	2	1705	1.071	76.5	3	4
18	2	2813	1.334	45.1	2	4
19	2	3030	1.463	49.9	3	3
20	2	1940	0.439	43.3	3	5
21	1	1270	0.773	29.6	2	4
22	1	917	1.400	64.8	1	3
23	1	1200	0.836	49.8	1	4
24	1	440	0.718	19.5	1	4
25	1	471	1.839	36.7	1	3
26	1	545	NA	NA	NA	NA
27	2	2778	0.519	21.4	2	3
28	2	2804	0.849	12.0	NA	NA
29	2	2992	0.664	67.8	1	3
30	4	4720	1.378	58.5	3	3
31	4	4845	1.835	35.4	2	4
32	4	3890	1.875	56.3	2	4
33	4	4879	2.398	62.6	1	3
34	4	4870	1.230	44.1	1	4
35	4	4140	1.538	79.8	1	4
36	4	2840	1.014	26.0	1	2
37	4	4500	0.915	50.6	NA	NA
38	4	4800	1.818	35.2	0	4
39	4	4650	0.992	72.4	2	4
40	4	4000	1.701	78.6	2	3
41	4	4750	1.282	77.4	NA	NA
42	4	4800	1.146	48.2	2	5
43	3	3765	0.871	67.9	3	4
44	3	3428	1.671	46.4	3	4
45	3	3668	0.102	71.5	3	4
46	3	3625	1.163	10.2	NA	NA
47	3	3610	4.391	79.6	NA	5
48	4	4132	0.749	87.4	3	3
49	4	3830	1.190	73.9	3	5
50	3	3655	0.968	84.9	2	3

Sample Number	Sector	Depth (M)	Sample Wt. (g)	Percent <63microns	Coccolith Abundance Index	Preservation
51	3	2956	0.767	93.8	2	4
52	3	2220	1.219	64.4	3	3
53	3	3283	1.391	81.7	3	2
54	3	3480	1.591	78.5	3	5
55	3	3690	1.462	92.0	3	2
56	3	3800	0.416	84.1	3	2
57	3	3760	1.150	36.4	3	5
58	3	3685	1.202	27.5	3	4
59	3	3740	0.691	98.3	2	4
60	3	3690	2.238	52.3	NA	NA
61	3	3965	2.226	35.7	3	5
62	3	4010	1.762	67.0	3	4
63	3	4010	1.510	96.0	3	3
64	3	3890	0.652	98.5	3	5
65	1	2110	0.770	34.6	2	2
66	5	2900	0.554	76.2	2	2
67	4	2960	0.632	94.9	3	4
68	4	3480	0.705	40.9	1	3
69	4	1580	0.793	86.4	3	5
70	3	1880	0.466	63.7	2	4
71	3	2910	0.435	91.9	1	4
72	3	3700	0.454	77.9	1	3
73	3	4080	0.405	98.8	NA	NA
74	4	2125	0.744	56.8	3	4
75	5	3300	0.734	44.5	3	4
76	3	1750	0.848	32.7	3	4
77	2	3014	0.338	89.0	1	4
78	2	2500	0.143	74.1	2	3
79	2	2395	0.902	16.8	2	2
80	2	1910	0.767	28.9	1	3
81	2	2164	0.524	75.7	1	5
82	2	2325	0.664	43.9	3	2
83	2	2150	0.467	33.4	3	3
84	2	2340	0.288	63.8	NA	NA
85	2	2362	1.042	35.6	NA	NA
86	2	2400	0.641	42.9	NA	NA
87	2	2018	0.425	49.8	2	3
88	2	2018	1.071	57.5	3	2
89	2	2125	0.530	33.6	1	3
90	2	1850	0.584	45.0	3	3
91	2	1950	0.527	44.6	2	1
92	2	1838	0.578	72.6	2	4
93	2	1688	1.029	66.7	2	4
94	2	1577	0.793	82.4	2	4
95	2	1320	0.927	34.6	1	1
96	2	1340	0.903	69.5	0	3
97	2	1105	0.260	100.0	NA	NA
98	2	657	0.708	63.3	NA	NA
99	3	2924	4.729	60.7	NA	3
100	3	3630	2.182	86.5	NA	4

Table 4. Sample data. Sectors are M Maputo, D Durban, EL East London and PE Port Elizabeth. Sector number 5 corresponds to cores outside these locations (see Fig. 2). NA indicates samples for which no data was available.

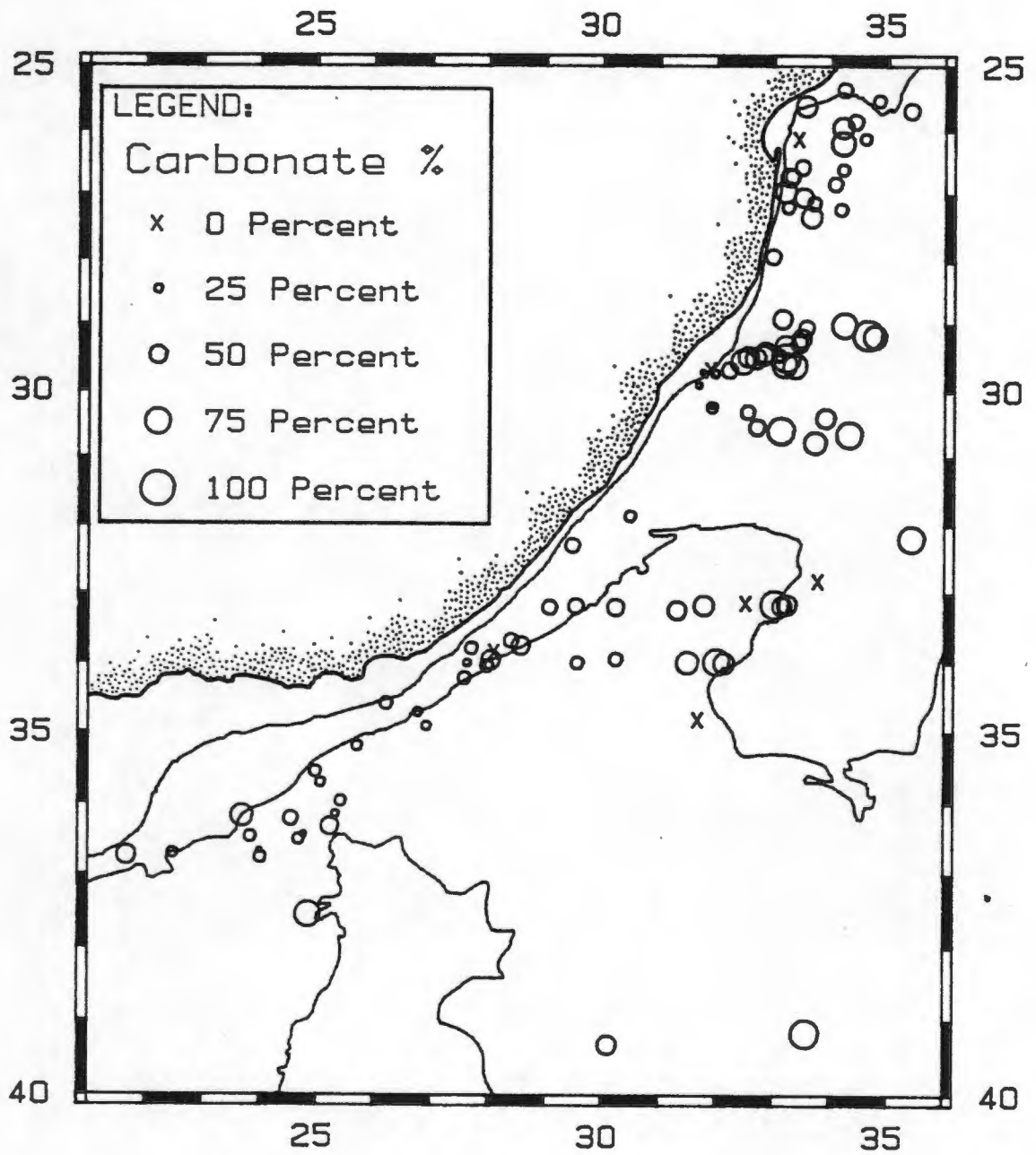


Figure 3.2 Percentage of carbonate material in samples.

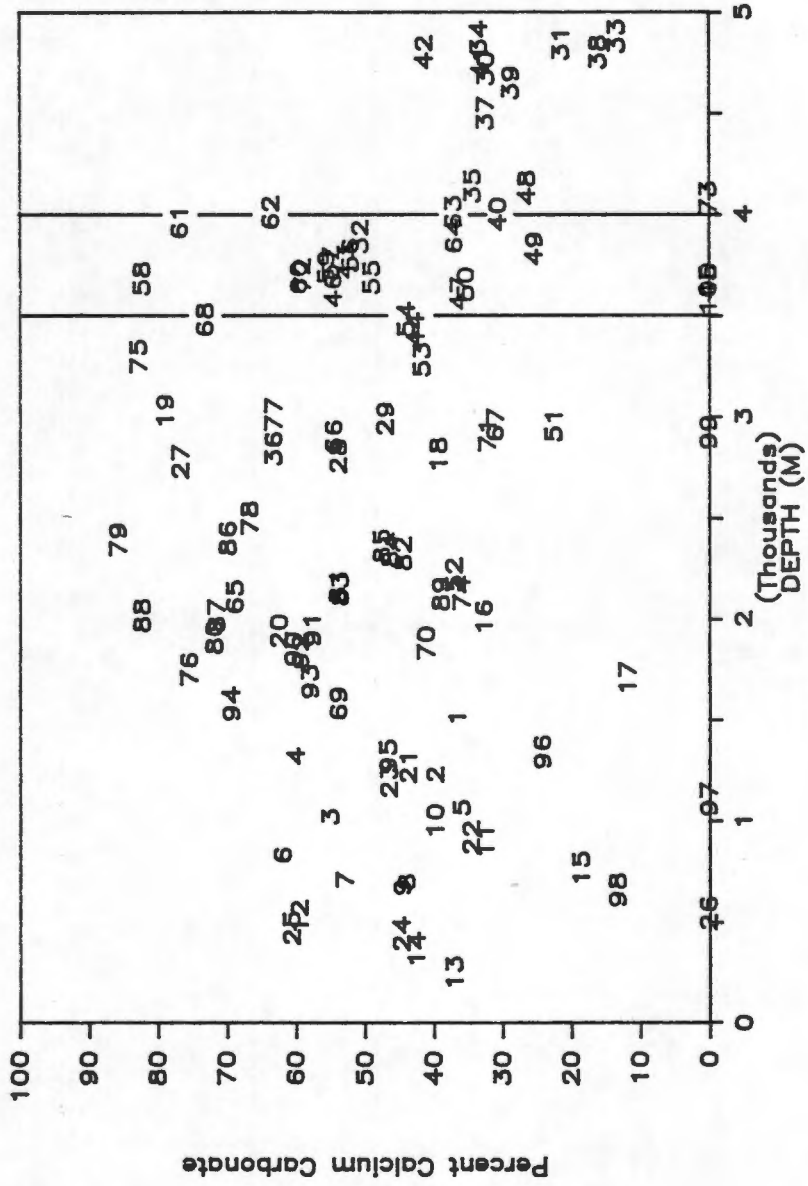


Figure 3.3 Plot of carbonate percentage vs. depth. Points are marked by sample numbers.

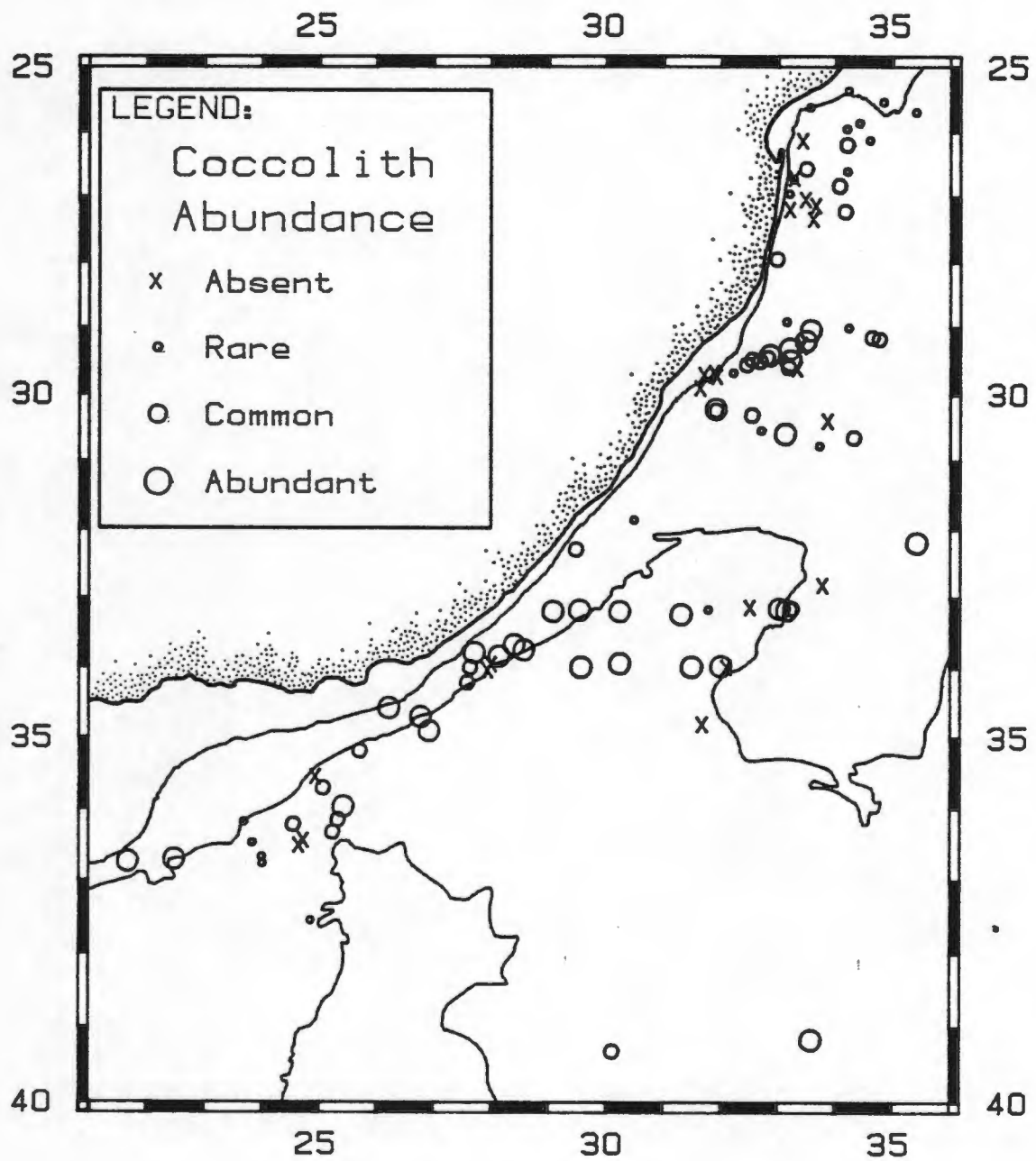


Figure 3.4 Relative abundance of coccoliths as determined using light microscopy.

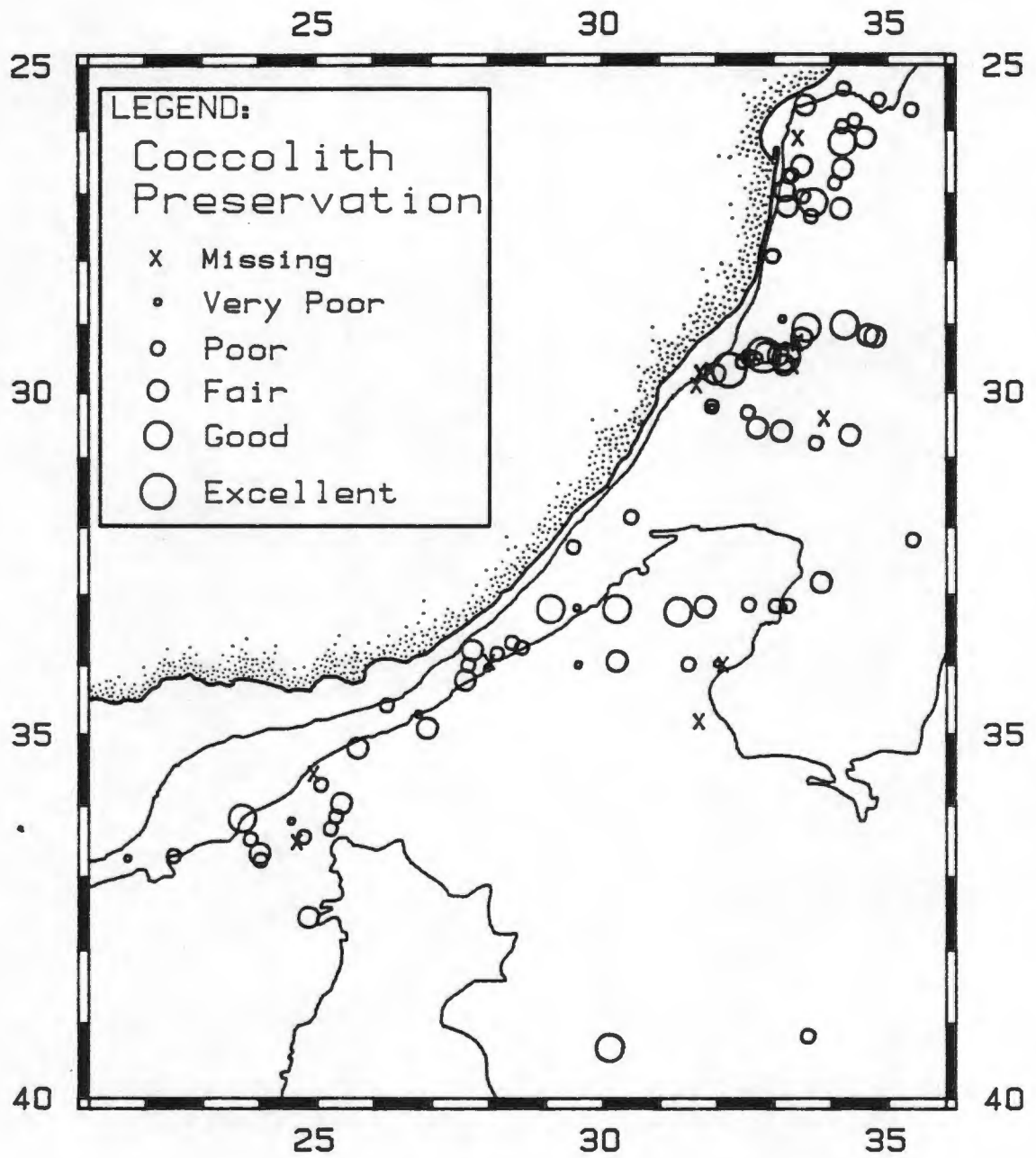


Figure 3.5 Distribution of coccolith preservations.

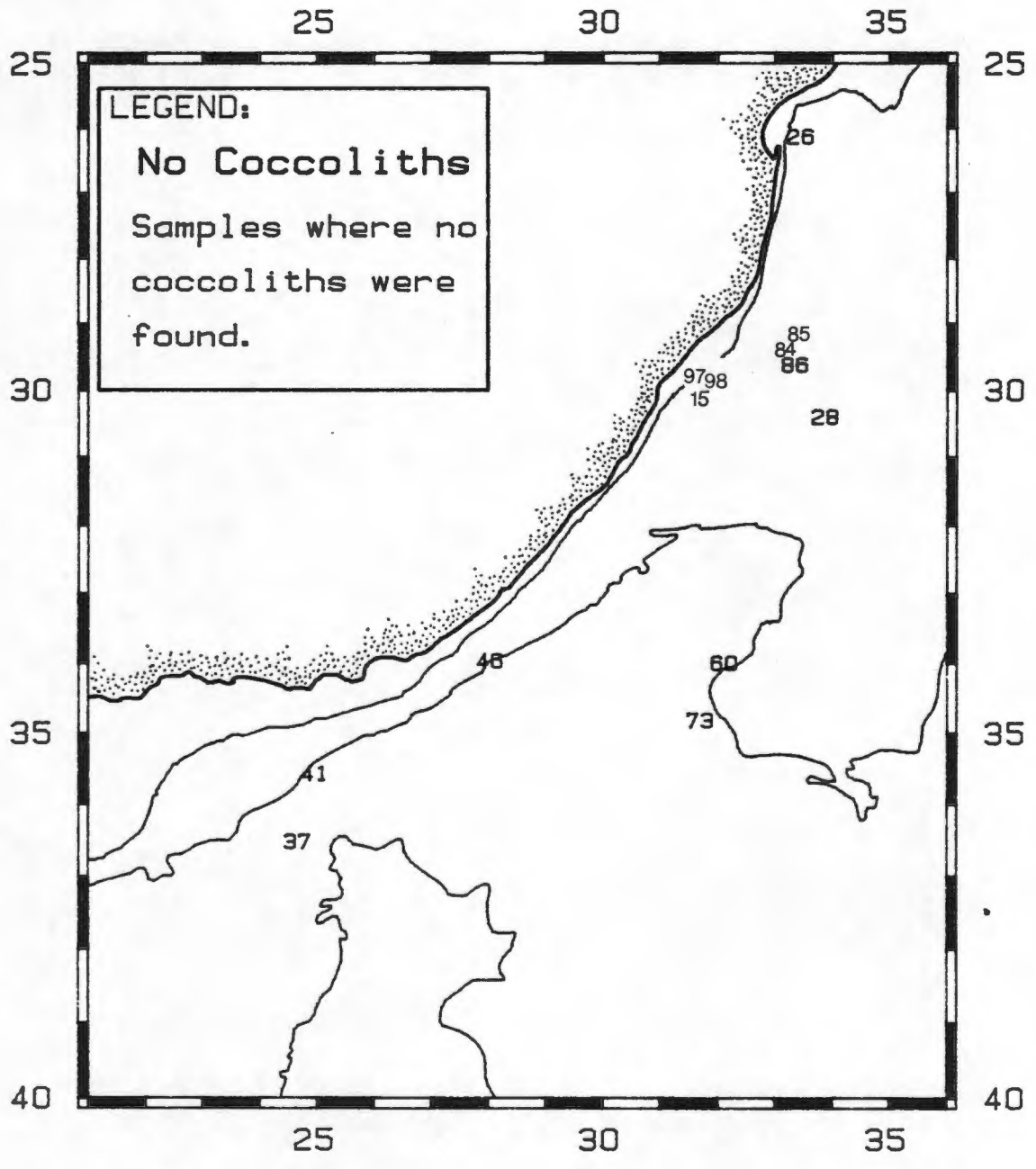


Figure 3.6 Samples in which no coccoliths were found under SEM. Locations are marked by sample numbers.

TABLE 5. Taxonomic list of coccolithophore species identified from the sediment surface in the southwest Indian Ocean. Most recent or best available micrographs are quoted for reference. Coccolithophore species that were also present in the water column (Friedinger and Winter 1985) are marked with an asterix.

Kingdom PLANTAE

Division CHRYSOPHYTA Pascher, 1914.

Class PRYMNESIOPHYCEAE Manton, 1964.

Order COCCOLITHOPHORALES Schiller, 1926.

CERATOLITHACEAE Norris, 1965.

- 1.* *Ceratolithus cristatus* Kamptner, 1950.
Wang and Samtleben, 1983. Pl. 2(164).

COCCOLITHACEAE Kamptner, 1928.

2. *Coccolithus pelagicus* (Wallich), 1892.
Siesser, 1975. Pl. 6(e,f).
3. *Crenalithus* sp. cf. *Crenalithus sessilis* (Lohmann), 1912.
Nishida, 1979. Pl. 3(3).
- 4.* *Calcidiscus leptoporus* (Murray and Blackman), 1890.
Wang and Samtleben, 1983. Pl. 1(10).
- 5.* *Emiliania huxleyi* (Lohmann), 1902.
Winter et al., 1979. Pl. 1(3).
- 6.* *Gephyrocapsa caribeanica* Bourdreaux and Hay, 1967.
Winter, 1982. Pl. 1(5).
- 7.* *G. ericsoni* McIntyre and B., 1967.
Winter et al., 1979. Pl. 1(6).
- 8.* *G. oceanica* Kamptner, 1943.
Okada and McIntyre, 1977. Pl. 3(1).
- 9.* *G. ornata* Heimdal, 1973.
Okada and McIntyre 1977. Pl. 3(1).
10. *G. protohuxleyi* McIntyre 1969.
Winter et al. 1978. Pl. 1(1-6).
- 11.* *Oolithus fragilis* (Lohmann) subsp. *cavum* Okada and McIntyre, 1977.
Okada and McIntyre 1977. Pl. 4(4,5).
- 12.* *Umbilicosphaera hulbertiana* Gaarder, 1970.
Wang and Samtleben, 1983. Pl. 1(13).
- 13.* *U. sibogae* (Webber-van Bosse), 1901.
Okada and McIntyre, 1977. Pl. 4(2).

HELICOSHAERACEAE Black, 1971 emend. Jafar and Martini, 1975.

- 14.* *Helicosphaera carteri* (Wallich), 1877.
Nishida, 1979. Pl. 9(4).
- 15.* *H. pavimentum* Okada and McIntyre, 1977.
Okada and McIntyre, 1977. Pl. 4(6,7).

PONTOSPHAERACEAE Lemmermann, 1908.

16. *Discolithina japonica* Takayama, 1967.
Okada and McIntyre, 1977. Pl. 6(3).
17. *Pontosphaera discophora* Schiller, 1925.
Borsetti and Cati, 1979. Pl. 2(3,4).
- 18.* *P. syracusana* Lohmann, 1920.
Okada and McIntyre, 1977. Pl. 5(7).

TABLE 5. cont.

RHABDOSPHERACEAE Lemmermann in Brandt and Apstein, 1908.

- 19.* *Acanthoica quattrosolina* Lohmann, 1903.
Nishida, 1979. Pl. 13(1).
- 20.* *Discosphaera tubifera* (Murray and Blackman), 1898.
Nishida, 1979. Pl. 13(1).
- 21.* *Neosphaera coccolithomorpha* Leccal-Schlauder, 1950.
Wang and Samtleben, 1983. Pl. 2(4).
- 22.* *Rhabdosphaera clavigera* Murray and Blackman, 1898.
Winter et al., 1979. Pl. 12(1).
- 23.* *Umbellosphaera irregularis* Paasche, 1955.
Wang and Samtleben, 1983. Pl. 2(2).
- 24.* *U.tenuis* (Kamptner), 1937.
Winter et al., 1979. Pl. III(1,2).

SYRACOSPHERA Lemmermann, 1908.

(CALCIOSOLENICEAE, Kamptner, 1937)

- 25.* *Anoploselenia brasiliensis* (Lohmann), 1919.
Borsetti and Cati, 1972. Pl. 16(1a,b).
- 26.* *Syracosphaera corolla* Leccal, 1965.
Borsetti and Cati, 1979. Pl. 3(5).
- 27.* *S.lamina* Leccal-Schlauder, 1951.
Nishida, 1979. Pl. 8(3).
- 28.* *S.mediterranea* Lohmann, 1902.
Okada and McIntyre, 1977. Pl. 10(4,5).
- 29.* *S.mediterranea* Lohmann var. *binodata* Kamptner, 1937.
Okada and McIntyre, 1977. Pl. 10(6).
- 30.* *S.pulchra* Lohmann, 1902.
Okada and McIntyre, 1977. Pl. 10(11,12).
31. *Syracosphaera* sp. cf. *variabilis* (Halldal and Markali), 1955.
Okada and McIntyre, 1977. Pl. 9(7,8).

CALYPTROSPHERACEAE Boudreaux and Hay, 1969.

32. *Calyptosphaera papillifera* Boudreaux and Hay, 1969.
Nishida, 1979. Pl. 23(3).

GENUS OF UNCERTAIN ORIGIN (Incertae sedis)

33. *Hyaster perplexus* (Bramlette and Riedel), 1954.
Wang and Samtleben, 1983. Pl. 2(1).

NON COCCOLITHOPHORE GENUS: CALCAREOUS DINOFLAGELATE.

(THORACOSPHERACEAE, Schiller, 1930)

- 34.* *Thoracosphaera* cf. *T.heimii* (Lohmann), 1919.
Winter et al., 1979. Pl. V(11).

DISCOASTERACEAE Vekshina, 1959.

35. *Discoaster broweri* Tan Sin Hok, 1927.
Buckry, 1971. Pl. 3(2). Range: Late Miocene to late Pliocene.
36. *D.exilis* Martini and Bramlette, 1963.
Martini and Bramlette, 1963. Pl. 104(1-3). Epoch: Middle Miocene.
37. *D.deflanderi* Bramlette and Reidel, 1954.
Buckry, 1971. Pl. 4(4). Range: mid Eocene to mid Miocene.
38. *D.siapanensis* Bramlette and Reidel, 1954.
Haq, 1980. Pl. 23(f). Range: mid to late Eocene.

TABLE 5. cont.

OTHER REWORKED COCCOLITHS

39. *Dictyococcites daviesi* (Haq), 1976.
Haq, 1976. Pl. XI(11). Epoch: Cenozoic.
40. *Ericsonia cava* (Hay and Mohler), Perch-Nielsen, 1
Hay and Mohler, 1967.
41. *Pseudoemiliana lacunosa* (Kamptner), 1963.
Samtleben, 1978. Pl. 3(1).
42. *Aperlapetra gronosa* (Stover), 1966.
Buckry, 1970. Pl. 6(6). Range: Albian-Campanian.
43. *Prediscophaera cretacea* (Arkhangelsky), 1912.
Haq, 1980. Pl. 15(d). after Buckry, 1969. Range: Albian-Campanian.
44. *Cyclicargolithus floridanus* (Roth and Hay) 1967, Buckry 1971. Roth, 1973. Pl.
6(2+3). Range: Eocene to Miocene.

Plate I Fossil coccoliths I(1-15).

1. Distal view of *Ceratolithus cristasus*.
2. Proximal view of *C. cristasus*.
3. Distal view of *Coccolithus pelagicus*.
4. Proximal view of *C. pelagicus*.
5. Distal view of *Crenalithus sp. cf. Crenalithus sessilis*. The central area and outer elements are dissolved.
6. Proximal view of *Crenalithus sp. cf. Crenalithus sessilis*.
7. Distal view of *Calcidiscus leptoporus*.
8. Proximal view of *C. leptoporus*.
9. The underside of a distal shield of *Calcidiscus leptoporus* that has been separated (probably by dissolution) from its proximal shield.
10. Distal view of *Emiliana huxleyi*.
11. Proximal view of *Emiliana huxleyi*.
- 12 & 13. Distal views of *Gephyrocapsa caribbeanica*.
14. A semi-complete *Gephyrocapsa ericsoni* coccosphere skeleton.
15. Distal view of a single *G. ericsoni* coccolith.

Plate I

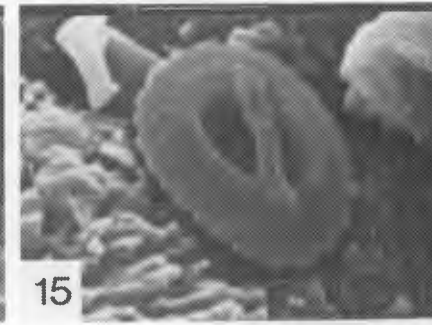
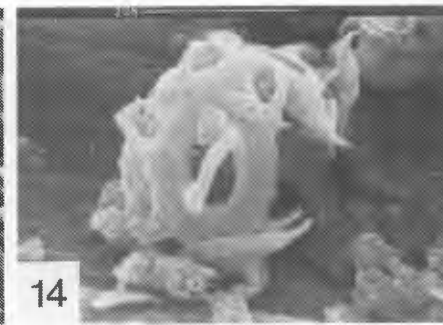
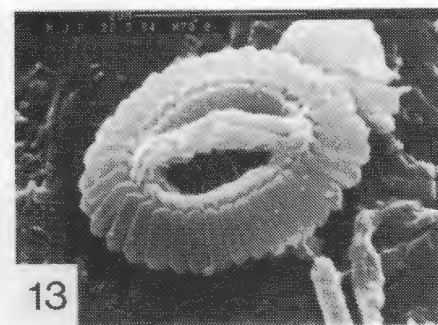
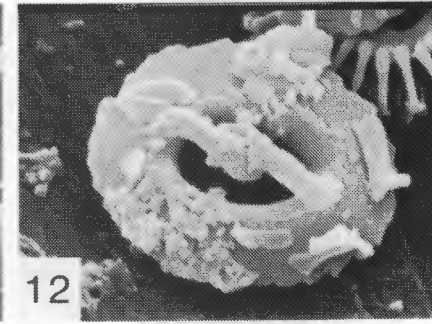
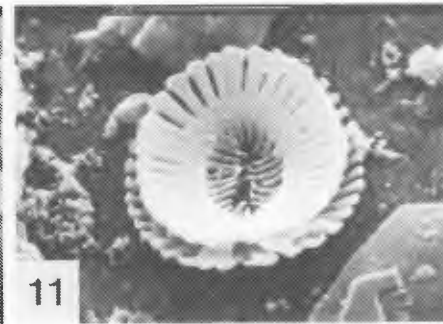
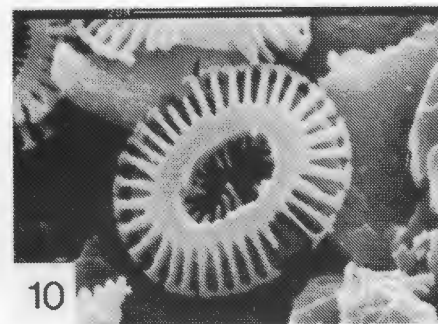
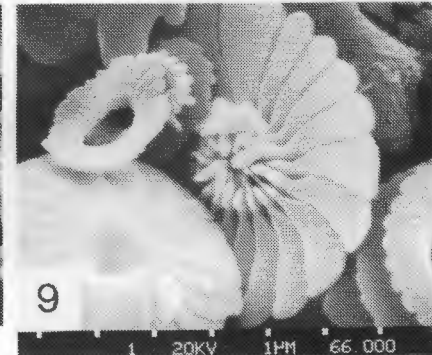
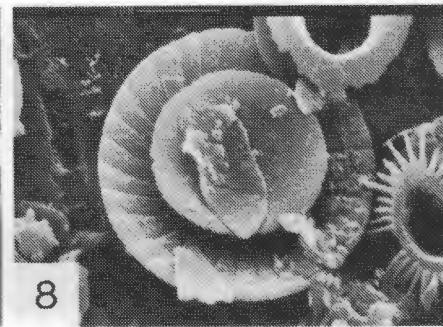
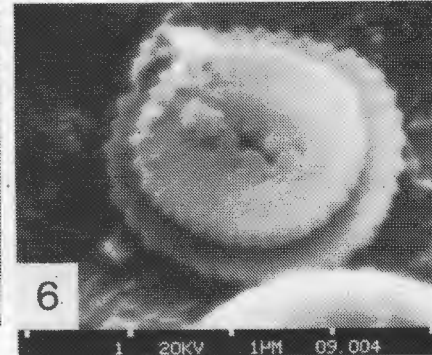
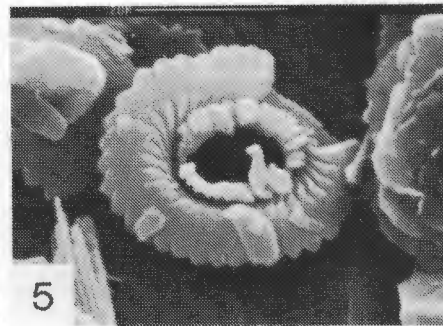
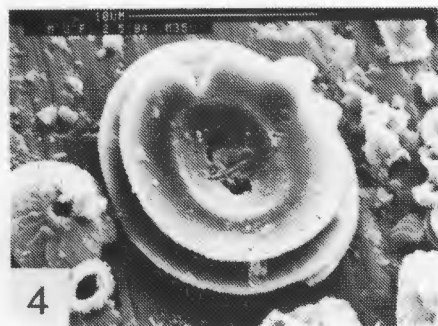
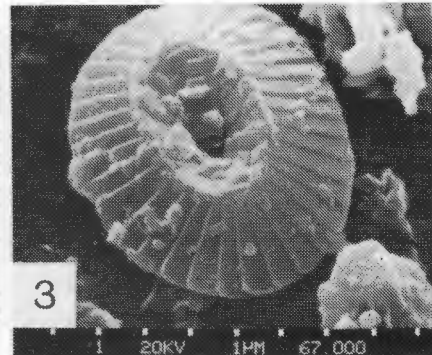
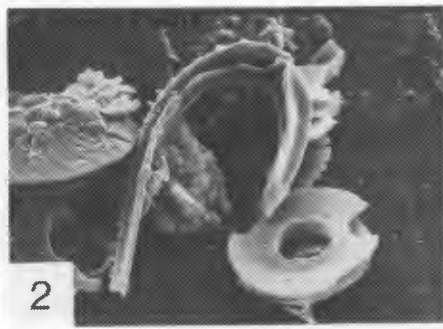
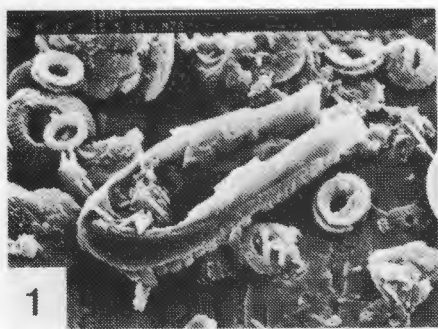


Plate II Fossil coccoliths II(1-15).

1. Distal view of *Gephyrocapsa oceanica*.
2. Proximal view of *G.oceanica*.
- 3 & 4. Proximal views of *Gephyrocapsa* specimens that could not be positively identified (since the central bridge is either absent or obscured due to the orientation on the SEM stub) but are most likely *G.oceanica*.
5. Distal view of *Gephyrocapsa ornata*.
- 6 & 7. Distal views of two specimens of *Gephyrocapsa protohuxleyi*.
8. Distal view of *Oolithus fragilis*.
9. Proximal view of *O. fragilis*.
10. Distal view of *Umbellosphaera hulbertiana*.
11. Proximal view of *U. hulbertiana*.
12. Distal view of *Umbilicosphaera sibogae*.
- 12 & 13. Proximal view of *U.sibogae*.
14. Distal view of *Helicosphaera carteri*.
15. Proximal view of *H. carteri*.

Plate II

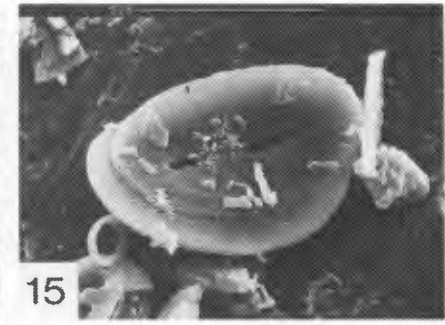
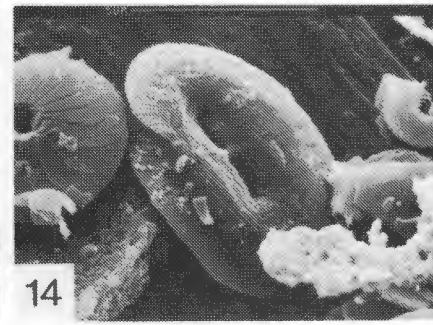
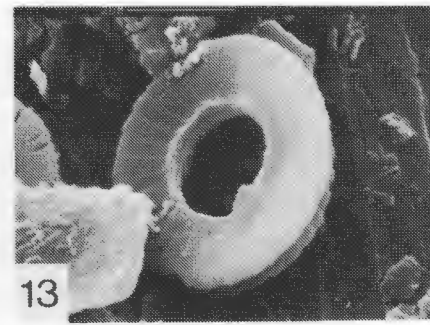
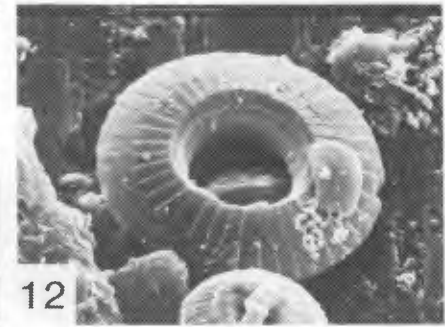
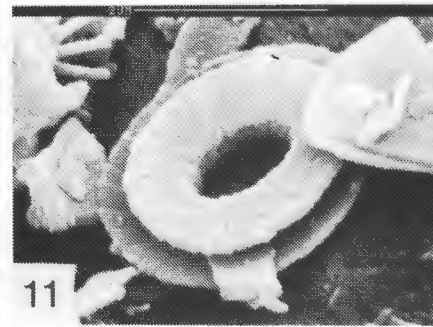
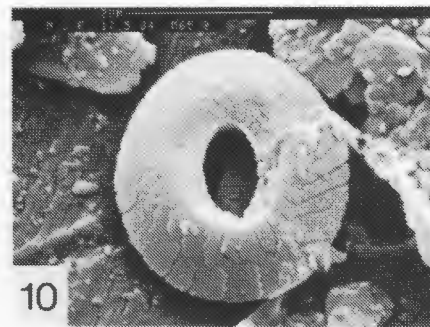
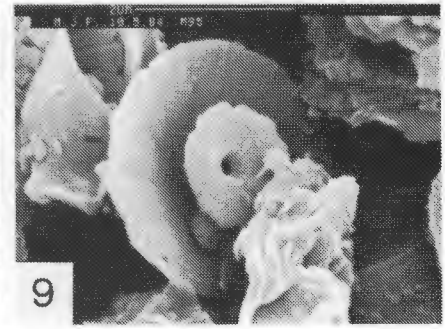
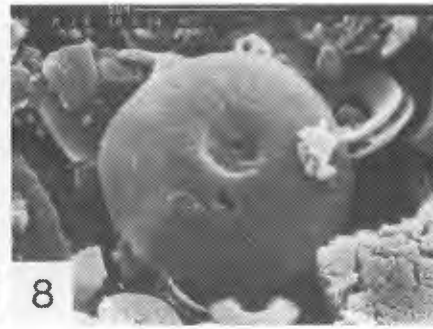
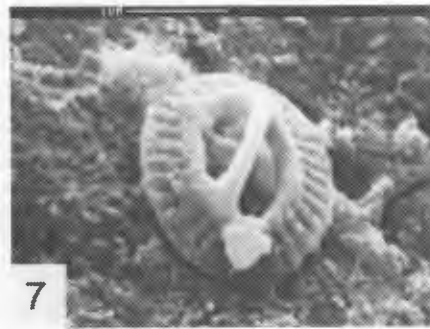
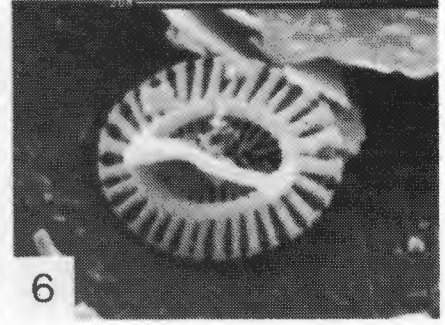
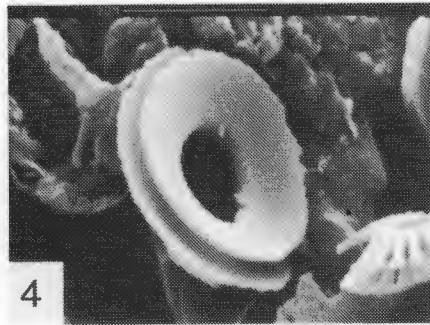
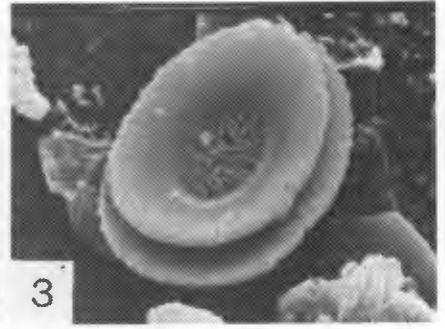
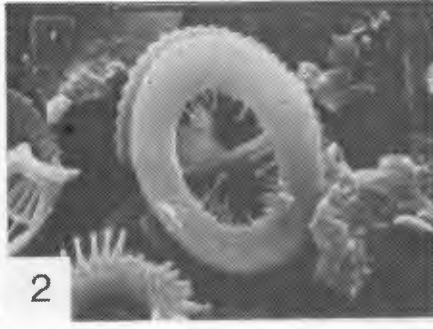


Plate III Fossil coccoliths III(1-15).

1. Distal view of *Helicosphaera pavementum*.
2. Distal view of *Discolithina japonica*.
3. Proximal view of *D. japonica*.
4. Distal view of *Pontosphaera discophora*.
5. Proximal view of *P. discophora*.
6. Proximal view of *P. syracusana*.
7. Distal view of *Acanthoica quattrosipina*.
- 8 & 9. Two different views of *Discosphaera tubifera* rhabdolith, both have lost their base shields, probably through dissolution.
10. Distal view of *Neosphaera coccolithomorpha*.
11. An intact rhabdolith of *Rhabdosphaera clavigera*.
12. Distal view of *R. clavigera* cyrtolith.
13. Proximal view of *R. clavigera* cyrtolith.
14. Distal view of *Umbellosphaera irregularis*.
15. Proximal view of *U. irregularis*.

Plate III

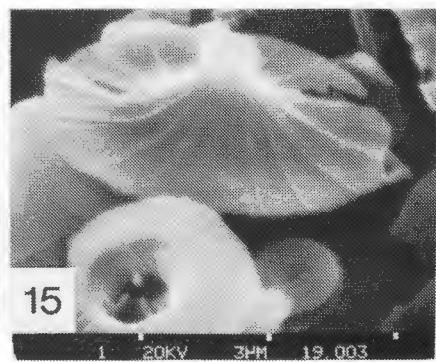
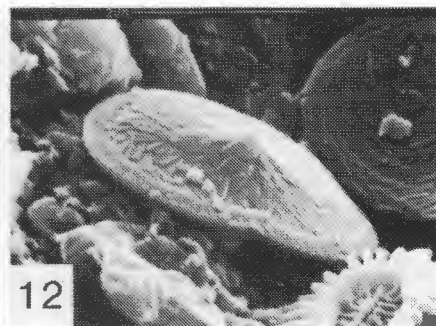
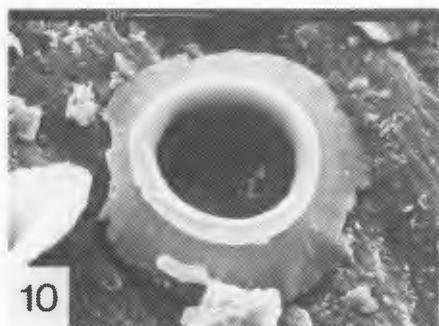
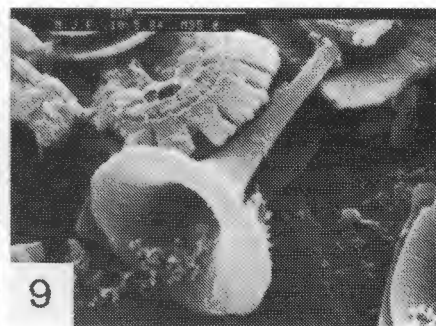
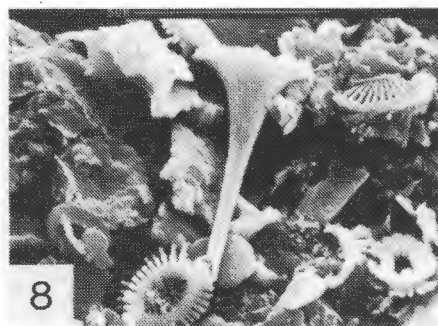
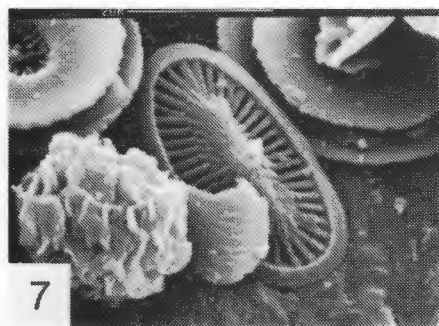
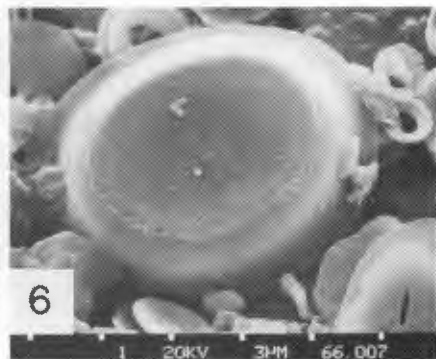
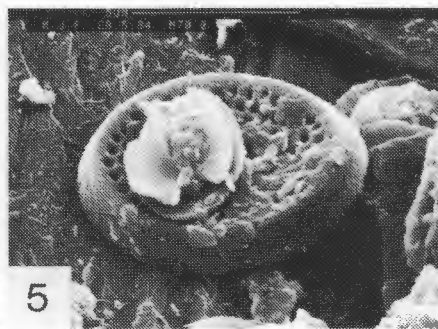
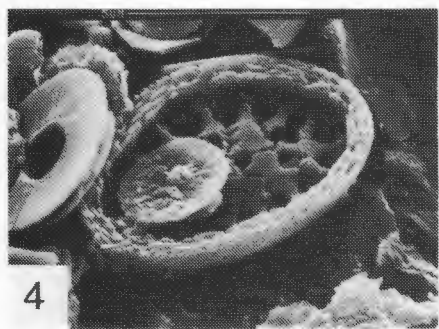
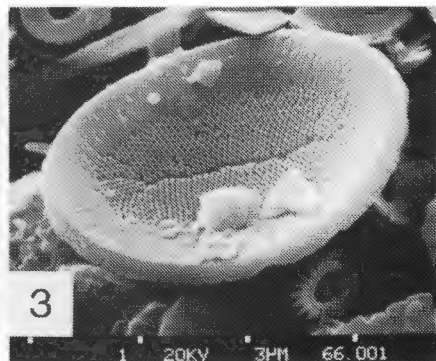
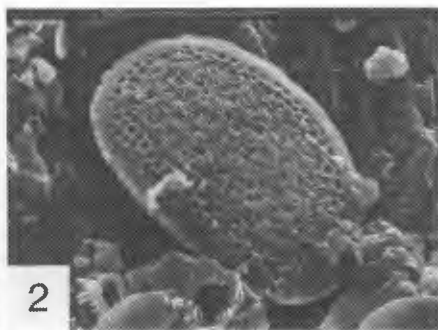
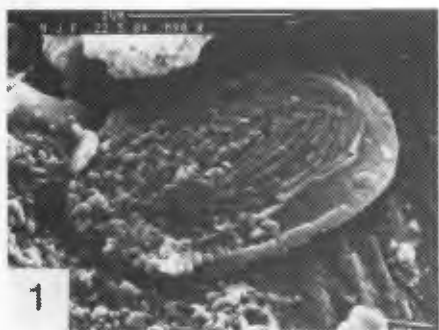


Plate IV Fossil coccoliths IV(1-15).

1. Distal view of *Umbellosphaera tenuis* specimen with calcite overgrowth.
2. Proximal view of dissolved *U.tenuis* specimen.
3. Distal view of *Anoploselenia brasiliensis*.
4. Proximal view of *A. brasiliensis*.
- 5 & 6. Proximal views of two different scapholiths of *A. brasiliensis*.
7. Proximal view of *Syracosphaera corolla*.
- 8 & 9. Two proximal views of *Syracosphaera lamina* specimens.
10. Distal view of specimen of *Syracosphaera mediteranea*.
11. Distal view of specimen of *S.mediteranea* Lohmann var. *binodata*.
12. Distal view of *Syracosphaera pulchra*.
13. Proximal view of *S.pulchra*.
14. Distal view of dissolved specimen of *Syracosphaera* sp. cf. *variabilis*.
15. Proximal view of *Syracosphaera mediteranea* specimen.

Plate IV

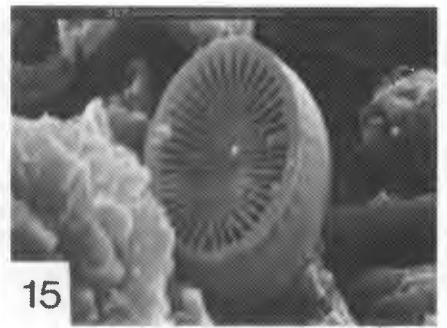
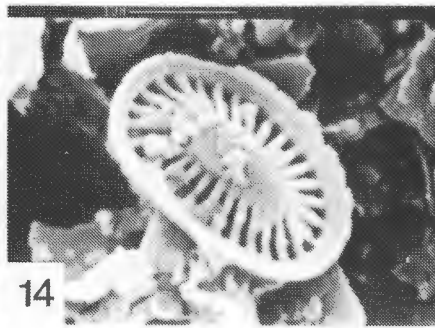
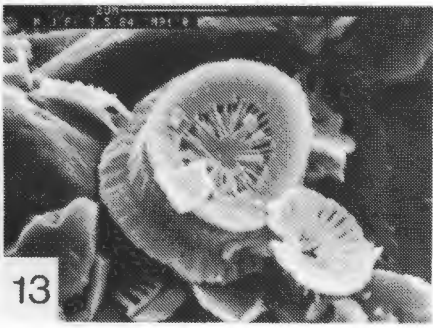
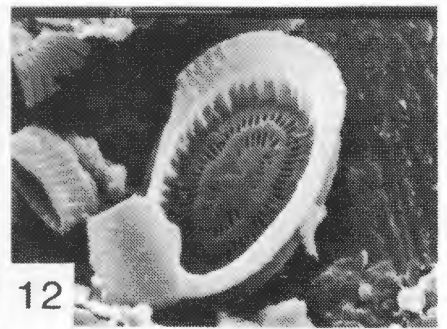
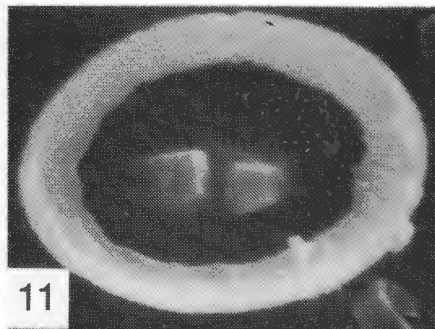
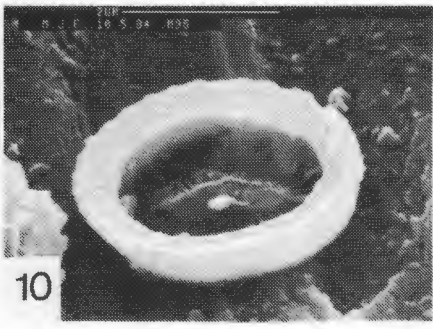
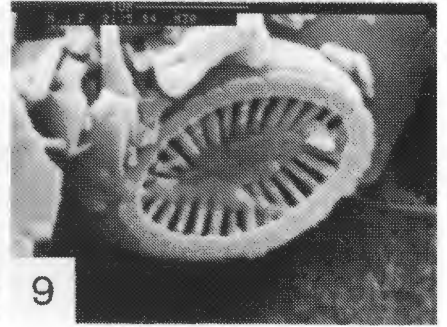
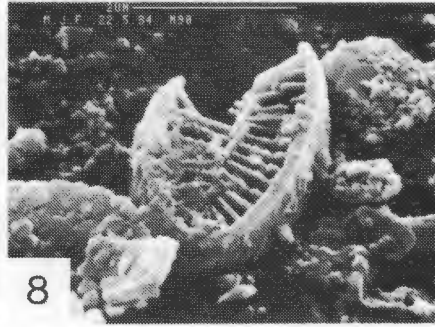
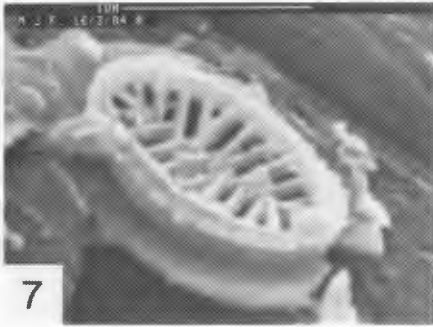
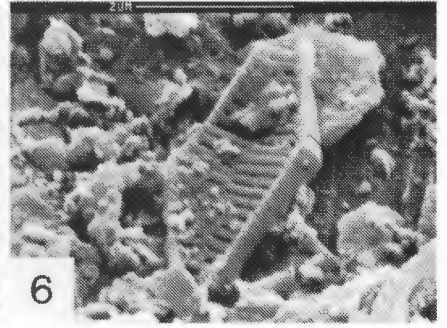
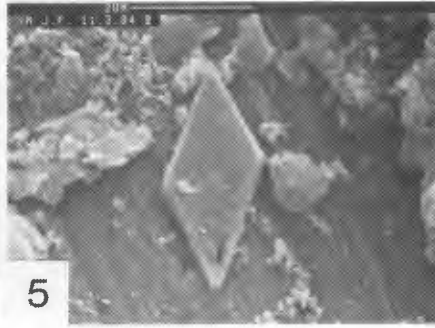
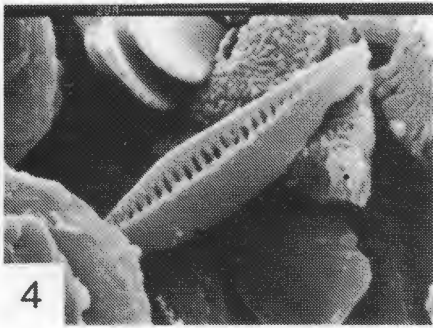
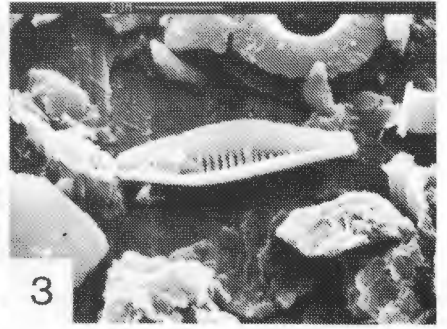
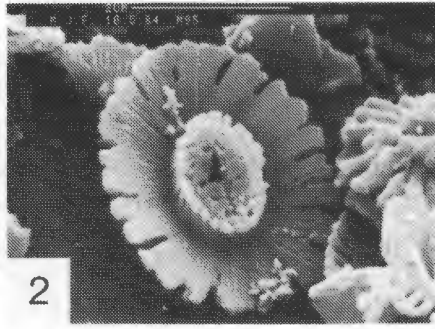


Plate V Fossil coccoliths V(1-15).

1. Proximal view of unidentified *Syracosphaera* Sp.A.
2. Distal view of *Calyptosphaera papillifera*, (the only holococcolith found in the study).
3. Proximal view of *Discoaster broweri*.
4. Proximal view of *Discoaster exilis*.
5. Distal view of *Discoaster deflanderi*.
6. Proximal view of *Discoaster siapanensis*.
7. Distal view of *Hyaster perplexus*.
8. Proximal view of *H. perplexus*.
- 9 & 10. Two views of *Thoracosphaera* cf. *T.heimii*.
- 11 & 12. Two distal views of specimens of *Dictyococcites daviesi*.
13. Distal view of *Ericsonia cava*.
14. Proximal view of *Cyclicargolithus floridanus*.
15. Unidentified coccolith Sp.B.

Plate V

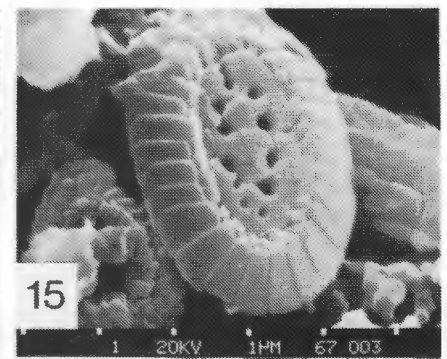
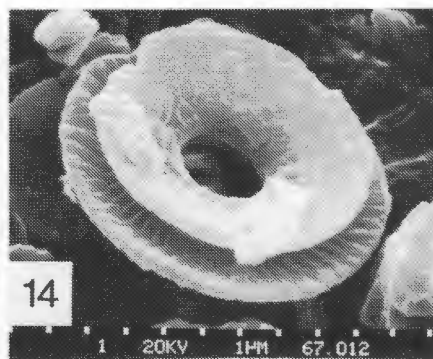
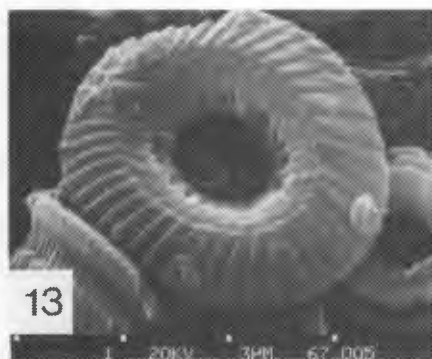
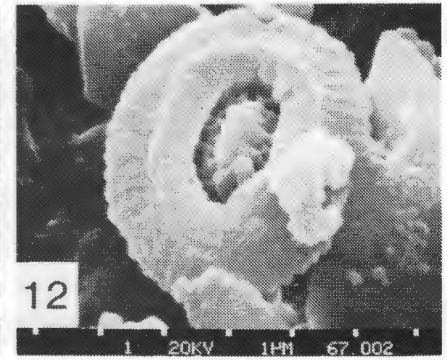
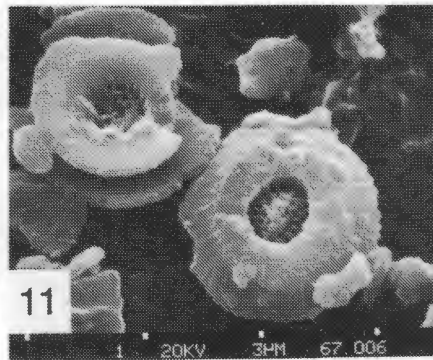
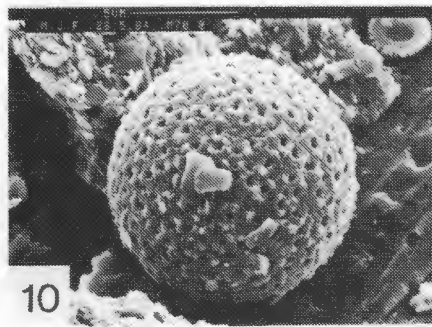
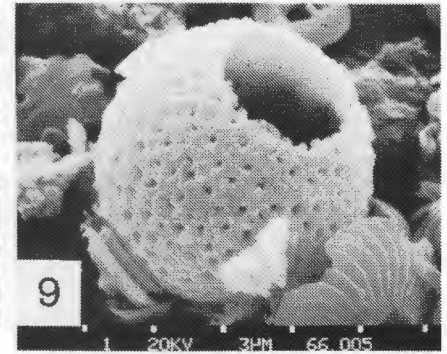
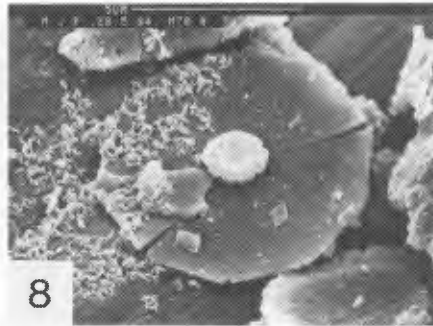
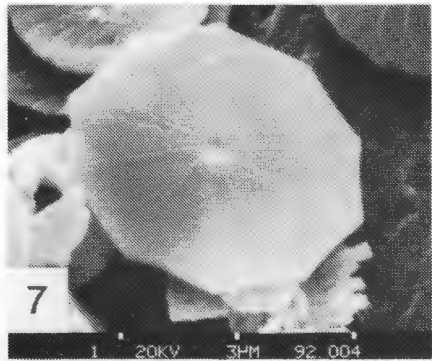
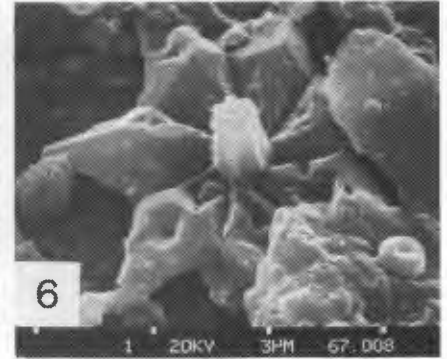
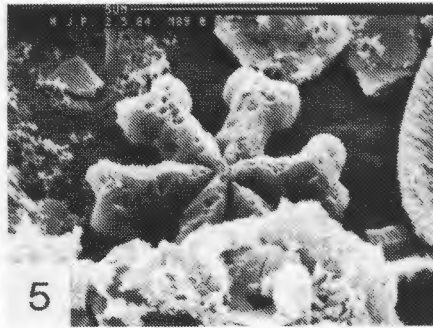
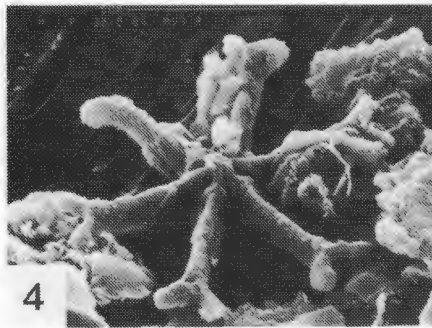
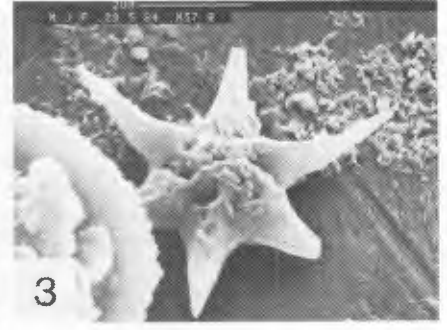
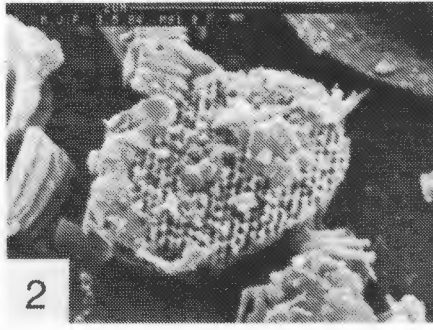
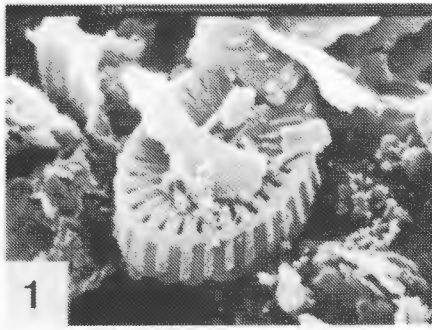


Plate VI Fossil coccoliths VI(1-15).

1. Unidentified coccolith *Sp.B.*
2. Unidentified coccolith *Sp.B.*
3. Distal view of *Chiasmolithus grandis*.
4. Distal view of *Pseudoemiliana lacunosa*.
- 4,5 & 6. Proximal views of *P. lacunosa*.
- 7 & 8. Distal views of highly dissolved *Aperlapetra gronosa* specimens.
9. Unidentified coccolith *Sp.C.*
10. Specimen of *Prediscophaera cretacea*.
11. *Cruciplacolithus Sp.D* specimen.
12. Unidentified coccolith *Sp.E.* (identification made difficult by extensive calcite overgrowth).
13. Unidentified coccolith *Sp.E.*
14. Unidentified coccolith *Sp.F.*
15. Unidentified coccolith *Sp.G.*

Plate VI

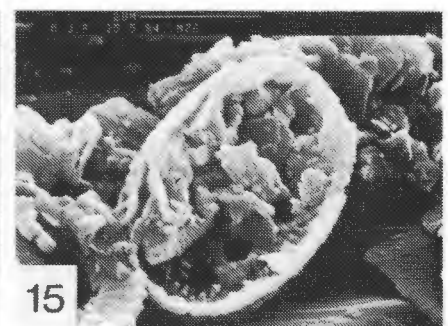
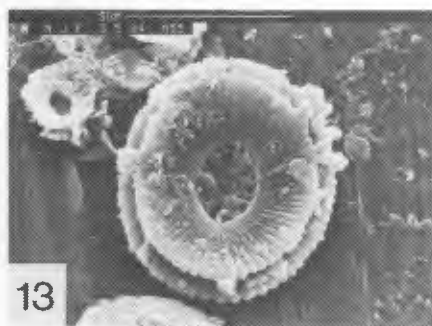
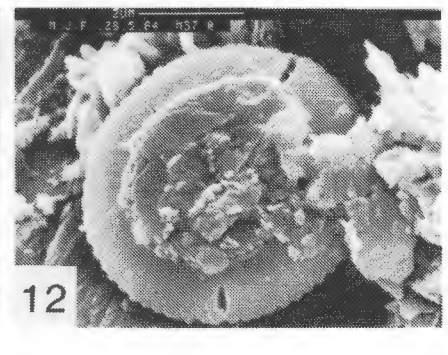
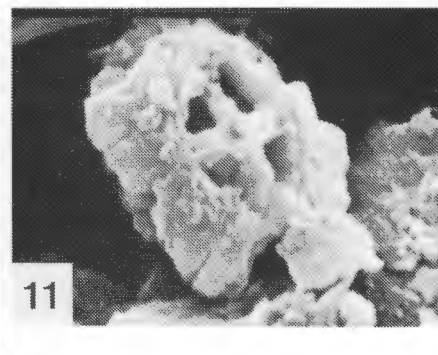
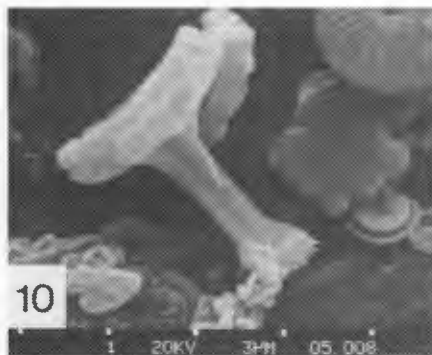
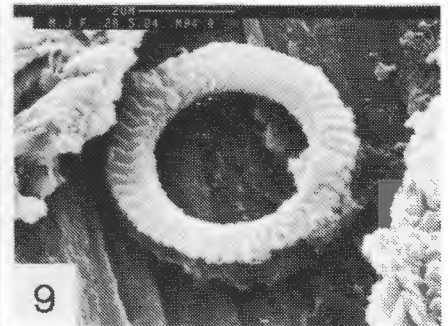
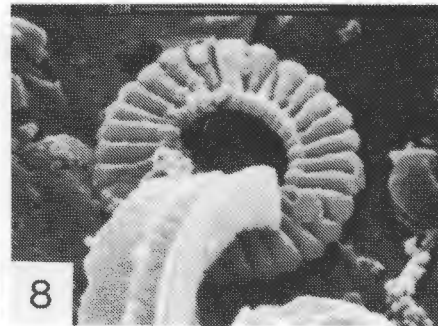
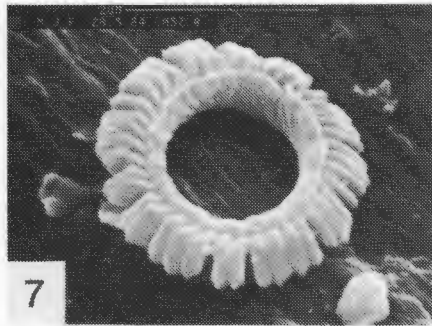
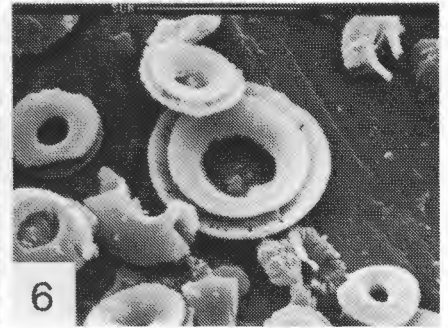
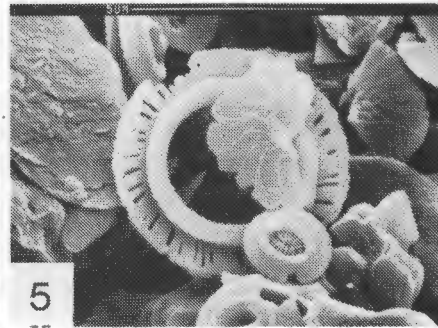
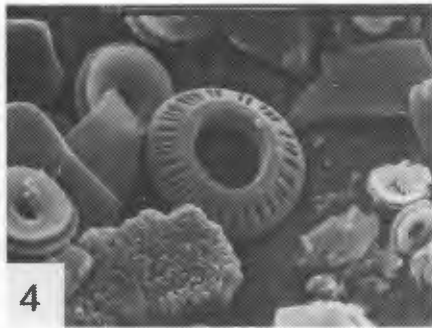
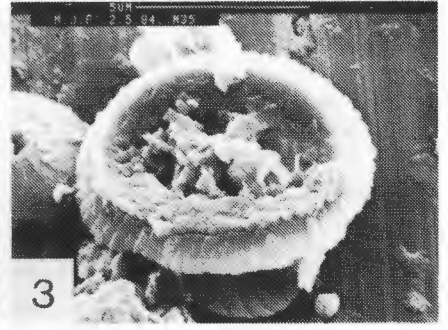
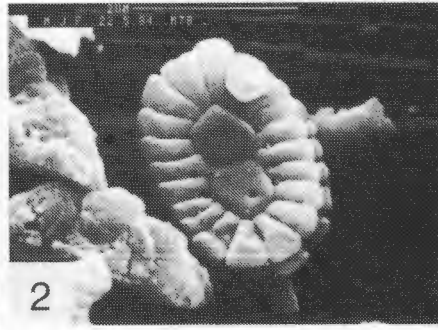
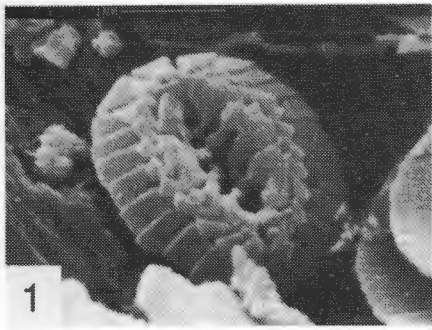
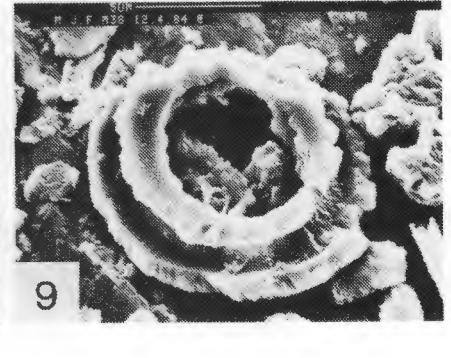
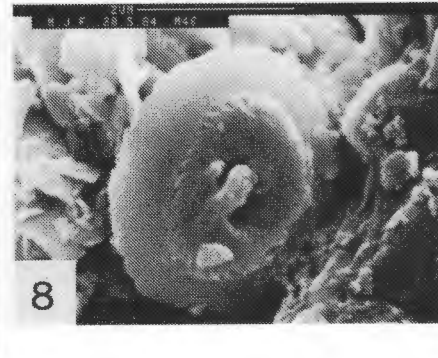
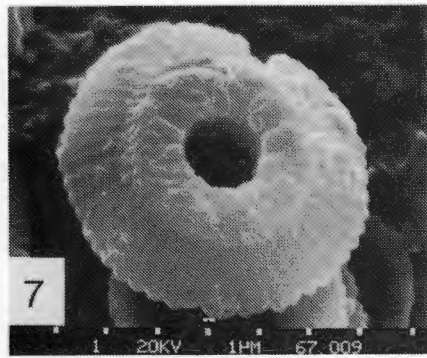
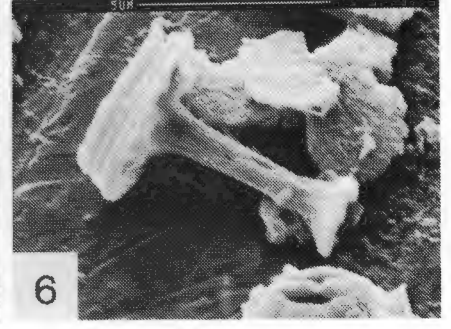
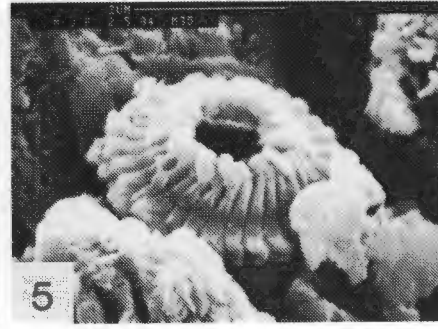
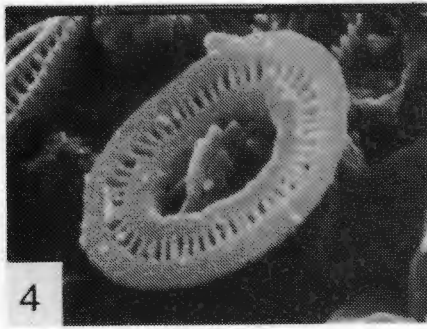
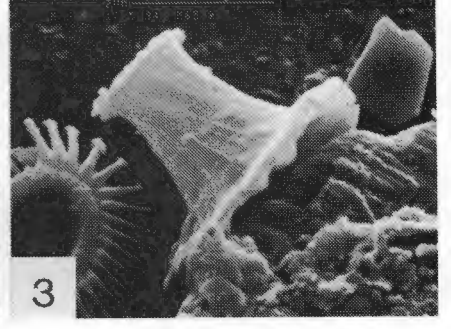
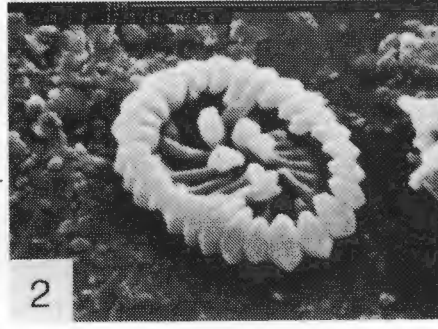
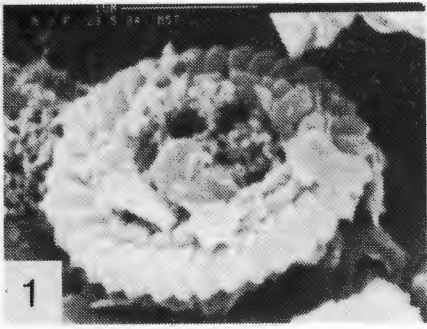


Plate VII Fossil coccoliths VII(1-9).

1. Unidentified coccolith *Sp.H.*
2. Unidentified coccolith *Sp.I.*
3. Unidentified coccolith *Sp.J.*
4. Unidentified coccolith *Sp.K.*
5. Unidentified coccolith *Sp.L.*
6. Unidentified coccolith *Sp.M.*
7. Distal view of *Cyclicargolithus floridanus*.
8. Unidentified coccolith *Sp.N.*
9. Unidentified coccolith *Sp.O.*

Plate VII



comprised less than 1% of the assemblage composition in our samples.

3.3.2 Assemblage composition

Four placolith bearing species dominated the coccolith assemblages at the sediment surface: *Gephyrocapsa oceanica*, *Emiliana huxleyi*, *Calcidiscus leptoporus* and *Umbilicosphaerashpaera sibogae* (Fig. 3.7). Each of these species contributed at least 10% to the total assemblage composition (Table 6) and together they were responsible for about 86% of the total coccolith assemblage. Four species: *Helicosphaera carteri*, *Rhabdosphaera clavigera*, *Syracosphaera pulchra*, and *Gephyrocapsa ericsoni* each comprised between one and ten percent of the assemblage composition (Table 7) and contributed, together, about seven percent to the total coccolith assemblage (Fig. 3.7). Thirty-six species (some relict), each with an average abundance of less than one percent, contributed to the remaining seven percent of the total coccolith population in the samples.

3.3.2.1 Major species

Emiliana huxleyi occurs in all but one sediment surface sample (No.13) and contributed up to 50.5% (No.87) of the coccolith assemblage. The relative abundance of *E. huxleyi* in core-tops decreases with southerly latitude (Fig. 3.8), reaching lowest values south of Port Elizabeth (sector four). High values on the Limpopo Cone and Central Terrace (sector one) are separated by a narrow band of low values lying beneath the path of the Agulhas Current, running northeast to southwest. Highest percentage occurrences are found at depths less than 3500 m.

Gephyrocapsa oceanica is present in all of the samples. Its maximum relative abundance is about 92% (sample No.74) and its mean percentage of the total population is about 35%. Highest concentrations of *G. oceanica* occur on the Limpopo Cone off Maputo (sector one), though east of this region the percentage composition decreases (Fig. 3.9). High abundances of *G. oceanica* also occur in the Agulhas Passage (sector four), while low percentages are concentrated east of Durban (sector two).

Calcidiscus leptoporus has been observed in every sample, contributing on average about 15% of the coccolith assemblage reaching a maximum of 43% (No.39). *C. leptoporus* increases in percent abundances from north to south and highest abundances are recorded at

depths below 3000 m (Fig. 3.10), in contrast to *E. huxleyi* which shows the opposite trend.

Umbilicosphaera sibogae contributes, on average, just over 10% of the total coccolith assemblage, it is present in all but one of the samples (No. 67) and has maximum abundance of 24% (No.1). Highest values are found to the north, parallel to the coast (Fig. 3.11), lying in a narrow band under the mean flow path of the Agulhas Current. Maximum values occur at depths of between 1 and 3 km.

3.3.2.2 Minor species

Helicosphaera carteri is found in all but one sample (No.67), has a maximum occurrence of about 7% (No.44), and a mean of 2.6%. Maximum abundances are found in the southern part of the study area (sectors three and four), close to the continental margin. The highest relative percentage abundances of *H. carteri* are found at depths between three and four thousand meters.

Rhabdosphaera clavigera is absent from seven of the core-top samples (Nos.4,11,13, 24,39,47 and 74), has a maximum relative abundance of about 7% (No.81), and a mean of 1.8%. High relative values are concentrated on the continental shelf off Durban and East London in sectors two and three. Highest percentages of *R. clavigera* occur between 1500 and 2500 m.

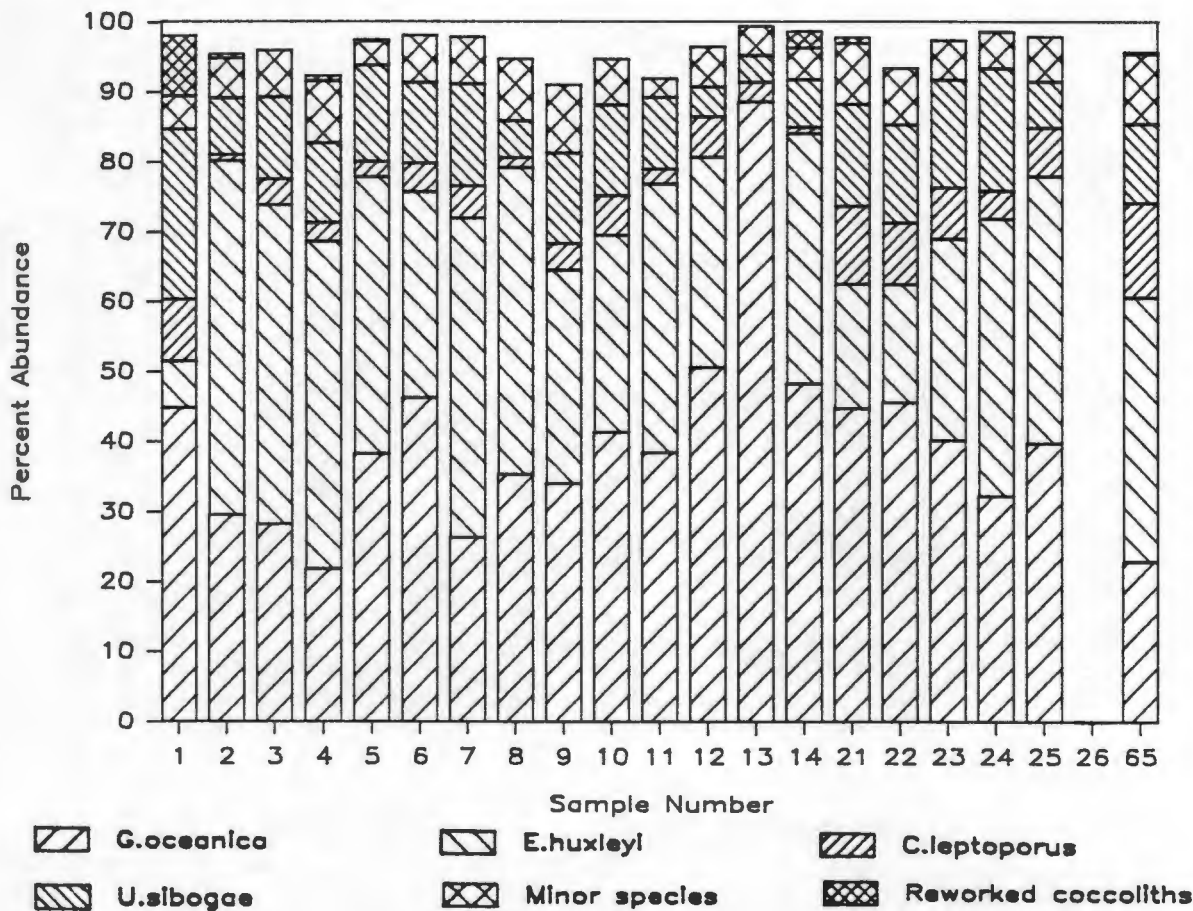
Syracosphaera pulchra is found in all but five of the core-top samples (Nos.38,39, 47,59 and 81), has a mean abundance of 1.8% and a maximum of about 6% (No.92). Highest relative percentages were found in the north of the region (sectors one and two) and is most abundant at depths less than 4000 m.

Gephyrocapsa ericsoni was absent from twenty-one of the samples (Nos.1,10,31-2, 38,47,50,54-7,65-8,71-2,76,80,82 and 92), has a maximum relative abundance of about 8% (No.36) but an average of only 1.1%. Highest abundances are concentrated in the north (sectors one and two) close to the coast, though some high values exist on the flanks of the Mozambique Ridge (sector three). Generally speaking *G. ericsoni* becomes less abundant with depth.

3.4 FORAMINIFERAL COUNTS

Samples containing high relative percent abundances of foraminiferal fragments are located in the Agulhas Passage (sector four) and in shallow water sediments east of Maputo (sector one). Fragment percentages are low

Sector 1



Sector 2

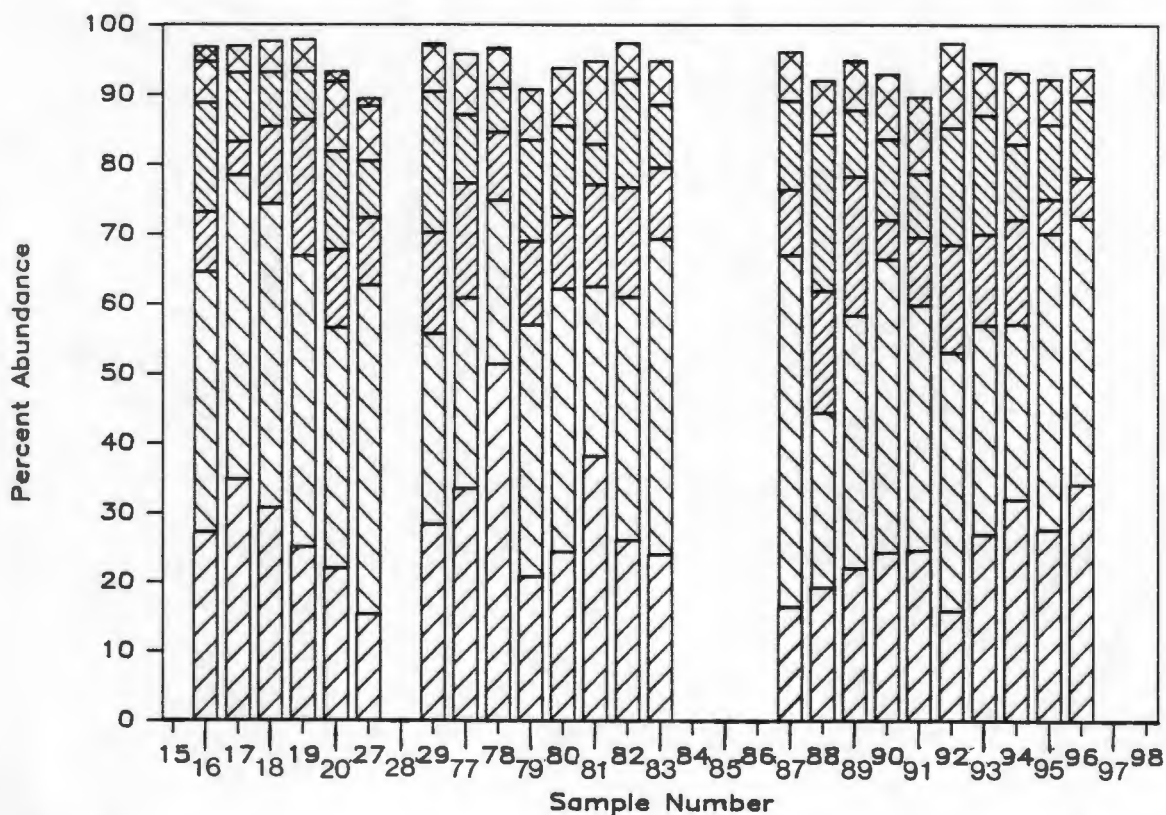


Figure 3.7 Stacked bar graphs for each sector, showing the relative abundances of the four most abundant species (*Gephyrocapsa oceanica*, *Emiliania huxleyi*, *Calcidiscus leptoporus* and *Umbilicosphaera sibogae*), and the relative proportions contributed in total by minor species and reworked/unidentified coccoliths in each sample.

Sector 3

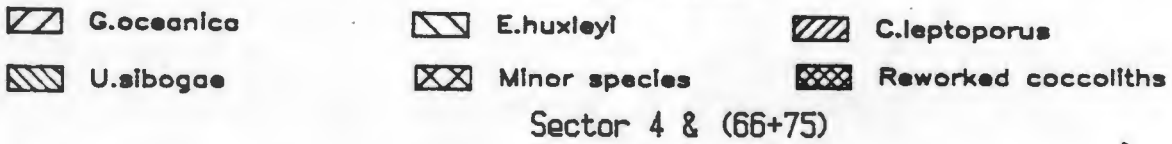
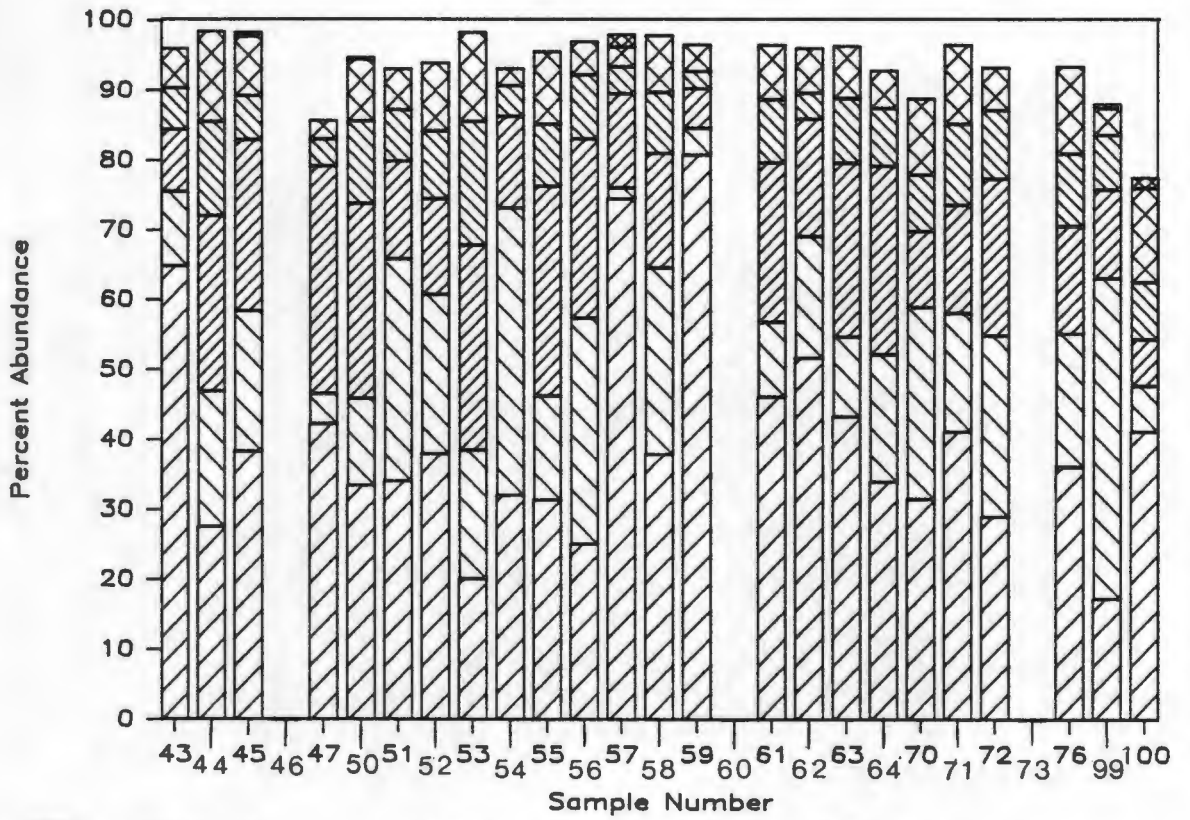


Figure 3.7 Stacked bar graphs for each sector, showing the relative abundances of the four most abundant species (*Gephyrocapsa oceanica*, *Emiliana huxleyi*, *Calcidiscus leptopus* and *Umbilicosphaera sibogae*), and the relative proportions contributed in total by minor species and reworked/unidentified coccoliths in each sample.

TABLE 6.

Sample Number
Gephyrocapsa oceanica
Emiliania huxleyi
Calcidiscus leptoporus
Umbilicosphaera sibogae

1 44.9 6.7 8.8 24.3
2 29.6 50.6 0.9 8.1
3 28.3 45.6 3.7 11.7
4 21.9 46.8 2.7 11.4
5 38.3 39.6 2.2 13.7
6 46.3 29.5 4.1 11.5
7 26.4 45.7 4.6 14.5
8 35.4 43.9 1.4 5.3
9 34.1 30.5 3.8 12.9
10 41.4 28.2 5.7 12.9
11 38.5 38.5 2.1 10.2
12 50.6 30.1 4.2 4.2
13 88.6 0.0 2.8 3.8
14 48.3 35.8 0.9 6.8
15 NA NA NA NA
16 27.3 37.3 8.6 15.6
17 34.9 43.6 4.8 9.9
18 30.8 43.6 11.0 7.8
19 25.2 41.7 19.5 6.9
20 22.0 34.6 11.1 14.1
21 44.8 17.8 11.2 14.5
22 45.6 16.9 8.8 14.0
23 40.2 28.8 7.3 15.4
24 32.3 39.6 4.0 17.5
25 79.6 NA 6.9 6.6
26 NA NA NA NA
27 15.4 47.3 9.7 8.1
28 NA NA NA NA
29 28.5 27.3 14.5 20.1
30 29.1 44.4 4.7 7.1
31 35.5 9.7 42.1 5.9
32 28.6 26.4 17.7 12.1
33 45.1 16.4 15.5 14.8
34 36.9 5.5 40.0 6.5
35 35.9 14.2 31.1 9.4
36 46.6 7.4 11.0 15.1
37 NA NA NA NA
38 39.8 4.6 25.9 12.1
39 39.2 6.5 43.2 0.0
40 37.9 8.1 30.1 11.1
41 NA NA NA NA
42 36.0 2.1 35.0 6.6
43 64.9 10.7 8.9 5.9
44 27.6 19.4 25.1 13.4
45 38.3 20.1 24.5 6.3
46 NA NA NA NA
47 42.3 4.3 32.6 3.8
48 50.0 0.0 16.5 20.1
49 41.5 16.2 23.6 8.1
50 33.5 12.4 27.9 11.8

TABLE 6. (cont.)

Sample Number
Gephyrocapsa oceanica
Emiliania huxleyi
Calcidiscus leptoporus
Umbilicosphaera sibogae

51 34.1 31.8 14.0 7.3
52 38.0 22.8 13.7 9.7
53 20.1 18.4 29.3 17.7
54 32.1 41.1 13.1 4.4
55 31.4 14.9 30.0 8.9
56 25.1 32.3 25.7 9.1
57 74.5 1.6 13.5 3.8
58 37.9 26.7 16.4 8.7
59 80.8 3.8 5.6 2.5
60 NA NA NA NA
61 46.2 10.7 22.8 9.0
62 51.7 17.4 16.8 3.7
63 43.3 11.4 24.9 9.2
64 34.0 18.2 27.0 8.2
65 23.0 37.7 13.5 11.3
66 27.5 16.2 30.8 11.7
67 1.9 8.9 0.2 0.0
68 25.4 19.2 34.9 7.0
69 52.7 7.8 15.6 8.4
70 31.5 27.4 10.9 8.1
71 41.2 16.9 15.5 11.6
72 29.0 25.9 22.5 9.8
73 NA NA NA NA
74 91.6 0.9 1.2 1.5
75 31.0 11.2 40.6 8.2
76 36.2 19.0 15.4 10.4
77 33.6 27.3 16.4 9.8
78 51.4 23.5 9.7 6.3
79 20.9 36.2 11.9 14.5
80 24.5 37.7 10.4 12.9
81 38.2 24.3 14.6 5.8
82 26.2 34.9 15.7 15.4
83 24.1 45.2 10.2 9.0
84 NA NA NA NA
85 NA NA NA NA
86 NA NA NA NA
87 16.5 50.5 9.4 12.7
88 19.3 25.1 17.5 22.3
89 22.1 36.3 19.9 9.5
90 24.4 42.0 5.7 11.5
91 24.7 35.1 9.7 9.1
92 15.9 37.2 15.4 16.7
93 27.0 30.0 13.0 17.0
94 32.0 25.1 15.0 10.8
95 27.7 42.5 4.9 10.6
96 34.2 38.1 5.8 11.1
97 NA NA NA NA
98 NA NA NA NA
99 17.3 45.8 12.7 7.8
100 41.2 6.6 6.6 8.2

Table 6. Relative percent abundances of the four most abundant coccolith species occurring in the study area (*Gephyrocapsa oceanica*, *Emiliania huxleyi*, *Calcidiscus leptoporus* and *Umbilicosphaera sibogae*). Species are ranked in order of decreasing mean percent abundance and fall in the range 10-100%. NA indicates samples for which no data was available.

TABLE 7.		TABLE 7. (cont)							
Sample Number	<i>Helicosphaera carteri</i>	<i>Rhabdosphaera clavigera</i>	<i>Syracosphaera pulchra</i>	<i>Gephyrocapsa ericsoni</i>	Sample Number	<i>Helicosphaera carteri</i>	<i>Rhabdosphaera clavigera</i>	<i>Syracosphaera pulchra</i>	<i>Gephyrocapsa ericsoni</i>
1	2.5	1.7	0.6	0.0	51	1.9	2.5	1.2	0.3
2	0.9	0.9	1.2	2.7	52	4.6	2.1	2.4	0.6
3	1.5	1.5	2.5	1.2	53	6.8	4.1	0.9	0.9
4	0.8	0.0	4.0	4.0	54	0.3	1.9	0.3	0.0
5	0.6	0.3	1.3	1.3	55	4.1	4.1	2.2	0.0
6	1.7	0.6	2.4	2.1	56	0.3	2.2	2.3	0.0
7	1.3	0.3	1.6	3.6	57	2.2	0.3	0.3	0.0
8	1.1	1.1	2.0	4.7	58	1.3	1.0	1.6	4.2
9	2.9	1.5	3.8	1.5	59	1.9	0.3	0.0	1.6
10	3.0	3.0	0.6	0.0	60	NA	NA	NA	NA
11	1.8	0.0	0.6	0.3	61	3.4	1.4	0.8	2.2
12	3.4	0.3	0.6	1.5	62	3.7	0.6	0.6	1.5
13	0.6	0.0	0.6	3.0	63	3.3	2.4	1.5	0.3
14	0.6	0.3	1.5	2.1	64	2.1	1.5	0.3	1.5
15	NA	NA	NA	NA	65	3.4	2.5	4.1	0.0
16	0.6	1.6	0.9	2.8	66	3.8	2.8	3.1	0.0
17	1.2	0.6	1.5	0.6	67	0.0	1.7	2.6	0.0
18	1.5	1.2	1.5	0.3	68	3.2	1.7	1.7	0.0
19	2.2	0.9	1.2	0.3	69	4.9	2.3	1.7	0.3
20	1.6	0.9	5.0	2.5	70	3.7	4.9	2.0	0.3
21	2.1	3.0	3.0	0.6	71	5.1	3.4	2.8	0.0
22	1.4	0.6	4.4	1.7	72	1.5	1.8	2.8	0.0
23	2.0	0.8	2.3	0.6	73	NA	NA	NA	NA
24	2.2	0.0	2.5	0.6	74	1.5	0.0	0.9	1.2
25	1.9	1.2	0.9	2.5	75	5.4	2.2	0.8	0.3
26	NA	NA	NA	NA	76	2.1	7.4	2.9	0.0
27	0.9	2.2	4.4	0.3	77	2.7	3.7	0.9	1.4
28	NA	NA	NA	NA	78	2.5	2.2	0.3	0.6
29	3.5	0.9	1.7	0.6	79	0.9	3.5	2.6	0.3
30	0.6	2.0	2.6	0.9	80	3.1	2.4	2.8	0.0
31	4.7	0.6	0.6	0.0	81	3.6	7.1	0.0	1.2
32	2.2	1.9	4.3	0.0	82	1.6	1.2	2.5	0.0
33	2.8	1.6	0.3	3.2	83	2.4	1.8	1.5	0.6
34	4.6	3.4	0.3	0.6	84	NA	NA	NA	NA
35	2.8	2.6	1.4	1.4	85	NA	NA	NA	NA
36	3.8	0.5	0.8	8.5	86	NA	NA	NA	NA
37	NA	NA	NA	NA	87	1.9	1.6	2.8	0.7
38	1.3	1.0	0.0	0.0	88	1.2	1.2	4.5	0.9
39	3.7	0.0	0.0	0.3	89	2.5	2.2	0.6	0.6
40	4.2	2.7	1.8	0.3	90	2.7	1.8	3.3	1.5
41	NA	NA	NA	NA	91	1.6	3.8	4.7	0.9
42	5.7	0.6	0.3	0.3	92	3.8	2.5	5.9	0.0
43	2.4	1.5	0.6	1.2	93	1.9	2.2	2.9	0.3
44	7.4	2.8	1.2	1.5	94	1.8	4.8	3.3	0.3
45	6.3	1.3	0.6	0.3	95	0.9	2.1	1.2	2.4
46	NA	NA	NA	NA	96	1.3	0.6	1.3	1.3
47	2.7	0.0	0.0	0.0	97	NA	NA	NA	NA
48	3.2	0.4	0.4	1.4	98	NA	NA	NA	NA
49	3.2	2.9	0.6	0.3	99	0.3	1.6	1.6	0.3
50	4.6	2.1	2.1	0.0	100	1.6	1.6	4.1	6.2

Table 7. Relative percent abundances of the four species of coccolith occurring with mean percent abundances in the range 1-10% (*Helicosphaera carteri*, *Rhabdosphaera clavigera*, *Syracosphaera pulchra* and *Gephyrocapsa ericsoni*). They are ranked in order of decreasing abundance. NA indicates samples for which no data was available.

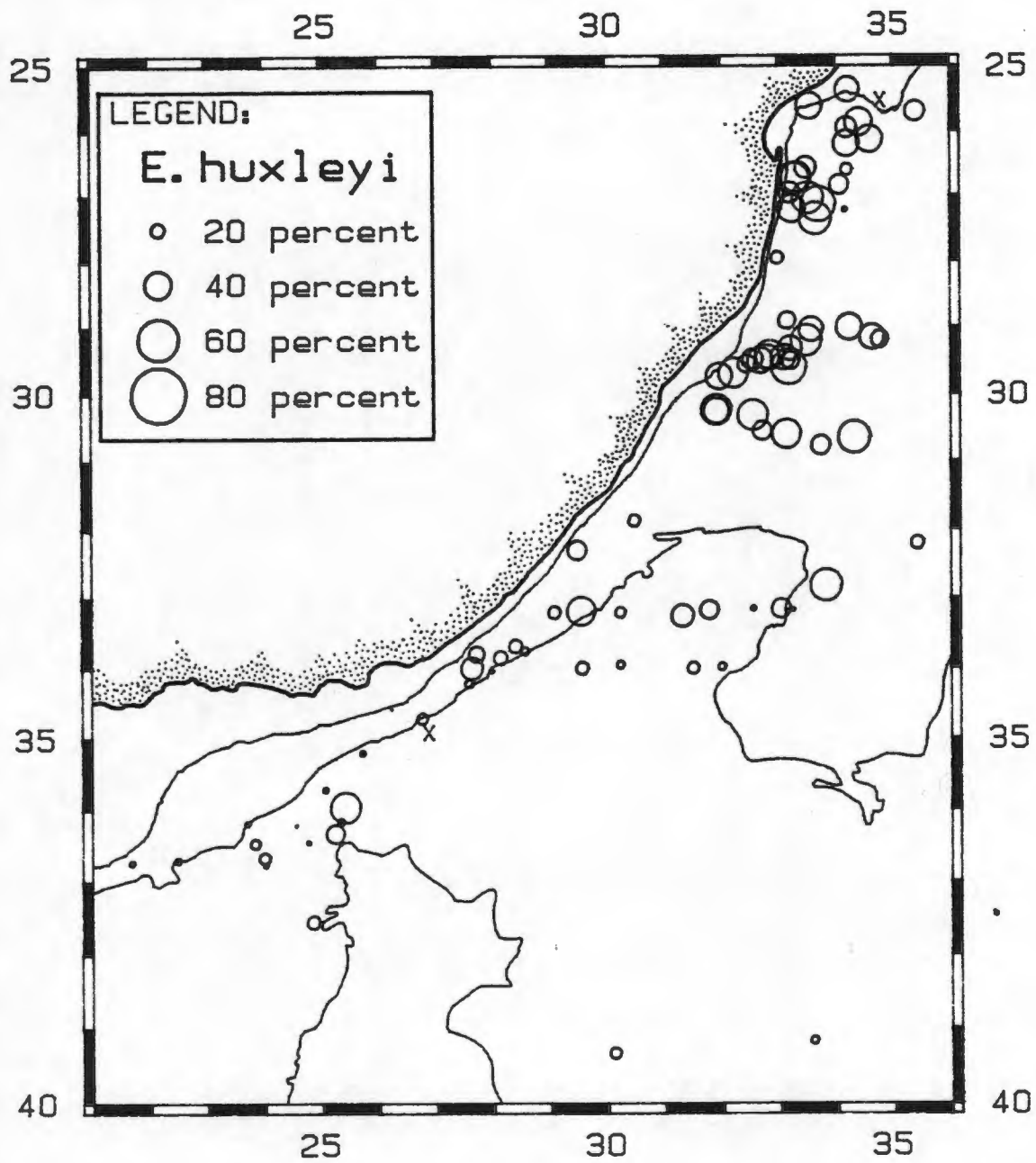


Figure 3.8 Percent of *Emiliana huxleyi* among identified coccoliths in sample.

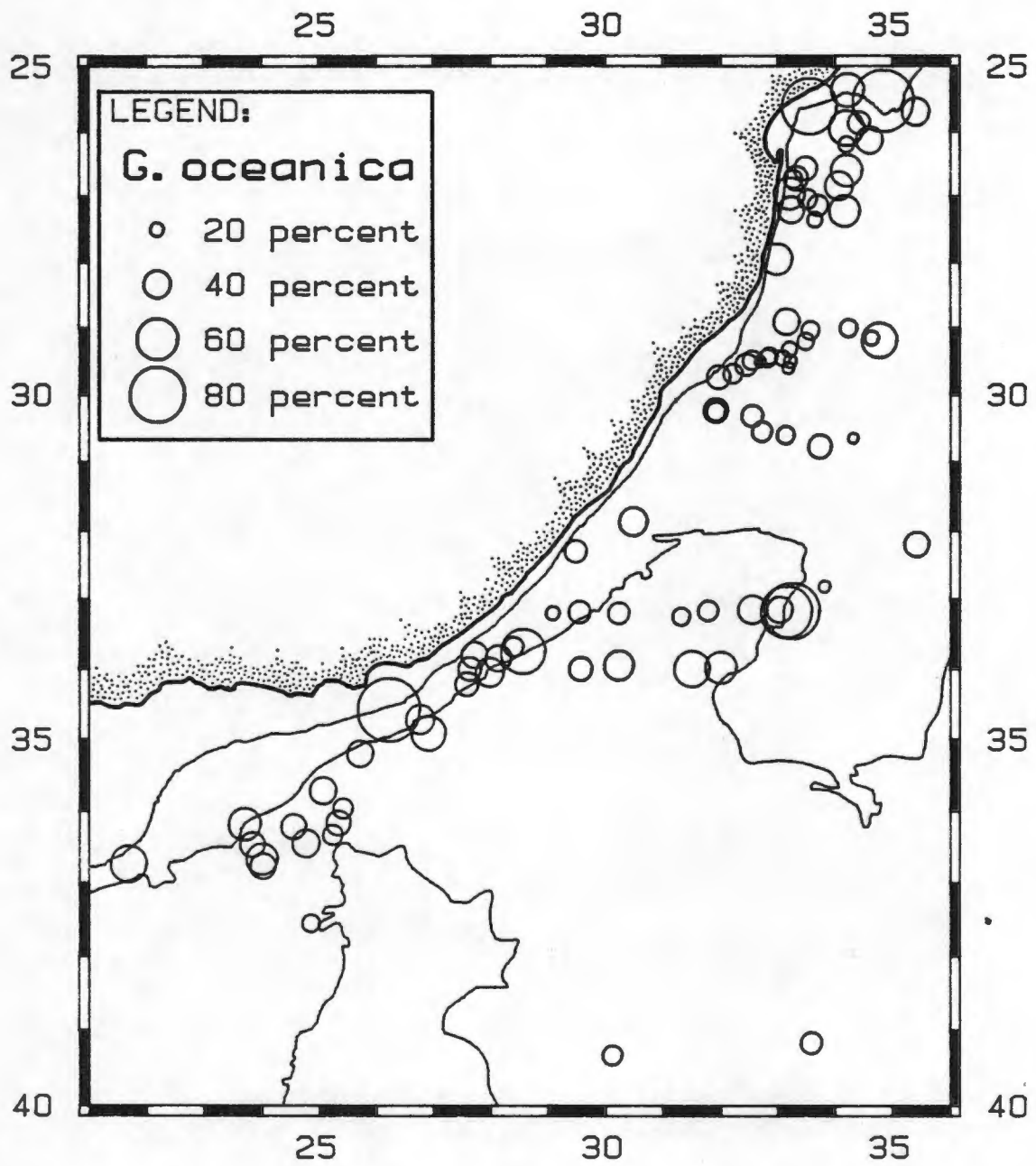


Figure 3.9 Percent of *Gephyrocapsa oceanica* among identified coccoliths in sample.

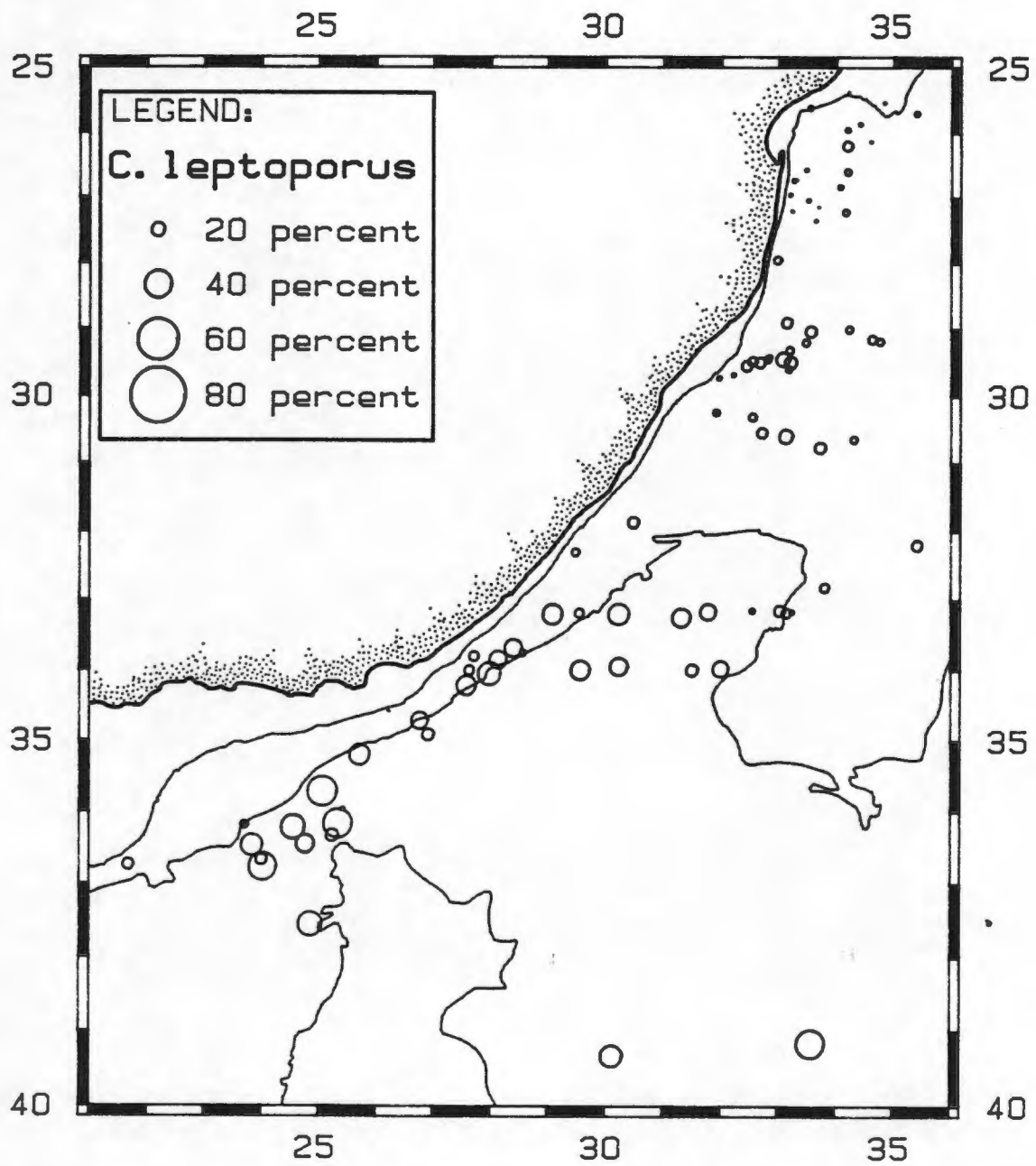


Figure 3.10 Percent of *Calcidiscus leptoporus* among identified coccoliths in sample.

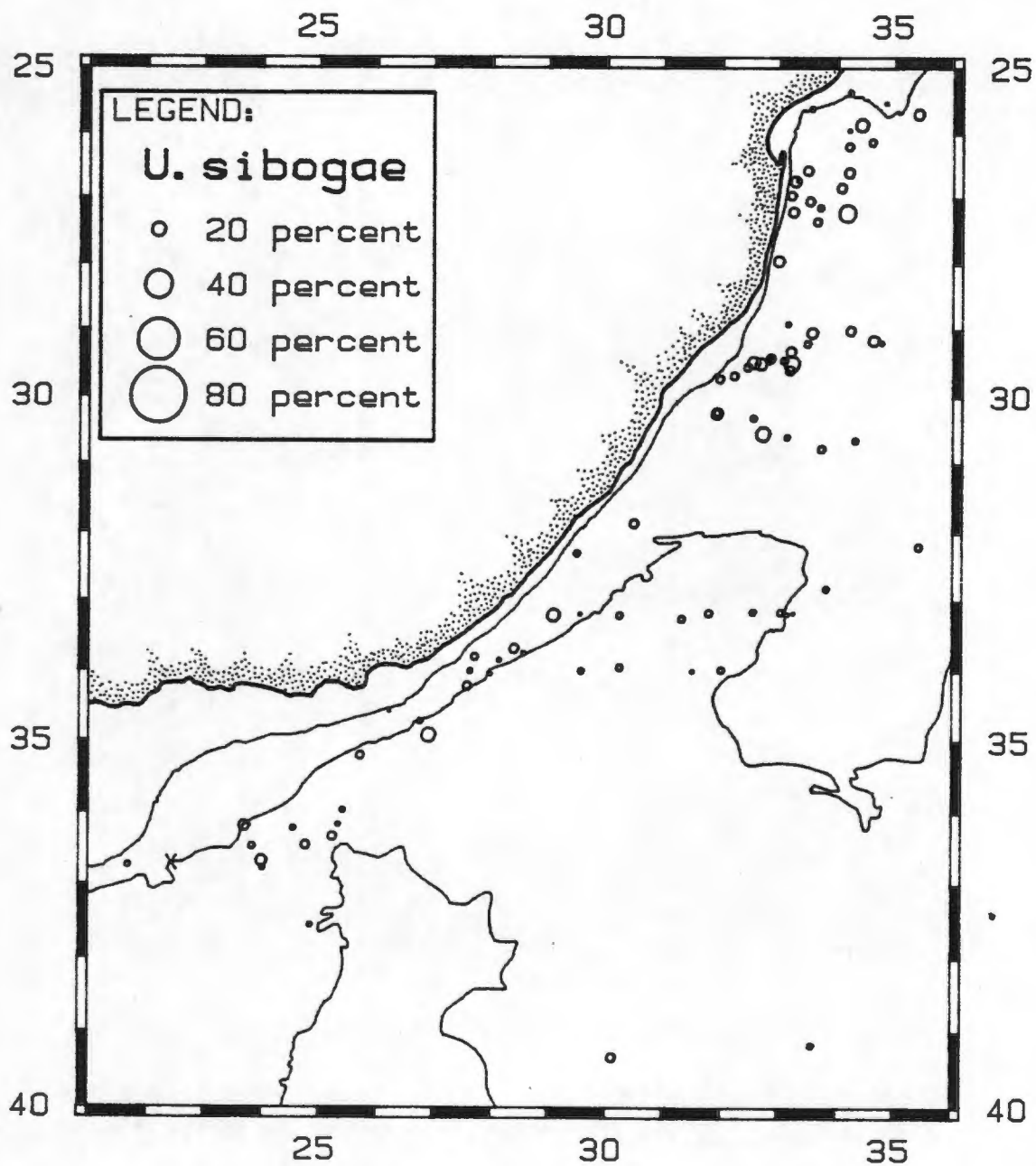


Figure 3.11 Percent of *Umbilicosphaera sibogae* among identified coccoliths in sample.

off Durban and East London (sectors two and three) and decrease with distance from the coast (Fig. 3.12). Relative percent abundances of foraminiferal fragments decrease with depth (Figure 3.13). Lowest values occur between two and four km. However, a sharp increase in fragments occurs at about 3650 m.

3.5 OXYGEN ISOTOPE ANALYSIS

Specimens of *Globigerinoides sacculifer* were rare or absent from samples taken from depths greater than four thousand meters. These samples were mostly located in the Agulhas Passage and could not be considered for isotopic analysis (Fig. 3.14).

Isotope ratios and derived temperatures are presented in Table 8, and plotted geographically in Fig. 3.15. Ninety percent of the samples had isotope ratios in the range -1.5 and 0.0 per mil. Eight of the eighty-two samples run have isotope values that fall outside of this range. These eight samples were found at depths in excess of 3500 m or in unstable areas, such as in the paths of mass gravity flows.

Derived temperature values ranged from 18.5° to 25.1°C. This range of values is close to surface-water temperatures in the Agulhas Current region (Wyrski, 1971). Warmest isotopic temperatures lie in a narrow band located parallel and close to the coast and temperatures decrease with distance from coast and towards the south.

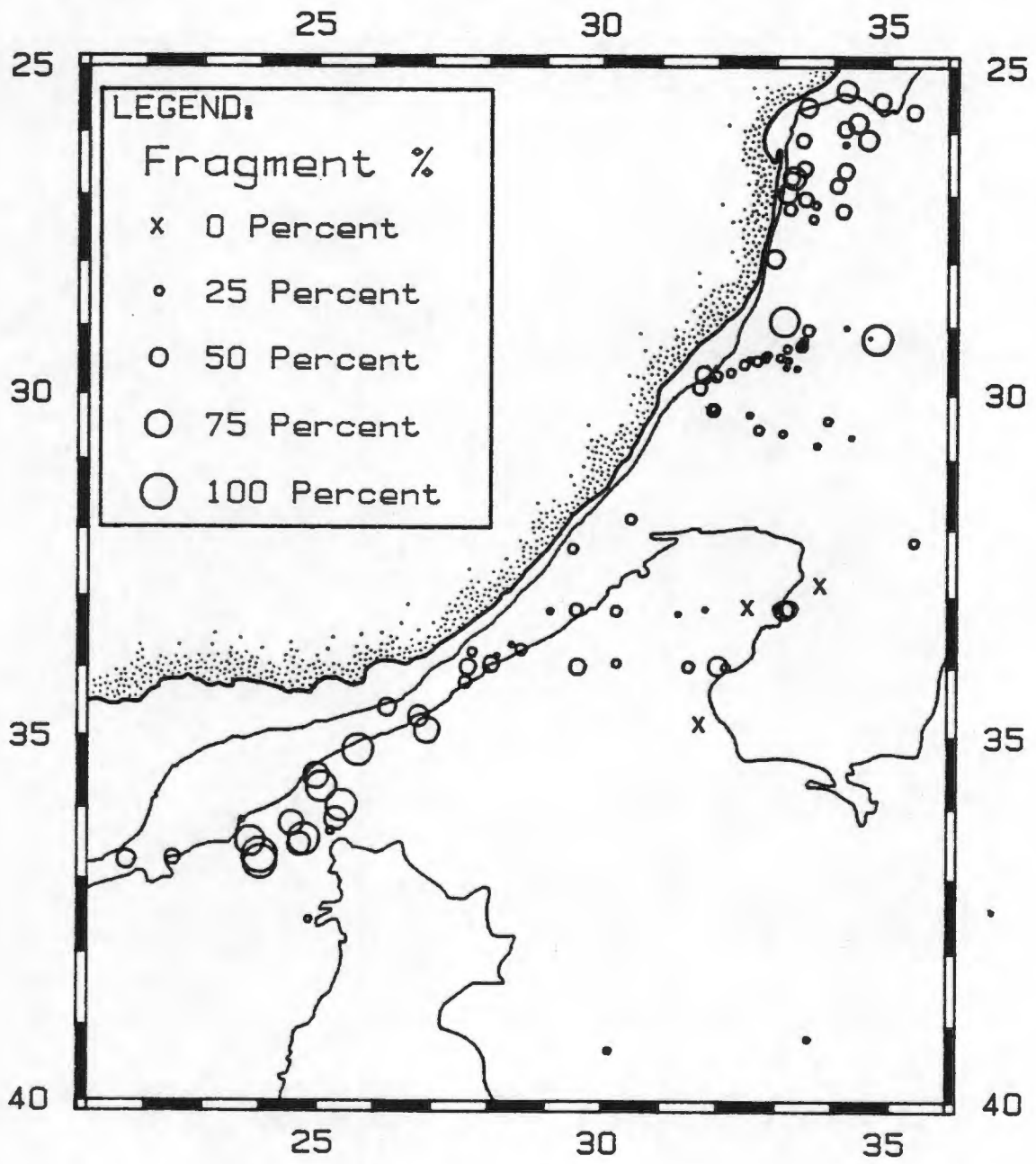


Figure 3.12 Percent foraminiferal fragments from the greater than 150 micron size fraction.

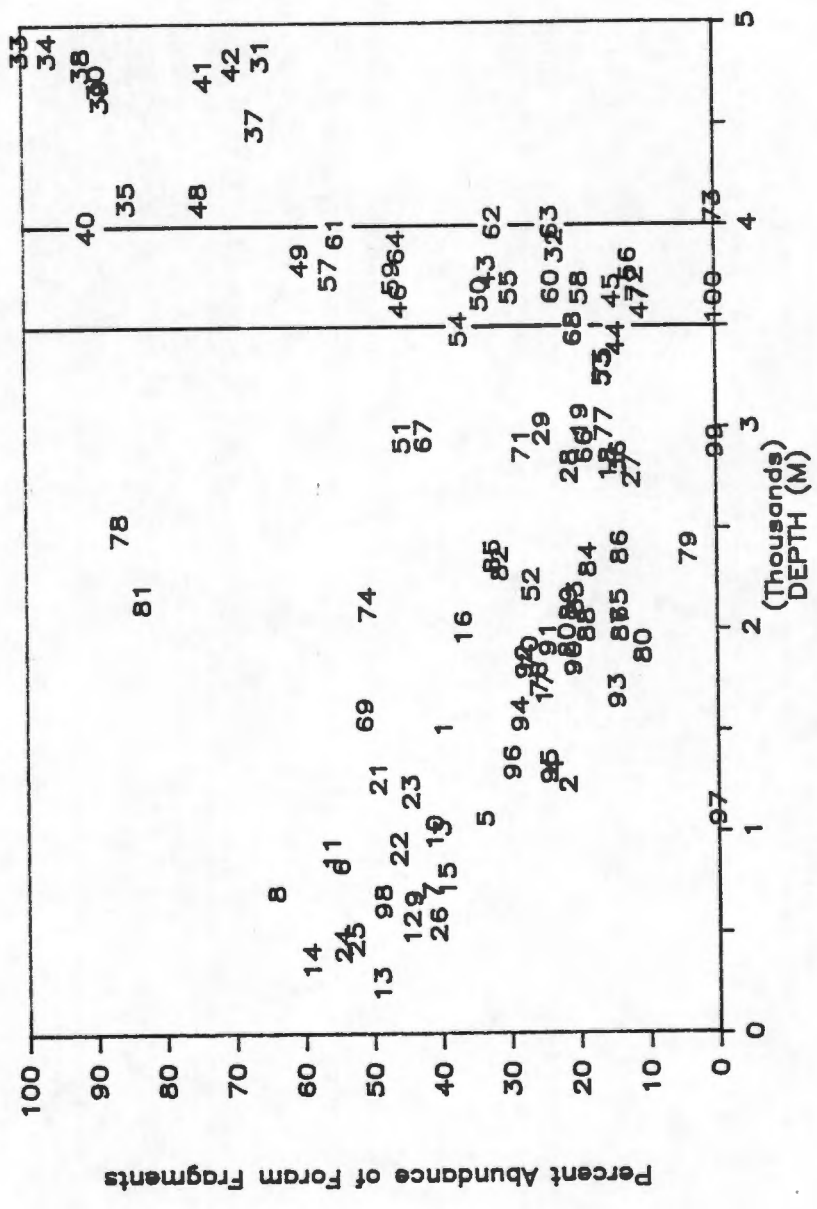


Figure 3.13 Plot of depth vs. percent foraminiferal fragments. Points are marked by sample numbers.

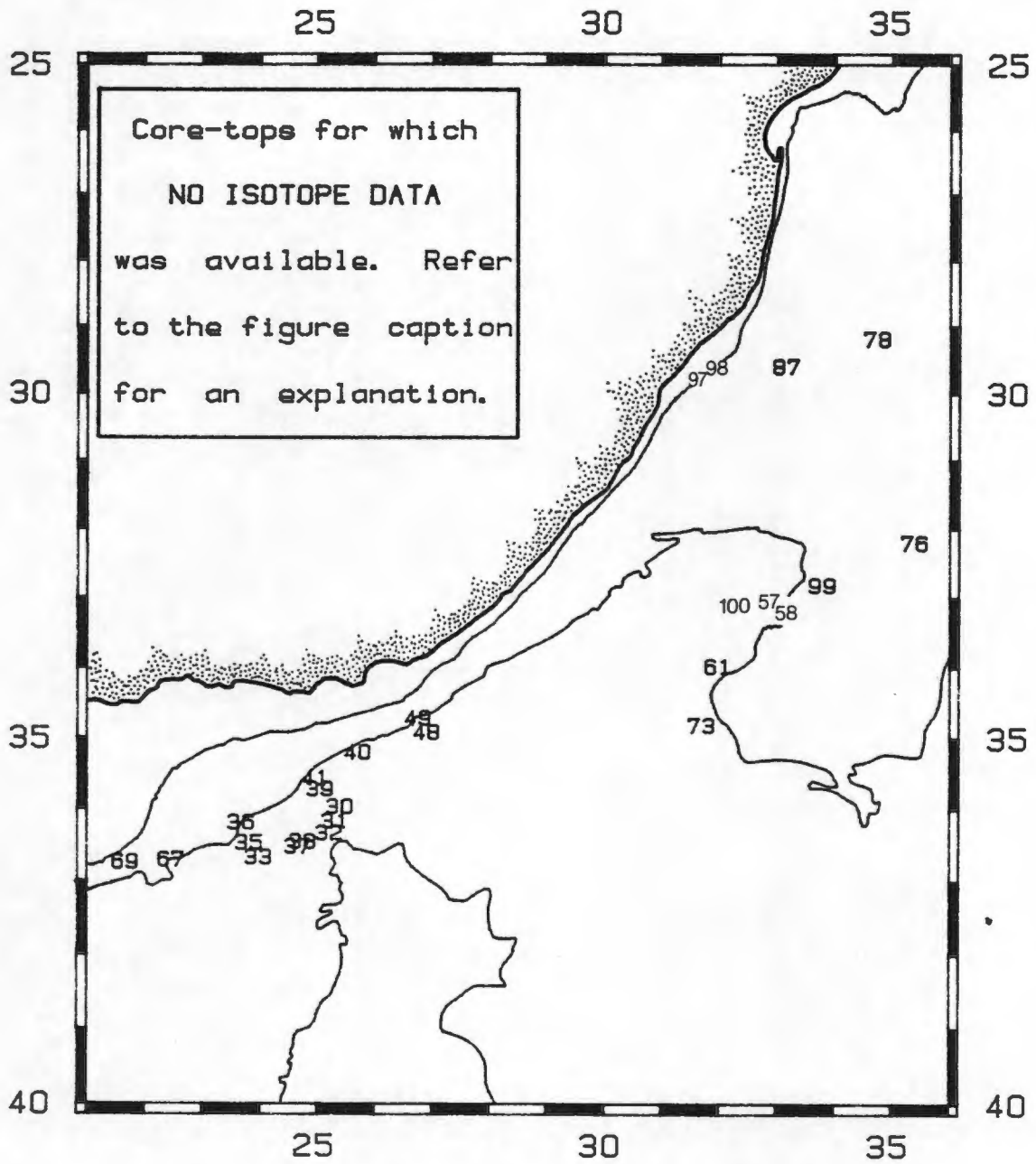


Figure 3.14 Cores-tops for which no isotope data was available (30-1,35,37-41,48-9,67,69,73,78 and 97-100) or were outside the glacial-interglacial range (Nos. 32,36,57,58,61,76 and 87) are marked by sample numbers.

TABLE 8.						TABLE 8. (cont.)					
Sample Number	Fragment Percent	CaCO ₃ Percent	Oxygen 18 PDB	Derived Temp.		Sample Number	Fragment Percent	CaCO ₃ Percent	Oxygen 18 PDB	Derived Temp.	
1	39.6	36.5	-0.694	21.4		51	45.3	22.4	-0.119	18.8	
2	21.5	39.7	-1.127	23.4		52	26.7	37.0	-0.223	19.2	
3	39.9	54.9	-0.882	22.2		53	16.2	41.6	-1.285	24.1	
4	23.5	59.9	-1.246	23.9		54	36.9	43.8	-0.157	18.9	
5	33.6	35.9	-0.645	21.1		55	29.5	48.8	-1.228	23.8	
6	54.6	61.8	-0.521	20.6		56	54.6	51.9	-0.379	19.9	
7	41.5	52.8	-1.060	23.0		57	55.8	54.7	0.094	17.8	
8	64.0	43.9	-1.089	23.2		58	19.3	82.2	0.338	16.7	
9	44.1	44.5	-1.085	23.2		59	46.6	55.4	-0.257	19.4	
10	41.0	39.7	-1.205	23.7		60	12.4	59.4	-0.333	19.7	
11	56.0	32.4	-1.193	23.7		61	54.7	76.7	0.095	17.8	
12	44.3	59.4	-0.647	21.1		62	31.8	63.4	-0.152	18.9	
13	48.7	37.0	-1.489	25.1		63	23.5	37.0	-0.503	20.5	
14	59.0	42.5	-0.668	21.2		64	45.8	36.9	-0.542	23.5	
15	39.2	18.5	-1.334	24.3		65	14.0	68.7	-0.542	20.7	
16	36.6	32.6	-1.006	22.8		66	18.8	54.3	-0.816	21.9	
17	24.9	11.8	-1.072	23.1		67	42.2	30.9	NA	18.2	
18	15.4	39.2	-1.014	22.8		68	20.3	73.0	-0.310	19.6	
19	19.5	78.8	-0.665	21.2		69	51.0	53.7	NA	18.2	
20	21.6	62.3	-1.125	23.3		70	27.0	41.0	-0.249	19.3	
21	49.1	43.6	-1.110	23.3		71	28.0	32.1	-0.975	22.6	
22	46.2	34.5	-1.429	24.8		72	11.3	58.9	-0.621	21.0	
23	44.4	46.4	-1.196	23.7		73	NA	NA	NA	18.2	
24	54.4	44.6	-0.514	20.5		74	50.5	35.9	-0.594	20.9	
25	52.6	60.5	-0.726	20.5		75	16.0	82.7	-0.055	18.5	
26	40.5	NA	-0.425	20.1		76	25.6	75.3	0.584	15.7	
27	12.0	76.6	-0.693	21.3		77	16.0	63.1	-0.209	19.2	
28	21.0	53.7	-0.503	20.5		78	86.3	66.6	NA	18.2	
29	25.0	46.9	-0.831	22.0		79	4.0	85.7	-0.664	21.2	
30	89.0	32.2	NA	18.2		80	10.7	71.7	-0.924	22.4	
31	65.2	21.3	NA	18.2		81	83.1	53.8	-1.045	23.0	
32	22.8	50.5	0.533	15.9		82	31.2	44.3	-0.762	21.7	
33	100.0	13.2	NA	18.2		83	20.3	53.4	-1.312	24.2	
34	96.0	33.2	-1.064	23.1		84	18.4	46.2	-1.065	23.1	
35	84.8	34.2	NA	18.2		85	32.3	47.4	-0.888	22.2	
36	14.0	63.1	0.522	15.9		86	13.9	69.7	-0.325	19.7	
37	66.2	32.3	NA	18.2		87	13.9	71.4	-1.648	25.8	
38	91.2	15.9	NA	18.2		88	18.7	82.2	-0.606	21.0	
39	88.4	28.6	NA	18.2		89	21.3	38.9	-1.322	24.3	
40	90.7	30.5	NA	18.2		90	20.7	60.3	-1.343	24.4	
41	73.5	33.0	NA	18.2		91	24.3	57.5	-1.093	23.2	
42	69.4	41.2	-0.243	19.3		92	27.8	59.2	-1.447	24.9	
43	32.7	52.6	-0.879	22.2		93	14.4	57.8	-1.135	23.4	
44	14.1	42.5	-0.734	21.5		94	28.4	69.2	-0.898	22.3	
45	14.6	NA	-1.334	24.3		95	24.2	46.5	-0.817	21.9	
46	45.5	54.4	-0.640	21.1		96	29.6	24.1	-1.025	22.9	
47	10.7	36.2	-0.721	21.5		97	NA	NA	NA	18.2	
48	74.4	26.3	NA	18.2		98	48.5	13.2	-1.936	27.2	
49	59.9	25.2	NA	18.2		99	NA	NA	NA	NA	
50	33.8	35.2	-1.142	23.4		100	NA	NA	NA	NA	

Table 8. Relative percent abundances of foraminifera species and fragments. Oxygen 18 PDB ratios are in parts per mil, while derived temperatures are in degrees centigrade. NA indicates samples for which no data was available.

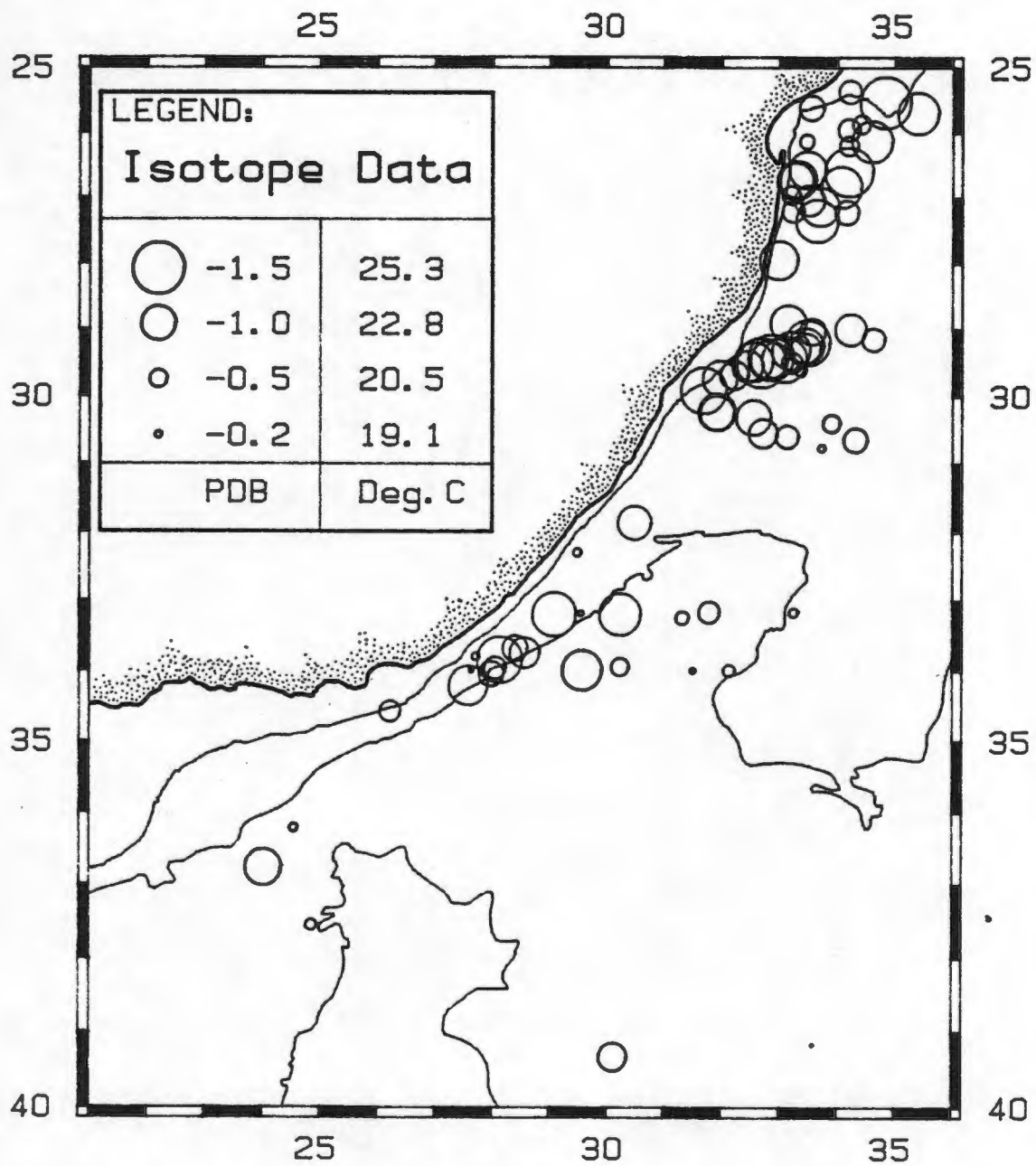


Figure 3.15 Isotope Data. The oxygen isotope ratios, (δO^{18} PDB) and derived isotopic temperatures are given in parts per mil and degrees centigrade respectively.

4. COMMUNITY STRUCTURE

Coccolith assemblages from the southwest Indian Ocean are dominated by epipelagic, placolith-bearing species. *G. oceanica* and *E. huxleyi*, the two dominant species in the study area, are also the two most important coccolithophore species in tropical to subtropical waters (McIntyre and Be 1967). Their biogeographical distribution is not well understood but, since they are the two most abundant coccolithophore species in Quaternary sediments, of great interest. *E. huxleyi* is the most abundant and ubiquitous coccolithophore species living in today's oceans, occurring at relative percent abundances of between 60 and 80% (McIntyre and Be 1967, Okada and McIntyre 1979). It has the widest biogeographic range and is one of the most euryhaline and eurythermal coccolithophore species (McIntyre and Be 1967, McIntyre et al, 1970, Winter et al, 1983). The distribution of *G. oceanica*, in contrast, apparently has a more limited range, currently preferring warmer waters and marginal seas (Okada and Honjo 1975). *G. oceanica* has a smaller salinity tolerance range than *E. huxleyi* and is found in normal to high salinities from 32-45 per mil (Okada and Honjo 1975, Winter 1982). *G. oceanica* also occurs abundantly in upwelling areas of low latitude and in warm highly saline and fertile waters where it often replaces *E. huxleyi* as the dominant species (Winter 1982 and 1985).

Only very few studies have been made of the ecological affinities of the remaining common coccolithophore species which occur at the sediment surface in the study area. *C. leptoporus* seems to prefer subtropical waters and has a wide biogeographical range, similar to but slightly smaller than, that of *E. huxleyi* (McIntyre and Be 1967, Schneidermann 1977). This species usually contributes only a small percentage to living coccolithophores in the world's oceans (McIntyre and Be 1967). Like *G. oceanica*, *C. leptoporus* seems to prefer high fertility waters (Roth and Berger 1975). Winter (1982) also reported that *C. leptoporus* increased in abundance during presumed times of high fertility in the Red Sea.

U. sibogae is usually found in medium to high fertility regions (Roth and Berger, 1975) and occurs in water between 18° and 24°C (McIntyre and Be 1967, Okada and McIntyre 1979). *R. clavigera* is one of the common

rhabdoliths in today's oceans, preferring subtropical and transitional waters (McIntyre and Be 1967) and reaching highest values in low fertility waters (Roth and Berger 1975). *H. carteri* is most abundant in subtropical waters of medium to high fertility (Roth and Berger 1975) but may extend into transitional waters (McIntyre and Be 1967). *S. pulchra*, the only *Syracosphere* species found in significant abundances in sediments of the southwest Indian Ocean, occurs occasionally in the equatorial to transitional zones of the Pacific and North Atlantic (Okada and McIntyre 1977) and seems to prefer low fertility waters (Roth and Berger 1975). *G. ericsoni*, although less abundant, displays a similar surface water distribution pattern to that of *G. oceanica* (McIntyre and Be 1967). *G. ericsoni* is also one of the most abundant species of coccolithophore presently living in the gulf of Aqaba, suggesting a higher than normal salinity tolerance (Winter et al, 1979).

5. DISCUSSION

5.1 PRESERVATION OF CORE-TOP MATERIAL

The interplay of three important parameters, dissolution, dilution and winnowing, seems to be controlling the state in which sediment material is preserved in the study area. Dissolution is likely to impair coccolith preservation by first etching element structures and eventually disintegrating coccoliths. Dissolution of carbonate material probably also biases sediment size range distributions towards the fine fraction.

Most samples examined under the SEM were generally well preserved though dissolved coccoliths were present. Best preserved coccoliths were concentrated in sectors one and two where the sea floor is well above the lysocline and core-top sediments are not subject to accelerated dissolution (Fig. 3.5). This relatively dissolution free environment is also reflected in the percent carbonate values, which are generally higher in the north than in the south of the study area (Fig. 3.2). Surprisingly, however, foraminiferal fragments (Fig. 3.12) contribute between 40 and 60% of the coarse fraction (>150 microns) found in the sediments off Maputo (sector one). Upwelling of relatively cool nutrient rich water does occasionally occur near Maputo (Martin 1984 and Orren 1963). Increased productivity associated with upwelled water could enhance the dissolution of carbonate. The CO₂ produced by respiration reduces the concentration of dissolved carbonate ions and so promotes undersaturation (Broecker 1974). The solubility of carbonate is also greater in cold water. These two effects could combine to increase dissolution on a regional basis such as off Maputo.

Less well preserved coccoliths are found in sector three and are concentrated close to the continental shelf. Poorer preservation is expected here since the sea floor is mostly below the lysocline. Evidence for dissolution is also found in the carbonate percentages which are generally lower in sector three than they are in the northern two sectors.

Worst coccolith preservations and lowest carbonate percentages are found in the Agulhas Passage (Sector 4), where sediments are not only well below the lysocline, but also probably eroded by Antarctic Bottom Water. Fine fraction percentages and relative coccolith

abundances are also low in this region, reflecting this winnowing action of the Antarctic Bottom Water. The relative abundances of *E. huxleyi* as well as *C. leptoporus* decrease significantly on the ocean floor at depths between 3500 and 4000 m (Figs. 5.1 & 5.2). The increase of foraminiferal fragments and decrease of carbonate percentages over this depth range (Figs. 3.12 & 3.3) is especially dramatic. Thus we assume that the lysocline begins at about 3500 m. Contributing to dissolution at depth is the cold and corrosive Antarctic Bottom Water which is forced through the Agulhas Passage at depths of about 4000 m and greater. Puzzling is the increase of coccolith abundances in some of the deepest samples in the Agulhas Passage. Perhaps these samples originated from recent turbidites that were buried quickly and therefore not so dissolved. Terrigenous material dilutes the carbonate content relative to other sediment components. The dilution of carbonate material with terrigenous minerals also seems to darken rock colours. The light brown hues of samples 13,15,17,44,71,96,97 and 98 (which are all found at or near the base of the continental shelf) are probably due to the mixing of pelagic sediments with large quantities of terrigenous material. For example samples 15,17,96,97 and 98 are situated near canyons in the Natal Valley which act as conduits for material from the Tuguela river (Flemming 1981).

Southern African continental shelf sediments of terrigenous origin are moved to the sea floor mainly by the activity of the Agulhas Current system which transports sediments along the continental shelf (Flemming 1981, Martin pers. com. 1986). When submarine canyons are encountered, sediments are trapped and transported to the oceanic sea floor in turbidity currents (Flemming 1981). Terrigenous sediments may also reach the deep sea floor and be incorporated into existing sediments if they are swept off the continental shelf by the Agulhas Current (Martin pers. com., 1986). Carbonate percentages tend to increase with distance from the southeast African coast as well as along the main flow path of the Agulhas Current. Both of these features are probably due to reduced dilution by terrigenous material (Fig. 3.2).

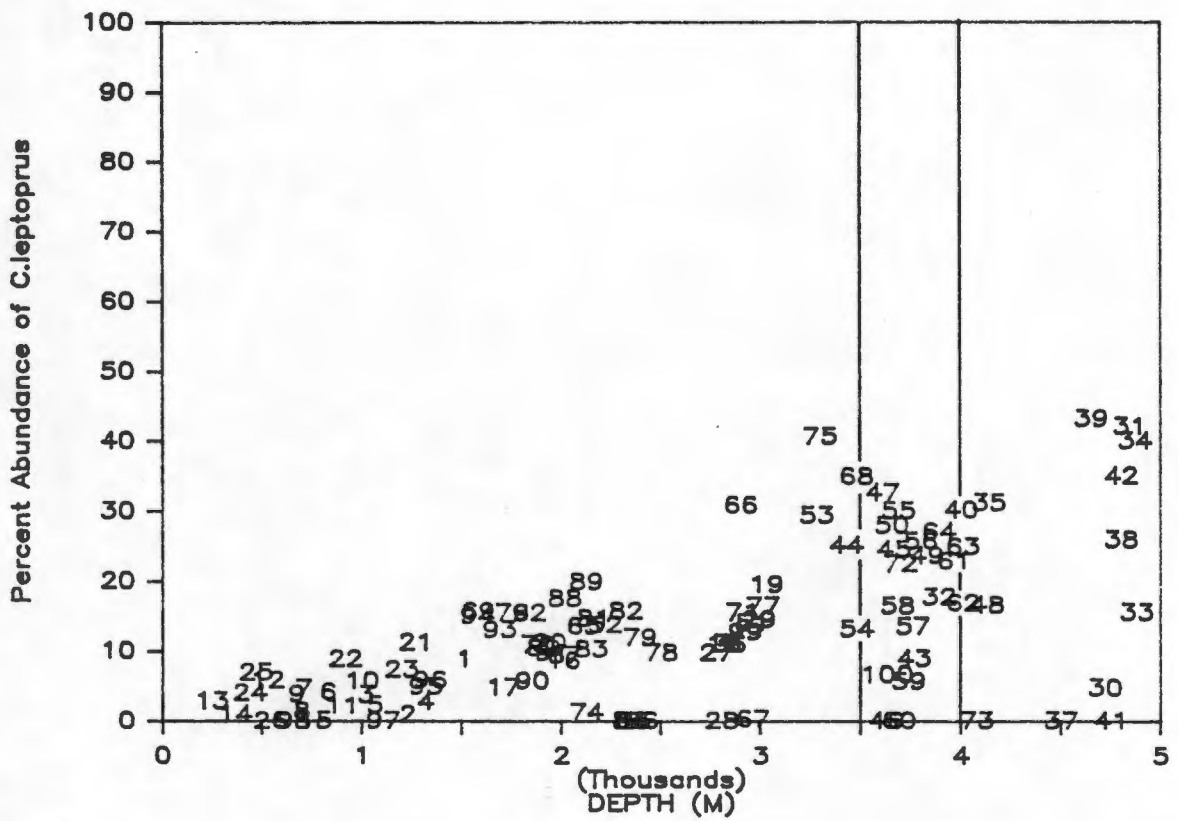


Figure 5.1 Plot of sample depth vs. percent *E. huxleyi*. Points are marked by sample numbers.

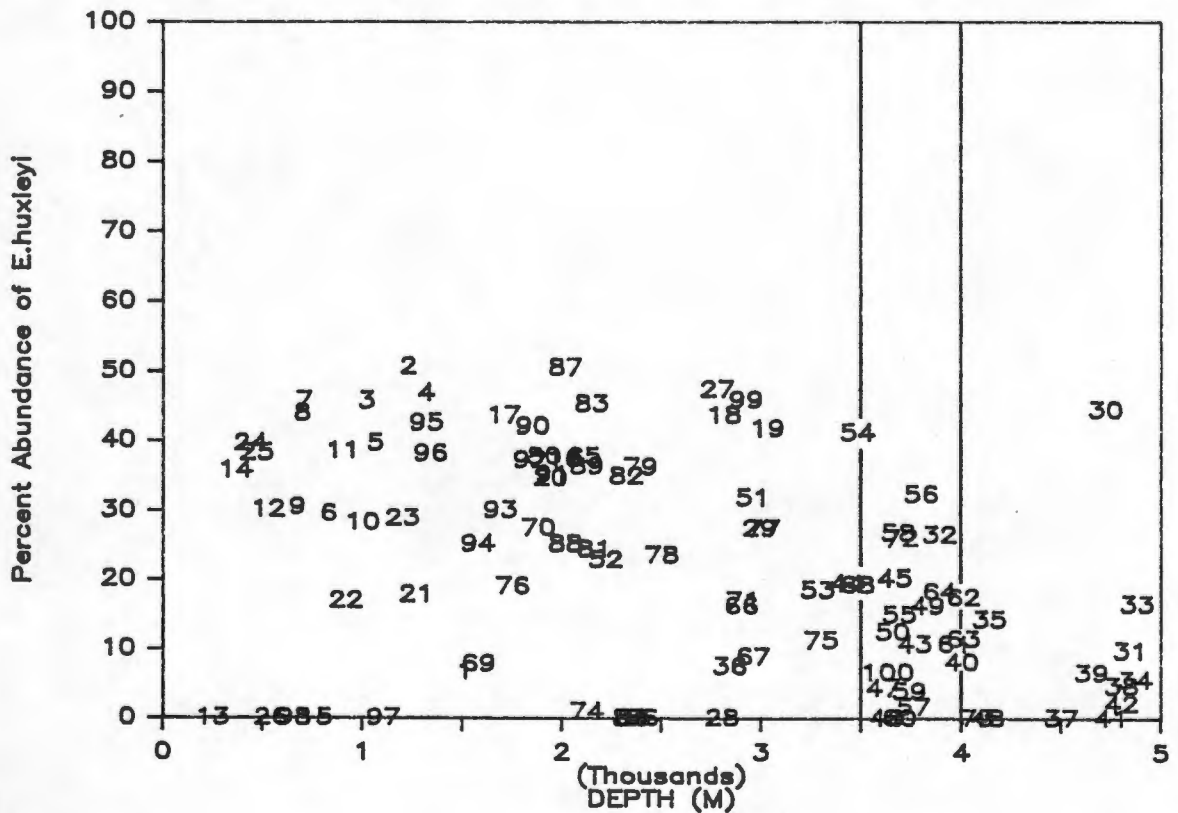


Figure 5.2 Plot of sample depth vs percent *C. leptoprus*. Points are marked by sample numbers.

The abundance of coccoliths which are found in the fine fraction of sediments may be reduced by winnowing, which is the selective removal of fine particles. This results in the build-up of coarse grained lag deposits (Goodlad 1986) and is a process which influences the distribution and sorting of marine sediments. Coarse lags have been correlated with high velocity currents by Huang and Watkins (1977). Goodlad (1986) found that the distribution of the greater than 150 micron fraction in sector two showed a close relationship with bottom current flow. Sectors one and two display lowest concentrations of fine material (coccoliths included) and may be explained by the winnowing effect of the Agulhas Current which can erode surface sediment material down to depths of 2500 m (Duncan 1970). Low coccolith abundances were also found in the Agulhas Passage (sector four), probably as a result of winnowing by Antarctic Bottom Water.

With the exception of these low values in the Agulhas Passage, coccolith and fine fraction abundances increase with southerly latitude (Figs. 3.4 & 3.1). This is probably due to diminished winnowing associated with increasing depth of sea floor. Fine fraction percentages and coccolith abundances are greatest in sector three probably because the sea floor is too deep to be winnowed by the Agulhas Current and mostly too shallow to be influenced by the Antarctic Bottom Water.

5.2 REWORKED COCCOLITHS

Small percentages of relict coccoliths were found in several samples, especially in the southern half of the study area, particularly in the Agulhas Passage (Fig. 5.3). Four discoaster species and eight extinct coccolithophore species were identified. An additional fifteen forms were too dissolved and broken to be identified. Small numbers of discoasters, extinct since the Tertiary (Bukry 1971), were found in seven samples (Nos. 1,29,57,65,69,89 and 93). The maximum concentration of discoasters in any one sample was only about 4% and it is therefore unlikely that these samples originated from outcrops of older material, especially since they contain high percentages of relatively modern species.

Extinct coccoliths species were also found in samples 5,6,7,8 & 99, but usually in extremely low abundances. Sample 67 (sector 4, in the extreme southwest of the study

area) is anomalous since it contains abundant (24%) *C. pelagicus* as well as large concentration of relict coccolith species such as *C. floridanus* (39%), *E. cava* (11.1%) and *D. daviesi* (5%). *C. pelagicus* is an extant coccolithophore species, presently preferring sub-arctic and cold temperate waters. It occurs commonly in the sub-polar waters of the northern hemisphere (McIntyre and Be 1967) though it has not been reported in the surface waters of the southern Indian Ocean (Friedinger and Winter 1985). *C. pelagicus*, does however, occur infrequently in core-top sediments from the study area (Samples 1,2, 4,14,16,20,21,27,65,69 & 89). *C. pelagicus* is a robust species which first appeared in the Upper Paleocene and its co-occurrence in samples with species that ranged through the Tertiary and Cretaceous suggest sediment reworking.

Samples containing unidentified coccoliths were concentrated in the Agulhas Passage (Nos. 30,33,35,38,40 & 46; Fig. 5.4) and are probably from turbidite or relict sediments that have been scoured by Antarctic Bottom Water.

Unidentified coccoliths were also found in sectors one and two (samples 1,10,13 and 63). Bioturbation may be responsible for the occurrence of reworked and unidentified coccoliths in the north of the study area since there is little evidence for the presence of turbidites or of sediment scouring. High bioturbation probably occurs in this region because of elevated nutrient concentrations associated with the Agulhas Current (R. Johnson, UCT Marine Geoscience Unit, pers. com. 1986) and may also be responsible for the destruction of foraminifera occurring off Maputo (section 5.1).

5.3 COCCOLITH CORE-TOP ASSEMBLAGE DISTRIBUTION

The area of this study encompasses approximately 15 degrees of latitude (25° to 40°S) and should include subtropical (10-30°S) and transitional (30-45°S) coccolith floral zones similar to the Atlantic and Pacific Oceans (McIntyre and Be 1967, Okada and Honjo 1973). Thus coccolith assemblages at the sediment surface from this region would be expected to differ from north to south as ecological ocean boundaries are crossed.

Three different coccolith assemblages have been recognized from the study area,

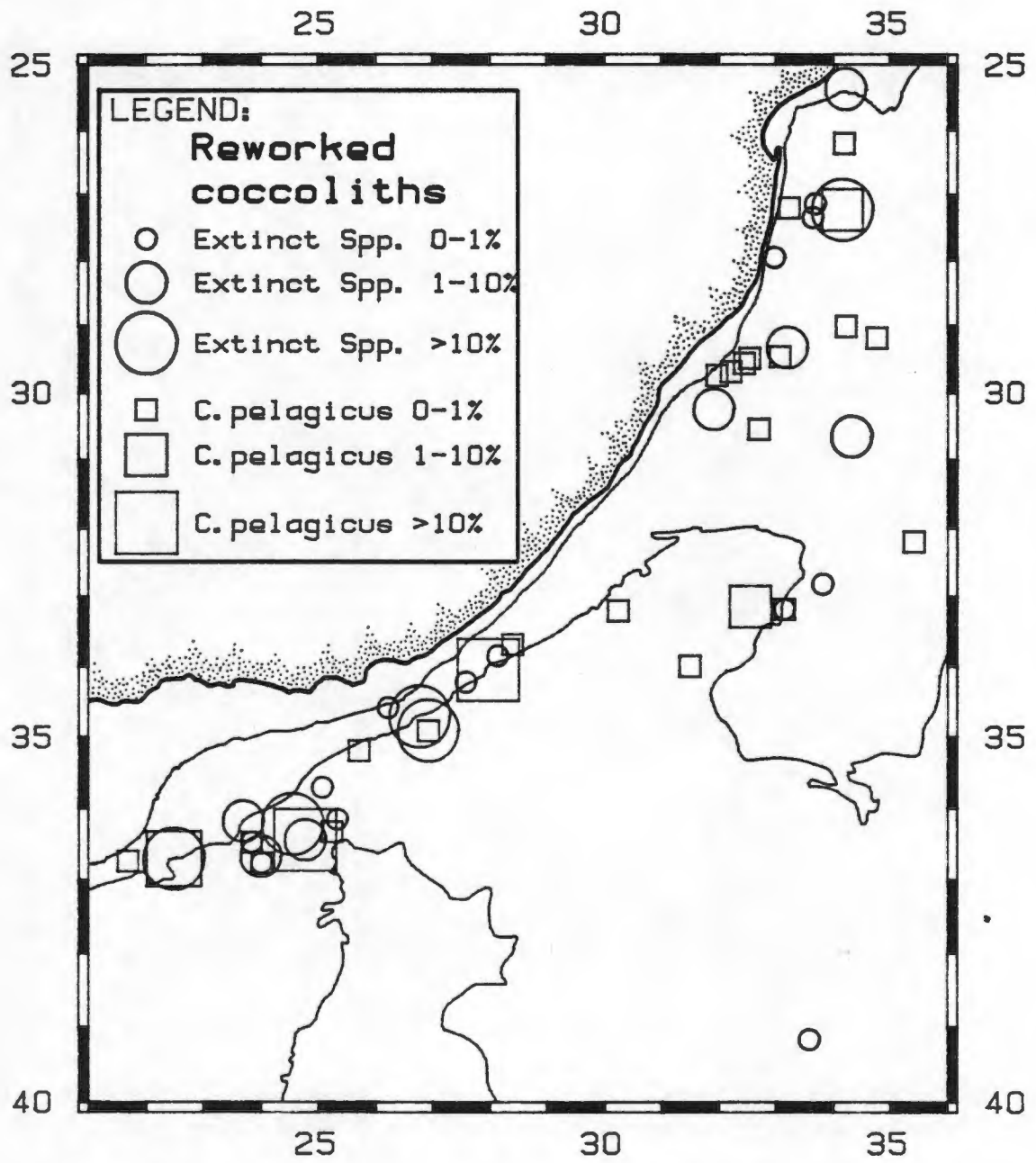


Figure 5.3 The distribution of reworked coccoliths.

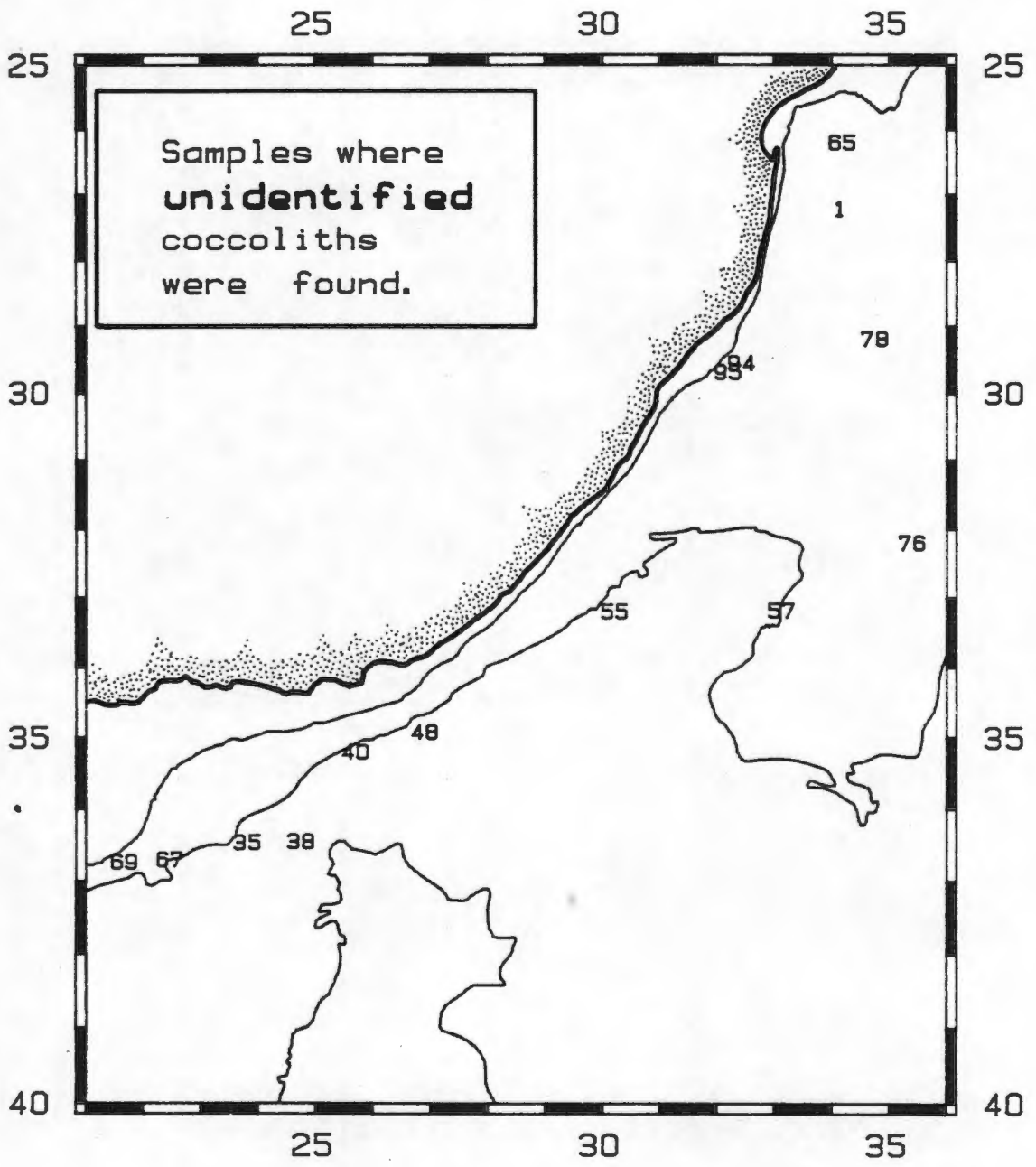


Figure 5.4 The distribution of unidentified coccoliths. Core-top locations are marked by sample numbers.

although some overlap occurs (Fig. 5.5): Maputo, Agulhas Current and Deep Water (Table 9). Each is associated with a specific oceanographic area and conditions. However, due to preferential dissolution and the integration of seasonal fluctuations by the sea floor, the three assemblages do not conform to the floral zones of McIntyre and Be (1967).

The Maputo assemblage (Samples 1-14, 21-25 and 65) is found on the shallow water continental shelf, inshore of the Agulhas Current (sector 1) and is characterized by *G. oceanica* (averaging 42%), *E. huxleyi* (33%), and lower concentrations of *U. sibogae* (12%), and *C. leptoporus* (5%). The high abundance of *G. oceanica* in this area is probably related to inshore return currents and the associated upwelling of nutrient rich waters. The controlling oceanographic features of this area are the shallow water bathymetry, low water temperatures (where there is upwelling) and the proximity of the warm Agulhas Current and its associated gyres.

The Agulhas Current assemblage (Samples 16-18, 20, 29, 44, 51-54, 70-71, 81-83 and 87-96) is restricted to a narrow band running offshore and parallel to the coast, directly beneath the mean flow path of the Agulhas Current (see section 1.6.1) through sectors one, two and three. *E. huxleyi* dominates the assemblage with an average abundance of 33%, *G. oceanica* only comprises 28% of the assemblage (10% lower than in the other two assemblages) while *C. leptoporus* and *U. sibogae* occur at average abundances of 13% and 12% respectively.

The deep-water or dissolution assemblage (Samples 30-35, 38-40, 42-43, 45, 47-50, 55-59, 61-64, 72, and 100) is situated in sectors three and four at depths greater than 3500 meters, with the deepest samples being found in the Agulhas Passage (4879 m). *G. oceanica* occurs at abundances of about 41%, *C. leptoporus* is the next most abundant species, occurring at an average abundance of 23% (five times more abundant than in the north). *E. huxleyi* and *U. sibogae* contribute about 15% and 8% respectively towards this assemblage. Since all of the deep-water samples occur at or below the lysocline (3500 m to 4000 m), dissolution is probably the major influence determining assemblage composition. The most abundant species found in the assemblage, *G. oceanica* and *C. leptoporus*, are also the most dissolution resistant (Berger 1973).

Two species, *E. huxleyi* and *C. leptoporus*, display significant differences in percent abundances from sediment surface samples from the north to the south of the study area. *E. huxleyi* decreases in relative percent abundance from north to south while *C. leptoporus* shows the reverse trend. Temperature and salinity are thought to be two important environmental factors controlling the distribution of these two species. However, the temperature range of between 15° and 26°C in the southwest Indian Ocean (Wyrтки et al, 1971) is well within the tolerance limit of both species (Okada and McIntyre 1979). Sea surface salinities vary only slightly, ranging between 35 and 35.6 per mil (Wyrтки et al, 1971). These salinity ranges are also well within the tolerance limits for both *E. huxleyi* and *C. leptoporus*.

Phosphate concentration in seawater may play an important role in influencing the distribution of coccolithophores (Reid 1962, Krey and Babenerd 1976, Winter 1982). Phosphate values in the study area range between about 0.2 and 1.0 mg at/l (Wyrтки et al, 1971). Generally values increase from north to south with occasional pockets of relatively high phosphate concentrations associated with dynamic upwelling off Maputo and Durban (Martin 1984). The strong nutrient gradient from north to south and the increase of *C. leptoporus* (Fig. 3.10) in the same direction, to the detriment of *E. huxleyi* (Fig. 3.8), seems to indicate fertility control in the distribution of *C. leptoporus*. Other coccolithophore species which have been reported to be sensitive fertility indicators such as *G. oceanica* and *H. carteri* (see community structure section above) are also found in areas of high nutrient concentrations in the study area. *G. oceanica* is most abundant in the shallow sediments off Maputo. Both species are abundant in the deeper, southern part of the study area. The high abundances of *G. oceanica* off Maputo support the affinity of this species for warm waters and high nutrient concentrations (Winter 1982 and 1985).

The ocean floor distribution pattern of *E. huxleyi* and *C. leptoporus* may not only be due to latitudinal environmental changes occurring in the water column but also to post-depositional dissolution. This is because there is a distinct sample-depth gradient from north to south, ranging from 248 m off Maputo (No.13) to 4879 m south of Port Elizabeth (No.33). The coccoliths of

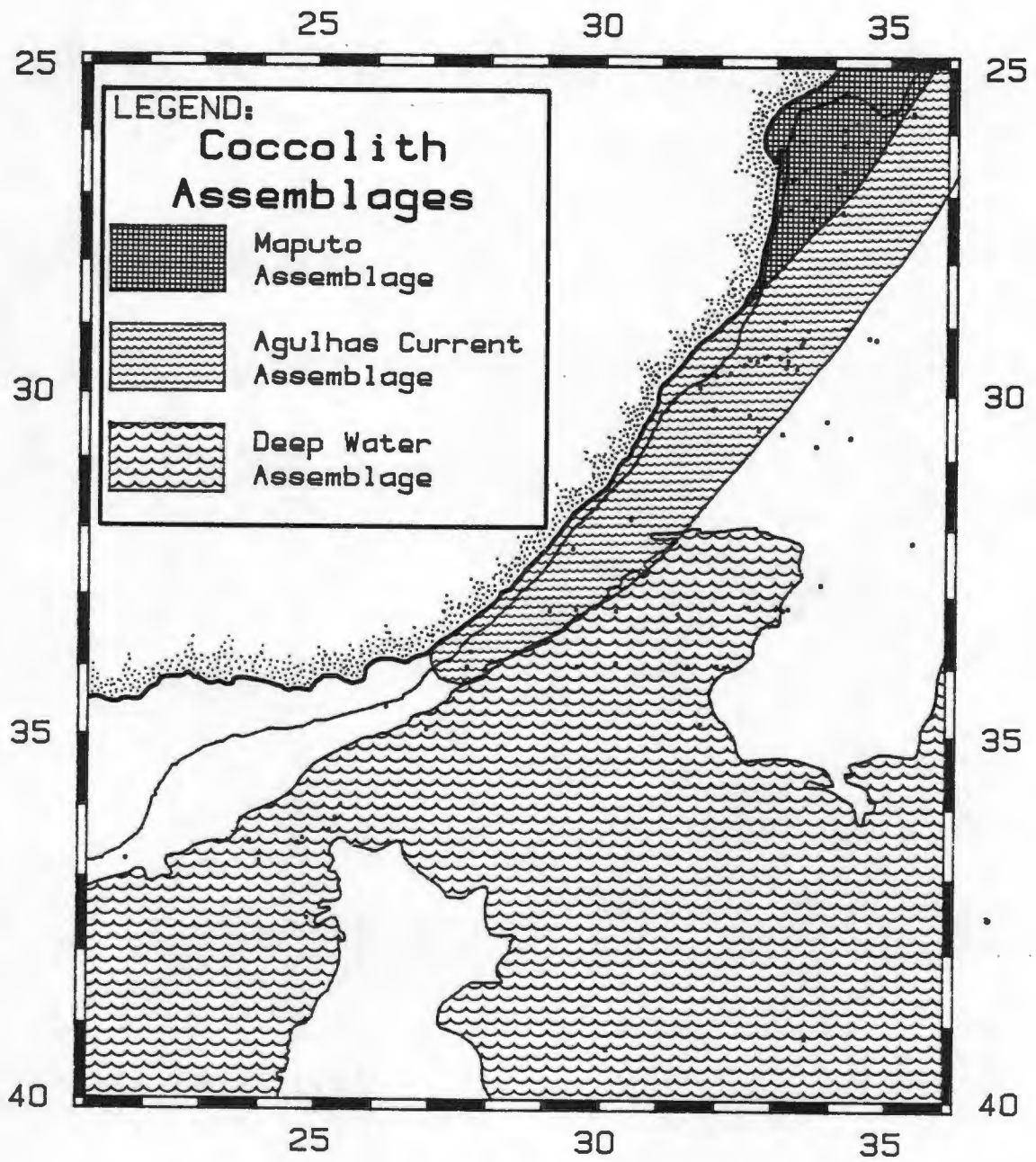


Figure 5.5 Coccolith assemblage distributions.

TABLE 9.

Core Top Assemblage	Temperature (°C)		Phosphate (Mic ats/l)		Assemblage Composition	
	Min	Max	Min	Max	Species	Abundance
1 MAPUTO	21	25	0.2	<0.8	<u>G.oceanica</u>	41.9 %
Summer	25	26	>0.2	0.4	<u>E.huxleyi</u>	32.5 %
Winter	21	22	0.6	<0.8	<u>U.sibogae</u>	11.5 %
Mean Depth = 925m					<u>C.leptoporus</u>	5.1 %
					<u>G.ericsoni</u>	1.7 %
2 AGULHAS CURRENT	20	26	<0.2	0.6	<u>E.huxleyi</u>	31.2 %
Summer	24	26	<0.2	0.2	<u>G.oceanica</u>	30.0 %
Winter	20	22	0.4	0.6	<u>C.leptoporus</u>	14.3 %
Mean Depth = 2143m					<u>U.sibogae</u>	11.1 %
					<u>S.pulchra</u>	2.5 %
3 DEEP WATER	15	23	<0.2	0.6	<u>G.oceanica</u>	34.8 %
Summer	19	23	<0.2	0.2	<u>C.leptoporus</u>	16.5 %
Winter	15	19	0.4	0.6	<u>E.huxleyi</u>	25.3 %
Mean Depth = 3653m					<u>U.sibogae</u>	10.5 %
					<u>H.carteri</u>	3.1 %

Table 9. Sea surface temperature and phosphate values for the Maputo, Agulhas Current and Deep Water assemblages (after Wyrski et al 1971). Mean values of significant coccolithophore species are also given.

C. leptoporus and *E. huxleyi* are both relatively dissolution resistant. However, *C. leptoporus* is somewhat more resistant to calcium carbonate dissolution than *E. huxleyi* (McIntyre and McIntyre 1971, Berger 1973, Roth and Berger 1975) probably due to its larger and more tightly packed elements (Schneiderman 1977). *C. leptoporus* is concentrated in samples below 3500 m (Figs. 3.9 & 5.2). On the other hand, *E. huxleyi* seems to remain relatively abundant in sediments shallower than 3500 m (Figs. 3.7 & 5.1), but decreases considerably in relative percent abundance at depths greater than this. Dissolution, therefore, seems to play a more important role in samples taken from the southern part of the study area where depths are greatest but can not explain the increase in the abundance of *C. leptoporus* with depth (Fig. 5.2) in the majority of samples taken from the northern two-thirds of the study area where we believe environmental factors play a more important role.

5.4 CORE-TOP AGE DETERMINATION

Emiliana huxleyi is believed to have evolved from *Gephyrocapsa protohuxleyi* somewhere between 270,000 and 250,000 years BP (McIntyre 1969) and became abundant between 73,000 to 85,000 years BP (Stage 4-5a: Thierstien et al 1977). Thus samples containing abundant *E. huxleyi* should be younger than 85,000 years BP. Indeed, all but one of the core-top samples taken in the study area contain *E. huxleyi* indicating that samples should all be younger than 270,000 years BP. Most of the samples, especially those from the north of the study area, contain relative percent abundances of *E. huxleyi* between 30 and 52% and can be assumed to be less than 85,000 years BP. In the south, samples from the deepest region (the Agulhas Passage) contain relative percent abundances of *E. huxleyi* of less than 10%, although the majority of samples contain relative abundances in the range 10-30%. Since samples from the south are generally from greater depths, dissolution probably diminishes percentages of *E. huxleyi*, thereby biasing results in favor of *C. leptoporus* and other resistant species. Had these samples been well preserved, *E. huxleyi* might have made up a larger fraction of the coccoliths identified, yielding values representative of 85,000 years BP or younger.

5.5 OXYGEN ISOTOPES

The oxygen isotopic ratio of water in the oceans is dependant on the amount of isotopically depleted ice stored on the continents (Dansgaard et al 1973): Water evaporates from the sea surface and subsequently precipitates at the polar ice caps. This results in an accumulation of ^{18}O depleted ice at the poles and the oxygen isotopic content of microfossil calcite is therefore heavier during interglacial than glacial periods. There is also a small isotopic fractionation between sea water and the calcite tests of marine plankton. At equilibrium this fractionation is controlled by temperature (Urey, 1947; Epstein et al 1951, 1953), and therefore, isotopic variations are also due to surface water temperature variations.

Seven samples (Nos. 32, 36, 57, 58, 61, 76 and 87) for which isotope ratios were evaluated gave anomalously high or low ratios outside the temperature range expected for holocene samples (Dansgaard 1964) for *G. sacculifer*. The locations of these cores (Fig. 3.14) in areas of accelerated dissolution and winnowing (in the Agulhas Passage) or at the bases of steep topography indicate that these samples may be highly dissolved or contaminated with glacial material (see below).

Remaining isotope ratios from core-top samples taken in the study area range from -1.5 to 0.0 parts per mil PDB. Lightest values of -1.49 to -1.0 per mil PDB (equals 23 to 25°C, Vincent and Shackleton 1980) occur in a narrow band on the sea floor beneath the "A" route of the Agulhas Current, in the northern part of the study area (Fig. 3.15). These values are about 0.5 per mil PDB lighter than samples analyzed on either side of this band. The isotopic temperatures fall within the summer temperature range of the Agulhas Current, 20 - 26°C (Wyrski et al, 1971). The 0.5 parts per mil enrichment in isotopic ratios of *G. sacculifer* specimens underneath the Agulhas Current can be explained by its elevated temperature at the ocean surface of between 2 to 3°C (one per mil change in O^{18} is equivalent to approximately 4°C; Emiliani 1955). Thus an oxygen isotope imprint of the Agulhas Current exists beneath it on the sea floor. Isotopic temperatures of *G. sacculifer* lying beyond the influence of the Agulhas Current range between 20.5 and 22.8°C and also reflect the summer average for sea-surface temperatures.

This would seem to indicate that *G. sacculifer* is more productive in the summer months and is in agreement with the findings of Vincent and Shackleton (1980).

South of about 28°S the occurrence of isotopically light samples decreases. This may be a result of decreasing temperatures of the Agulhas Current as it flows southward or due to carbonate dissolution. Dissolution of less resistant foraminifera species such as *G. sacculifer* tends to make them isotopically heavier (Berger and Killingley 1977) and many specimens of this species from depths greater than 3500 m were partly dissolved.

Some samples give isotope values greater than -0.5 parts per mil PDB (less than 20.5°C) and indicate temperatures below the seasonal range of modern surface temperatures. However, we believe that these values are positively biased since the samples are from depths equal to or greater than 3500 m and have probably experienced some dissolution. On the other hand, a few of these samples also occur on the slopes of topographic highs which are vulnerable sedimentary environments and thus may be outcrops of glacial material which have been exposed by mass gravity flows or current activity.

A few samples yielding unexpectedly warm estimated temperatures were found beyond the influence of the Agulhas Current or not directly related to its mean flow path. These may be core-tops of relict, reworked, or disturbed interglacial material, they occur chiefly off Durban near turbidite channels.

Most of the oxygen isotope ratios obtained from the carbonate tests of foraminifera indicated depletion of ^{18}O , yielding Holocene values similar to those of Vincent and Shackleton (1980). This supports the belief that most of our core-tops especially north of 32°S are probably of Recent age.

5.6 IMPLICATIONS FOR SEDIMENTOLOGY AND AGULHAS CURRENT STRENGTH

The Agulhas Current is probably the major factor influencing sedimentation, sediment distribution patterns, and geological features in the study area (Martin 1981). Evidence exists that the Agulhas Current may have influenced changing sedimentation throughout the past with major current activity centering between 90-100 Myr BP, 65 Myr BP and 38-22 Myr BP (Martin 1981). In the Pleistocene, fluctuations in the current probably

occurred in response to sea level changes and changing physiography (Martin 1981).

Vertical and lateral movements of the Agulhas Current during the past and particularly during glacial intervals are of special interest because of the current's role in transporting heat from the equator to the poles. Any shift in its temperature structure and velocity would effect inter- and intra-ocean heat transfer and the climate of southern Africa.

The furthest southerly penetration of the Agulhas Current is directly associated with the position of the subtropical convergence (STC), which separates warm saline subtropical water from cool low-salinity sub-polar water (Prell et al 1979). Currently positioned at about 40°S (Fig 1.2), the location of the subtropical convergence is linked to circulation patterns in the southern Indian Ocean (Duncan 1970).

At present about 20% of Agulhas Current is lost from the Indian to the Atlantic Ocean (Gordon 1985). The cold Antarctic Bottom Water which flows north through the Agulhas Passage at depths greater than 4000 m probably replaces some of this water but there is a net heat loss from the Indian to the Atlantic ocean. A greater than 5° shift northwards in the position of the subtropical convergence would prevent Agulhas Current spillage into the Atlantic ocean and thus alter the inter-ocean heat budget.

Borehole and acoustic data (Dingle et al 1978, Dingle and Camden-Smith 1979, Goodlad 1986, Martin et al 1982 and Martin 1984) has suggested that surface sediments in the study area are largely outcrops of relict material that have been exposed by the Agulhas Current during periods of intense flow. At present the Agulhas is voluminous and fast flowing and may erode and transport sediments 2500 meters below the surface (Duncan 1970).

Percent *E. huxleyi* present and oxygen-isotope ratios indicate that the majority of samples are most probably recent or at least not older than 85,000 years except for sediments found in the Agulhas Passage. This implies that sediments have accumulated on the ocean floor in the last 85,000 years and that the Agulhas Current does not have a pronounced erosional influence, at least in areas from which cores were retrieved for this study.

The data presented here show that the position of the core of the Agulhas Current

can be determined using oxygen isotopic temperatures from surface sediments beneath the current in the southwest Indian Ocean. Oceanographers have shown that current core temperatures are related to current intensity. It should therefore be possible to determine past changes in current intensity by comparing isotopic temperatures of surface and downcore sediments.

The path of the Agulhas Current in the north of the study area is dictated by the location of its western boundary (the African continent) and therefore will not have changed much in the past. In the south of the study area, however, where the current has no solid boundary, its position may have changed during, say, the Pleistocene. Any changes in therefore be determined by comparing isotopic temperatures from undissolved surface and downcore material from this region.

For example, Winter (UCT Marine Geoscience Unit, pers. com. 1986) has found that the glacial-interglacial range in oxygen isotope ratios of *G. sacculifer* from cores taken east of East London can be explained solely by changes in ice volume. No temperature effect is superimposed on the isotope signal, suggesting that temperature (and perhaps intensity) of the Agulhas Current remained more or less constant, at least since stage 5.

If undissolved down-core sample material from the Agulhas Passage also indicated that the current core had not shifted in position or changed in intensity, this would imply that the inter-ocean heat transfer between the Indian and Atlantic Oceans (Gordon 1985) could not have changed considerably. The position of the subtropical convergence during glacial time could therefore not have shifted northward more than a few degrees.

This emphasises the usefulness for paleo-reconstructions of the core-top data presented in this thesis.

Dingle et al (1978), Martin et al (1982), Martin (1984) and Goodlad (1986) indicated that the north of the study area is scoured by powerful currents which have exposed Cretaceous and Tertiary strata. The data presented here indicates, however, that the majority of the core-top samples investigated, except those from the Agulhas Passage, are

younger than 85,000 years BP. This suggests that sediment accumulation rather than scouring has occurred since this time at the earliest and emphasises the usefulness of this kind of data in determining the age of undissolved surficial sediments from the study area.

6. CONCLUSIONS

Core-top samples from the southwest Indian Ocean show that:

1. Three processes, dilution, dissolution and winnowing, control the state in which sediment material is preserved.
2. Coccolith and foraminifera preservations deteriorate at depths greater than 3500 m, marking the beginning of the lysocline. Sediments in the Agulhas Passage (sector four: 3000-5000 m) are therefore frequently dissolved, especially since they are also swept by corrosive Antarctic Bottom Water.
3. Dilution of calcareous sediments is related to the flux of terrigenous material to the ocean floor, and is therefore greatest close to the continent.
4. Winnowing occurs in the shallow sediments of sectors one and two beneath the Agulhas Current and in the Agulhas Passage beneath Antarctic bottom water.
5. Three coccolith assemblages (Maputo, Agulhas Current and Deep water) have been recognized in the study area and are delineated by four ecologically significant coccolithophore species (*G. oceanica*, *E. huxleyi*, *C. leptoporus* and *U. sibogae*).
6. Dissolution seems to be important in determining coccolith community structure in the south where depths are greatest, whereas environmental factors (eg. nutrient concentration and water temperature) seem to play a more important role in the majority of samples taken from the northern two-thirds of the study area.
7. *E. huxleyi* percentages and isotope ratios from the carbonate tests of foraminifera indicate that the majority of core-top samples are less than 85,000 years BP except for sediments found in the Agulhas Passage.
8. Lightest isotope values (-1.5 to -1.0 per mil PDB) occur beneath the "A" route of the Agulhas Current and are about 0.5 per mil PDB lighter than samples analyzed beyond the current's influence; and thus reflects the Agulhas Current's elevated temperature of between 2 to 3 degrees centigrade.
9. In areas from which cores were retrieved for this study, sediments appear to have been accumulating over the last 85,000 years. This suggests that the current is not particularly erosive at these sites at present and demonstrates the useful application of this data in reconstructing the paleohistory of the Agulhas Current.

REFERENCES

- Be,A.W.H and Hutson,W.H. 1977. The ecology of planktonic foraminifera : biogeographic patterns of life and fossil assemblages in the Indian Ocean. Micropaleontology 23:369-414.
- Berger,W.H. 1973. Deep sea carbonates: evidence for a coccolith lysocline. Deep Sea Research 20:917-921.
- Berger,W.H. and Killingley,J.S. 1977. Glacial-Holocene transition in deep sea carbonates: selective dissolution of the stable isotope signal. Science 197:563-566.
- Berger,W.H. and Roth,P.H. 1975. Oceanic Micropaleontology: progress and prospect. Review of Geophysics and Space Physics 13:561-585.
- Bernard,F and Lecal,J. 1960. Plankton unicellulaire recolte dans l'ocean Indien par le Charcot (1950) et le Norsel (1955-6). Bulletin of the Institute of Oceanography, Monaco, 1166:1-54.
- Birch,G.F. 1981. The karbonate bombe: a precise, rapid and cheap method for determining calcium carbonate in sediments and rocks. Transactions of the Geological Society of South Africa 84:199-203.
- Borsetti,A.M and Cati,F. 1972. Il nannoplancton calcareo vivente nel tirreno centro meridionale. Parte I. Giornale di Geologia (Annali del museo Geologico di Bologna), Serie 2a 38:395-414.
- Borsetti,A.M. and Cati,F. 1979. Calcareous nannoplancton biostratigraphy of the vrica section Calabria, southern Italy. Giornale di Geologia, (Annali del museo Geologcodi Bologna) Serie 2a
- Braarrud,T. 1945. Forurensing og selvrening av sjovann. Naturen 7-8.
- Bramlette,M.N. 1958. Significance of coccolithophorids in calcium carbonate deposition. Bulletin of the Geological Society of America 69:121-126.
- Broecker,W.S. 1974. Chemical oceanography. Harcourt Brace Jovanovich, Inc. New York. 214pp.
- Bukry,D. 1970. Coccolith age determinations Leg 2, Deep Sea drilling Project. In: Peterson,M.N.A., Edgar,N,I. et al, 1970. Initial reports of the Deep Sea Drilling Project II. Washington (U.S. Government Printing Office).
- Bukry,D. 1971. Discoaster evolutionary trends. Micropaleontology 17(1):43-52.
- Craig,H. 1957. Isotopic standards for carbon and oxygen and correction factors. Geochim. Cosmochim. Acta. 12:1331-149.
- Dansgaard,W., Johnsen,S.J., Clausen,H.B. and Gunderstrup,N. 1973. Stable Isotope glaciology. Meddelser om Gronland 197(2):1-53.
- Dansgaard,W. 1964. Stable isotopes in precipitation. Tellus 16:436-468.
- Dingle,R.V.D. 1978. South Africa. In: Moullade,M. and Nairn,A.E.M (Eds). The Phanerozoic geology of the world,2. The Mesozoic. Elsevier, Amsterdam, 401-33.
- Dingle,R.V.D., Goodlad,S.W. and Martin,A.K. 1978. Bathymetry and stratigraphy of the Northern Natal Valley (southwest Indian Ocean): A preliminary report. Marine Geology 28:28-106.
- Dingle,R.V.D. and Camden-Smith,F. 1979. Acoustic stratigraphy an current generated bedforms in deep ocean basins off south-eastern Africa. Marine Geology 33:239-60.
- Dingle,R.V.D. and Robson,S.R. 1985. Slumps, canyons and related features on the continental margin off East London, SE Africa (SW Indian Ocean). Marine Geology 67:37-54.
- Duncan,C. 1970. The Agulhas Current. Phd thesis, University of Hawaii.
- Emiliani,C. 1955. Pleistocene temperatures. Journal of Geology 63:538-578.
- Epstein,S.R., Buchsbaum,H.A., Lowenstam,H.A. and Urey,H.C. 1951. Carbonate-water isotpic temperature scale. Geological Society of America Bulletin 62:417-426.
- Epstein,S.R., Buchsbaum,H.A., Lowenstam,H.A. and Urey,H.C. 1953. Revised carbonate-water isotopic temperature scale. Geological Society of America Bulletin 64:1315-1326.
- Erez,J. and Luz,B. 1983. Experimental paleotemperature equation for planktonic foraminifera. Geochemica et Cosmochimica Acta 47:1025-1031.
- Flemming,B.W. 1981. Factors controlling shelf sediment dispersal along the southeast African continental margin. Marine Geology 42:259-277.

- Friedinger and Winter 1985. Distribution of modern coccolithophore assemblages in the area of the Natal Valley (southwest Indian Ocean). Joint Geological Survey/University of Cape Town Marine Geoscience Unit Technical Report 14:146-150.
- Gaarder, K.R. 1971. Comments on the distribution of coccolithophorids in the oceans. In: Funnel, B.M. and Riedel, W.R. (Eds). The Micropaleontology of the Oceans. Cambridge Press 97-103.
- Gordon, A.L. 1985. Indian-Atlantic transfer of thermocline water at the Agulhas Retroflexion. Science 227:1030-1033.
- Goodlad, S.W. 1978. The bathymetry of the Natal Valley off the Natal and Zululand coasts (southern Africa). Joint Geological Survey/University of Cape Town Marine Geoscience Unit Technical Report 10.
- Goodlad, S.W. 1986. Tectonic and sedimentary history of the Mid-Natal Valley (S.W. Indian Ocean). Joint Geological Survey/University of Cape Town Marine Geoscience Unit Bulletin 15.
- Grundlingh, M.L. 1977. Drift observations from Nimbus VI satellite tracked buoys in the southwest Indian Ocean. Deep Sea Research 24:903-913.
- Geitzenauer, K.R., Roche, M.B. and McIntyre, A. 1977. Coccolith biogeography from North Atlantic and Pacific surface sediments. In: Ramsay, A.T.S., Oceanic micropaleontology. Academic Press, 973-1008.
- Haq, B.U. 1973. Transgression climatic change and the diversity of calcareous nannoplankton. Marine Geology 15:M25-M30.
- Haq, B.U. 1976. Coccoliths in cores from the Bellingshauen Abyssal Plain and Antarctic continental basin. Leg 35 of the Deep Sea Drilling Project. Initial reports of the Deep Sea Drilling Project XXXV:557-567. Washington (U.S. Government Printing Office).
- Haq, B.U. 1980. Biogeographic history of the Miocene calcareous nannoplankton and paleoceanography of the Atlantic Ocean. Micropaleontology 26(4):414-443.
- Harris, T.F.W. 1978. Review of coastal currents in southern African waters. South African National Scientific Programmes Report 30.
- Harris, T.F.W. and van-Foreest, D. 1977. The Agulhas Current system. Department of Oceanography, University of Cape Town. 36p.
- Hart, G.F., Pienaar, R.N. and Caveney, R. 1965. An aragonite coccolith from South Africa. South African Journal of Science 61:425-426.
- Hay, W.W. and Mohler, H.P. 1967. In: Hay, W.W., Mohler, H.P., Roth, P.H., Schmidt, R.R. and Boudreaux, J.E., (Eds) Calcareous nanoplankton zonation of the Cenozoic of the Gulf Coast and Caribbean-Antillean area and transoceanic correlation: Gulf Coast Association Geological Societies Transactions 17:428-480.
- Honjo, S. 1976. Coccoliths: production, transportation and sedimentation. Marine Micropaleontology 1:65-79.
- Honjo, S. 1977. Biogeography and provincialism of living coccolithophorida in the Pacific Ocean. In: Ramsay, A.T.S., Oceanic micropaleontology Academic Press, 951-972.
- Honjo, S. and Okada, H. 1974. Community structure of coccolithophores in the photic layer of the mid Pacific. Micropaleontology 20:209-230.
- Honjo, S. and Roman, M.R. 1978. Marine copepod faecal pellets: production, preservation and sedimentation. Journal of Marine Research 36:45-57.
- Huang, T.C. and Watkins, N.D. 1977. Contrasts between the Brunhes and Matuyama. Sedimentary records of bottom water activity in the south Pacific. Marine Geology 23:113-132.
- Hutchings, L., Holden, C. and Mitchell-Innes, B. 1984. Hydrological and biological shipboard monitoring of upwelling off the Cape Peninsula. South African Journal of Science 80:83-89.
- Hutson, W.H. 1980. The Agulhas Current during the Late Pleistocene: Analysis of modern faunal analogs. Science 207:64-66.
- Kennett, J.P. 1982. Paleo-oceanography: Global Ocean Circulation. Reviews of Geophysics and Space Physics 21(5):1258-1274. U.S. National report to the International union of Geodesy and Geophysics. 1979-1982.

- Kolla,V.,Sullivan,L.,Streeter,S.S. and Langseth,M.G. 1976. Spreading of the Antarctic Bottom water and its effects on the floor of the Indian Ocean inferred from bottomwater potential temperature, turbidity and sea floor photography. Marine Geology 21:171-189.
- Krey,I. and Babenerd,B. 1976. Atlas of the International Indian Ocean Expedition. Landesvermessungsamt Schleswig-Holstein Kiel.
- Malan,O.G. and Schumann,E.H. 1979. Natal shelf circulation revealed by Landsat imagery. South African Journal of Science 75:136-137.
- Manton,I and Leedale,G.F. 1963. Observations on the microanatomy of *Crystallolithus hyalinus* Gaarder and Markali. Arch.Mikrobiol. 47:115-136.
- Martin,A.K. 1981. The influence of the Agulhas Current on the physiographic development of the northernmost Natal Valley (SW Indian Ocean) Marine Geology 39:259-76.
- Martin,A.K. 1984. Plate tectonic status and sedimentary basin in-fill of the Natal Valley (S.W. Indian Ocean). Joint Geological Survey/University of Cape Town, Marine Geoscience Unit, Bulletin 14.
- Martin,A.K., Goodlad,S.W. and Salmon,D.A. 1982. Sedimentary basin in-fill in the northernmost Natal Valley, hiatus development and Agulhas Current palaeo-oceanography. Journal of the Geological Society of London 139:183-201.
- Martini,E. and Bramlette,M.N. 1963. Calcareous nannoplankton from the experimental Mohole drilling. Journal of Paleontology 37:845-856.
- McIntyre,A. 1967. Coccoliths as paleoclimatic indicators of Pleistocene glaciation. Science 158(3806):1314-1317.
- McIntyre,A. 1969. The coccolithophorida in red sea sediments. In: Degens,E.T. and Ross,P.A.,Eds. Hot brines and recent heavy metal deposits in the red sea. Berlin/Heidelberg/New York, Springer-Verlag 229-305.
- McIntyre,A., Be,A.W.H. and Roche,M.B. 1970. Modern Pacific coccolithophorids a paleontological thermometer. New York Academy of Science Transactions 32(6):720-731.
- McIntyre,A. and Be,A.W.H. 1967. Modern coccolithophoridae of the Atlantic Ocean. 1. Placoliths and cyrtoliths. Deep Sea Research 14:561-597.
- McIntyre,A. and McIntyre,R. 1971. Coccolith concentrations and differential solution in oceanic sediments. In: Funnel,B.M and Reidel,W.R. (Eds) The Micropaleontology of the Oceans Cambridge University press, 253-261.
- Muller,G., and Gastner,M. 1971. The "karbonate bombe", a simple device for the determination of carbonate content in sediments, soils and other minerals. N.Jb.Mineral. 10:466-469.
- Munsell Soil Colour Charts. 1975 Ed. Munsell Colour. Macbeth, Kollmorgen Corporation, 2441 North Calvert Street, Baltimore, Maryland 21218.
- Nishida,S. 1979. Atlas of Pacific nannoplanktons. News of Osaka Micropaleontologists. Soec. 3:1-29.
- Okada,H. and Honjo,S. 1973. The distribution of oceanic coccolithophorids in the Pacific. Deep Sea Research 20:355-374.
- Okada,H. and Honjo,S. 1975. Distribution of coccolithophores in marginal seas along the western Pacific Ocean in the Red Sea. Marine Biology 31:271-285.
- Okada,H. and McIntyre,A. 1977. Modern coccolithophores of the Pacific and north Atlantic oceans. Micropaleontology 23:1-55.
- Okada,H. and McIntyre,A. 1979. Seasonal distribution of modern coccolithophores in the western north Atlantic Ocean. Marine Biology 54:319-328.
- Orren,M.J. 1963. Hydrological observations in the southwest Indian Ocean. Investigative report of the Division of Sea Fisheries of South Africa. 45:1-61.
- Ostenfeld,C.H. 1900. Über Coccospheera. Zool.Anz. 23(612): 198-200.
- Parke and Adams 1960. The motile (*Crystallolithus hyalinus* Gaarder and Markali) and non-motile phases in the life history of *Coccolithus pelagicus* (Wallich) Schiller Journal of the Marine Biological Association of the United Kingdom 39:263-274.
- Parsons,T.R., Takahashi,M. and Hargrave,B. 1977. Biological Oceanographic Processes (2nd Edition). Pergamon Press.
- Pearce,A.F. 1977. Some features of the upper 500 m of the Agulhas Current. Journal of Marine Research 35(4):731-751.

- Pearce, A.F., Schumann, E.H. and Lundie, G.S.H. 1978. Features of the shelf circulation of the Natal coast. South African Journal of Science 74.
- Peterson, L.C. and Prell, W.L. 1985. Carbonate dissolution in recent sediments of the eastern equatorial Indian Ocean: preservation patterns and carbonate loss above the Lysocline. Marine Geology 64:259-290.
- Pienaar, R.N. 1966. Microfossils from the Cretaceous system of Zululand, studies with the aid of the electron microscope. South African Journal of Science 61:425-426.
- Pienaar, R.N. 1968. Upper Cretaceous coccolithophorids from Zululand, South Africa. Paleontology 11:361-7.
- Prell, W.L., Hutson, W.H. and Williams, D.F. 1979. The southern tropical convergence and late Quaternary circulation in the southern Indian Ocean. Marine Micropaleontology 4:225-234.
- Reid, J.L. 1962. On circulation, phosphate-phosphorous content and zooplankton volumes in the upper part of the Pacific Ocean. Limnology and Oceanography 7:28736.
- Roche, M.B., McIntyre, A. and Imbrie, J. 1975. Quantitative paleoceanography of the late Pleistocene-Holocene north Atlantic: coccolith evidence. In: Saito, T. and Burckle, L.H. (Eds) Late Neogene epoch boundaries. Micropaleontology special publication 1:199-225.
- Roth, P.H. 1973. Calcareous nannofossils - leg 17, Deep Sea Drilling Project. In: Winterer, E.L. and Ewing, J.L. 1973. Initial reports of the Deep Sea Drilling Project 17:695-795.
- Roth, P.H. and Berger, W.H. 1975. Distribution and dissolution of coccoliths in the south and central Pacific. Cushman Foundation of Foraminiferal Research, special publication 13:87-113.
- Roth, P.H. and Coulbourn, W.T. 1982. Floral and solution patterns of coccoliths in surface sediments of the north Pacific. Marine Micropaleontology 7:1-52.
- Roth, P.H., Mullin, M.M. and Berger, W.H. 1975. Coccolith sedimentation by faecal pellets: laboratory experiments and field observations. Geological Society of America Bulletin 86:1079-1084.
- Samtleben, C. 1978. Pliocene-Pleistocene coccolith assemblages from the Sierra Leone Rise Site 366, leg 41 Deep Sea Drilling Project. Initial reports of the Deep Sea Drilling Project VXL1:913-931. Washington (U.S. Government Printing Office).
- Shackleton, N.J. 1974. Attainment of isotopic equilibrium between ocean water and the benthonic Foraminifera genus *Uvigerina*: isotopic changes in the ocean during the pleistocene: Colloq.Int.C.N.R.S. (Les methodes quantitatives d'etude des variations du climat au cours du Pleistocene) 219:203-209.
- Shackleton, N.J. 1977. The oxygen isotope stratigraphy of the late Pleistocene. Philosophical Transactions of the Royal Society of London B280:169-182.
- Shackleton, N.J. and Opdyke, N.D. 1976. Oxygen isotope and paleomagnetic stratigraphy of equatorial Pacific core V28-239, Late Pliocene to Latest Pleistocene. In: Cline, R.M. and Hays, J.D. (Eds.), Investigation of late Quaternary Paleoceanography and Paleoclimatology. Geological Society of America Memoirs 145:449-464.
- Shannon, L.V., Stander, G.H. and Cambell, J.A. 1973. Oceanic circulation deduced from plastic drift cards. Investigation Report of the South African Division of Sea Fisheries 108, 31pp.
- Schneidermann, N. 1977. Selective dissolution of recent coccoliths in the Atlantic Ocean. In: Oceanic Micropaleontology Ramsay (ed).
- Siesser, W.G. 1975. Calcareous nannofossils in pleistocene sediment cores from the South African continental slope. Transactions of the Royal Society of Southern Africa 42(2):108-147.
- Silva, E.S. 1960. O microplankton de superficie nos meses de Setembro e Outubro na estacao de Inhaca (Mozambique). Mem.Junta.Invest.Utram. 2. Ser 18:1-15.
- Taylor, F.R.J. 1966. Phytoplankton of the southwestern Indian Ocean. Nova.Hedwigia 12:433-76.
- Thierstien, H.R., Geitzenauer, K.R., Molino, B. and Shackleton, N.J. 1977. Global synchronicity of late Quaternary coccolith datum levels: validation by oxygen isotopes. Geology 5:400-404.
- Travers, A. and Travers, M. 1965. Introduction a l'etude du phytoplancton et des Tintinnides de la region de Tulear (Madagascar). Ibid. 4:125-62.

- Urey, H.C. 1947. The thermodynamic properties of isotopic substances. Journal of the Chemical Society 1947:562-581.
- Ushakova, M.G. 1970. Coccoliths in suspension and in the surface layer of sediment in the Pacific Ocean. In: Funnel and Reidel Eds. The micropaleontology of the Oceans. Cambridge University press.
- Vincent, E. and Shackleton, N.J. 1980. Agulhas Current temperature distribution delineated by oxygen isotope analysis of foraminifera in surface sediments. Cushman Foundation for foraminiferal research Special Publication 19:89-95.
- Wang, P. and Samtleben, C. 1983. Calcareous nannoplankton in surface sediments of the east China Sea. Marine Micropaleontology 8:249-259.
- Webber, M. 1902. Introduction et description de l'expédition. In Siboga-Expeditice 1:1-159.
- Webber-van-Bosse, A. 1901. E'tudes sur les algues de l'Archipel Malaisien. III. Note préliminaire sur les resultants algologiques de l'expédition du Siboga. Jard.Bot.Buitenz., Ann. 17(2):126-141.
- Westall, F. 1984. Current-controlled sedimentation in the Agulhas Passage, SW Indian Ocean. Joint Geological Survey/University of Cape Town, Marine Geoscience Unit, Bulletin 12.
- Wilbur, K.M. and Watabe, N. 1963. Experimental studies on calcification in molluscs and the alga *Coccolithus huxleyi*. Annals of the New York Academy of Science 109:82-112.
- Winter, A. 1982. Paleoenvironmental interpretation of Quaternary coccolith assemblages from the Gulf of Aqaba (Elat), Red Sea. Revista Espanola de Micropaleontologia 14:291-314.
- Winter, A. 1985. Distribution of living coccolithophores in the California Current system, southern California borderland. Marine Micropaleontology 9:385-393.
- Winter, A., Reiss, Z., and Luz, B. 1978. Living *Geophyrocapsa protohuxleyi* (McIntyre) in the Gulf of Elat ('Aqaba). Marine Micropaleontology 3:295-298.
- Winter, A., Reiss, Z., and Luz, B. 1979. Distribution of living coccolithophore assemblages in the Gulf of Elat ('Aqaba). Marine Micropaleontology 4:197-223.
- Winter, A., Almogi-Labin, A., Erez, Y., Halicz, E., Luz, B. and Reiss, Z. 1983. Salinity tolerance of marine organisms deduced from Red Sea Quaternary record. Marine Geology 53:M17-M22.
- Wyrki, K., Bennet, E.B. and Rochford, D.J. 1971. Oceanographic Atlas of the International Indian Ocean Expedition. National Science Foundation Washington D.C. U.S. Government Printing Office 531pp.

APPENDIX

Percent abundances of the rare and unidentified species of coccolithophore represented in the surface sediments of the southwest Indian Ocean by their coccoliths. Species names are abbreviated and the plate reference is given for each species. The symbols NA indicate that coccoliths were not found in these samples.

Sample Number	U.ten IV(1)	A.bra IV(3)	G.car I(12)	O.fra II(8)	U.hul II(10)	D.tub III(9)	U.irr III(14)	C.ces I(5)
1	1.2	0.3	0.0	0.0	0.0	0.0	0.3	0.0
2	0.6	1.2	0.0	0.0	0.0	0.9	1.8	0.0
3	0.6	0.6	0.9	0.0	0.0	0.3	0.6	0.3
4	1.3	2.0	0.0	0.9	0.0	0.8	1.9	0.6
5	0.3	0.0	0.0	0.0	0.0	0.3	0.6	0.3
6	0.6	0.0	0.0	0.0	0.0	0.3	0.3	0.0
7	0.3	0.3	0.0	0.0	0.0	0.3	0.0	0.0
8	0.3	1.5	0.0	0.6	0.0	1.1	0.0	0.0
9	0.9	0.9	0.9	0.6	0.0	1.7	0.0	2.9
10	0.3	0.6	0.0	0.0	0.0	0.3	1.2	3.0
11	0.0	0.0	0.0	0.3	1.5	0.3	0.3	4.2
12	0.0	0.0	1.2	0.0	0.0	0.3	0.0	1.5
13	0.3	0.0	0.0	0.0	0.0	0.0	0.0	0.0
14	0.0	0.6	0.0	0.0	0.0	0.3	0.0	0.0
15	NA	NA	NA	NA	NA	NA	NA	NA
16	0.0	2.2	0.0	0.3	0.0	0.0	0.0	0.0
17	0.9	0.6	0.3	0.0	0.0	0.0	0.3	0.0
18	0.6	0.3	0.3	0.0	0.0	0.3	0.0	0.0
19	0.3	0.0	0.0	0.0	0.0	0.0	0.0	0.0
20	0.6	1.2	0.0	0.0	0.0	0.6	0.3	2.7
21	0.6	0.0	0.6	0.0	0.0	0.0	0.0	1.5
22	1.7	0.3	0.0	0.0	0.0	0.8	4.4	0.0
23	0.8	0.8	0.0	0.0	0.0	0.0	0.0	0.0
24	0.0	0.3	0.3	0.0	0.0	0.3	0.0	0.0
25	0.3	0.3	0.0	0.0	0.0	0.0	0.0	0.6
26	NA	NA	NA	NA	NA	NA	NA	NA
27	1.8	1.2	0.0	0.6	3.8	0.6	0.6	1.6
28	NA	NA	NA	NA	NA	NA	NA	NA
29	0.3	0.0	0.6	0.0	0.0	0.0	0.0	1.7
30	3.5	1.8	0.0	1.5	0.0	0.9	0.0	0.0
31	0.3	0.0	0.6	0.0	0.0	0.0	0.0	0.6
32	0.9	0.6	0.0	0.0	0.6	0.0	0.0	2.7
33	12.0	0.0	0.0	0.0	0.0	0.9	1.9	0.3
34	0.0	0.0	0.9	0.0	0.0	0.0	0.0	1.2
35	0.3	0.0	0.9	0.0	0.0	0.0	0.0	1.4
36	0.8	0.8	0.5	0.0	0.0	0.0	0.5	0.0
37	NA	NA	NA	NA	NA	NA	NA	NA
38	0.0	0.0	0.7	0.0	0.0	0.0	0.0	0.0
39	0.0	0.9	0.0	0.0	0.0	0.0	0.0	0.3
40	0.6	0.0	0.3	0.0	0.0	0.0	0.0	2.7
41	NA	NA	NA	NA	NA	NA	NA	NA
42	0.0	0.0	1.2	0.0	0.0	0.0	0.0	1.8
43	0.0	0.3	5.9	0.0	0.0	0.0	0.0	3.6
44	0.0	0.0	0.0	0.0	0.6	0.0	0.0	0.6
45	0.0	0.6	0.0	0.6	0.0	0.0	0.0	0.0
46	NA	NA	NA	NA	NA	NA	NA	NA
47	0.0	0.0	0.0	0.0	0.0	0.0	0.0	0.0
48	0.7	0.0	0.0	0.0	0.0	0.0	0.0	5.0
49	0.0	0.0	0.0	0.0	0.0	0.0	0.0	0.0
50	0.0	0.0	0.3	0.0	0.9	0.0	0.0	3.4
51	0.3	0.6	0.3	2.9	0.0	0.0	0.0	2.2
52	0.9	0.0	0.0	0.0	0.0	0.0	0.0	3.1
53	0.9	0.0	0.6	0.3	0.0	0.0	0.0	0.0
54	2.5	2.5	1.9	1.2	0.0	0.0	0.0	0.6
55	1.6	0.6	0.6	0.6	0.0	0.0	0.0	0.9
56	1.9	0.0	0.0	0.0	0.0	0.0	0.0	0.0
57	0.0	0.0	0.0	0.0	0.0	0.0	0.0	1.6
58	0.3	2.3	0.3	0.0	0.0	0.0	0.0	0.0
59	0.3	0.0	0.0	0.0	0.0	0.3	0.0	2.8
60	NA	NA	NA	NA	NA	NA	NA	NA
61	1.1	0.3	3.1	0.6	0.6	0.0	0.0	0.8
62	0.9	0.0	5.2	1.5	0.0	0.0	0.0	0.6
63	1.2	0.3	0.9	0.0	0.0	0.0	0.0	0.0
64	0.9	0.0	0.3	0.6	0.0	0.0	0.6	0.2
65	0.6	0.0	0.0	1.6	0.9	0.3	0.0	0.0
66	0.0	0.3	0.3	0.0	0.0	0.0	0.0	1.5
67	0.0	0.0	0.0	0.0	0.0	0.0	0.0	0.0
68	0.9	0.0	0.6	0.6	0.9	0.0	0.0	3.2
69	0.6	0.0	0.0	0.0	0.0	0.0	0.0	0.0
70	1.2	1.4	2.0	0.3	0.0	0.0	0.0	1.2
71	0.3	0.0	0.6	0.0	0.0	0.9	0.0	4.4
72	0.9	0.9	0.6	3.4	0.0	0.0	0.0	1.7
73	NA	NA	NA	NA	NA	NA	NA	1.5
74	0.0	0.3	9.4	0.0	0.0	0.0	0.0	NA
75	0.0	0.0	0.8	0.0	0.0	0.0	0.0	0.0
76	1.2	0.9	1.2	2.1	1.2	0.3	0.0	0.0
77	0.3	0.0	0.0	0.0	0.0	0.0	0.0	1.1
78	0.6	0.3	2.5	0.6	1.6	0.0	0.0	0.0
79	1.4	0.9	1.2	3.5	0.6	0.0	0.6	0.3
80	0.6	1.5	0.3	0.3	1.2	0.6	0.0	1.2
81	0.0	1.6	1.6	0.0	0.9	0.3	0.0	1.2
82	0.6	0.3	0.0	0.0	0.0	0.3	0.9	0.0
83	1.2	0.9	0.0	1.2	0.0	0.9	0.0	0.9
84	NA	NA	NA	NA	NA	NA	NA	NA
85	NA	NA	NA	NA	NA	NA	NA	NA
86	NA	NA	NA	NA	NA	NA	NA	NA
87	1.2	0.9	0.0	0.0	0.0	1.2	0.5	0.0
88	5.4	0.0	0.6	1.5	0.0	0.0	0.0	0.0
89	0.3	0.9	0.3	0.0	1.9	0.0	0.0	0.0
90	0.3	1.2	0.6	1.2	2.7	0.0	0.0	0.9
91	3.4	3.1	0.0	0.9	0.6	1.3	0.0	0.3
92	0.3	0.9	0.9	0.0	0.0	0.0	0.3	0.0
93	0.9	0.6	0.0	0.9	0.3	0.0	0.0	0.0
94	1.2	1.8	0.0	1.2	0.3	0.0	0.3	1.5
95	1.5	1.5	0.0	0.0	0.0	0.3	0.6	1.8
96	2.3	0.3	0.0	0.0	0.0	2.6	0.3	0.0
97	NA	NA	NA	NA	NA	NA	NA	NA
98	NA	NA	NA	NA	NA	NA	NA	NA
99	1.6	1.3	1.3	4.2	0.7	0.0	0.7	1.3
100	0.8	3.3	0.0	2.5	5.8	0.0	0.0	1.2

Sample Number	Disc. V(3)	C.cri I(1)	P.cre VI(10)	P.lac VI(4)	D.dav V(11)	E.cav V(13)	C.flo VI(7)	C.gra VI(3)	Sample Number	Disc. V(3)	C.cri I(1)	P.cre VI(10)	P.lac VI(4)	D.dav V(11)	E.cav V(13)	C.flo VI(7)	C.gra VI(3)
1	3.9	0.0	0.0	0.0	0.0	0.0	0.0	0.0	51	0.0	0.0	0.0	0.0	0.0	0.0	0.0	0.0
2	0.0	0.0	0.0	0.0	0.0	0.0	0.0	0.0	52	0.0	0.0	0.0	0.0	0.0	0.0	0.0	0.0
3	0.0	0.0	0.0	0.0	0.0	0.0	0.0	0.0	53	0.0	0.0	0.0	0.0	0.0	0.0	0.0	0.0
4	0.0	0.0	0.0	0.0	0.0	0.0	0.0	0.0	54	0.0	0.0	0.0	0.0	0.0	0.0	0.0	0.0
5	0.0	0.0	0.3	0.0	0.0	0.0	0.0	0.0	55	0.0	0.0	0.0	0.0	0.0	0.0	0.0	0.0
6	0.0	0.0	0.0	0.0	0.0	0.0	0.0	0.0	56	0.0	0.0	0.0	0.0	0.0	0.0	0.0	0.0
7	0.0	0.0	0.0	0.0	0.0	0.0	0.0	0.0	57	1.2	0.0	0.0	0.0	0.0	0.0	0.0	0.0
8	0.0	0.0	0.0	0.0	0.0	0.0	0.0	0.0	58	0.0	0.0	0.0	0.0	0.0	0.0	0.0	0.0
9	0.0	0.0	0.0	0.0	0.0	0.0	0.0	0.0	59	0.0	0.0	0.0	0.0	0.0	0.0	0.0	0.0
10	0.0	0.0	0.0	0.0	0.0	0.0	0.0	0.0	60	NA	NA	NA	NA	NA	NA	NA	NA
11	0.0	0.0	0.0	0.0	0.0	0.0	0.0	0.0	61	0.0	0.0	0.0	0.0	0.0	0.0	0.0	0.0
12	0.0	0.0	0.0	0.0	0.0	0.0	0.0	0.0	62	0.0	0.3	0.0	0.0	0.0	0.0	0.0	0.0
13	0.0	0.0	0.0	0.0	0.0	0.0	0.0	0.0	63	0.0	0.0	0.0	0.0	0.0	0.0	0.0	0.0
14	0.0	0.0	0.0	0.0	0.0	0.0	0.0	0.0	64	0.0	0.0	0.0	0.0	0.0	0.0	0.0	0.0
15	NA	NA	NA	NA	NA	NA	NA	NA	65	0.3	0.0	0.0	0.0	0.0	0.0	0.0	0.0
16	0.0	0.0	0.0	0.0	0.0	0.0	0.0	0.0	66	0.0	0.0	0.0	0.0	0.0	0.0	0.0	0.0
17	0.0	0.0	0.0	0.0	0.0	0.0	0.0	0.0	67	0.0	0.0	0.0	0.0	5.0	11.1	38.9	0.0
18	0.0	0.0	0.0	0.0	0.0	0.0	0.0	0.0	68	0.0	0.0	0.0	0.0	0.0	0.0	0.0	0.0
19	0.0	0.0	0.0	0.0	0.0	0.0	0.0	0.0	69	0.6	0.0	0.0	0.0	0.0	0.0	0.0	0.0
20	0.0	0.0	0.0	0.0	0.0	0.0	0.0	0.0	70	0.0	0.0	0.0	0.0	0.0	0.0	0.0	0.0
21	0.0	0.0	0.0	0.0	0.0	0.0	0.0	0.0	71	0.0	0.0	0.0	0.0	0.0	0.0	0.0	0.0
22	0.0	0.0	0.0	0.0	0.0	0.0	0.0	0.0	72	0.0	0.0	0.0	0.0	0.0	0.0	0.0	0.0
23	0.0	0.0	0.0	0.0	0.0	0.0	0.0	0.0	73	NA	NA	NA	NA	NA	NA	NA	NA
24	0.0	0.0	0.0	0.0	0.0	0.0	0.0	0.0	74	0.0	0.0	0.0	0.0	0.0	0.0	0.0	0.0
25	0.0	0.0	0.0	0.0	0.0	0.0	0.0	0.0	75	0.0	0.0	0.0	0.0	0.0	0.0	0.0	0.0
26	NA	NA	NA	NA	NA	NA	NA	NA	76	0.0	0.0	0.0	0.0	0.0	0.0	0.0	0.0
27	0.0	0.0	0.0	0.0	0.0	0.0	0.0	0.0	77	0.0	0.0	0.0	0.0	0.0	0.0	0.0	0.0
28	NA	NA	NA	NA	NA	NA	NA	NA	78	0.0	0.0	0.0	0.0	0.0	0.0	0.0	0.0
29	0.3	0.0	0.0	0.0	0.0	0.0	0.0	0.0	79	0.0	0.0	0.0	0.0	0.0	0.0	0.0	0.0
30	0.0	0.0	0.0	0.0	0.0	0.0	0.0	0.0	80	0.0	0.0	0.0	0.0	0.0	0.0	0.0	0.0
31	0.0	0.0	0.0	0.0	0.0	0.0	0.0	0.0	81	0.0	0.3	0.0	0.0	0.0	0.0	0.0	0.0
32	0.0	0.0	0.0	0.0	0.0	0.0	0.0	0.0	82	0.0	0.0	0.0	0.0	0.0	0.0	0.0	0.0
33	0.0	0.0	0.0	0.0	0.0	0.0	0.0	0.0	83	0.0	0.0	0.0	0.0	0.0	0.0	0.0	0.0
34	0.0	0.0	0.0	0.0	0.0	0.0	0.0	0.0	84	NA	NA	NA	NA	NA	NA	NA	NA
35	0.0	0.0	0.0	0.0	0.0	0.0	0.0	0.3	85	NA	NA	NA	NA	NA	NA	NA	NA
36	0.0	0.0	0.0	0.0	0.0	0.0	0.0	0.0	86	NA	NA	NA	NA	NA	NA	NA	NA
37	NA	NA	NA	NA	NA	NA	NA	NA	87	0.0	0.0	0.0	0.0	0.0	0.0	0.0	0.0
38	0.0	0.0	0.0	0.0	0.0	0.0	0.0	0.0	88	0.0	0.0	0.0	0.0	0.0	0.0	0.0	0.0
39	0.0	0.0	0.0	0.0	0.0	0.0	0.0	0.0	89	0.3	0.0	0.0	0.0	0.0	0.0	0.0	0.0
40	0.0	0.0	0.0	0.0	0.0	0.0	0.0	0.0	90	0.0	0.0	0.0	0.0	0.0	0.0	0.0	0.0
41	NA	NA	NA	NA	NA	NA	NA	NA	91	0.0	0.0	0.0	0.0	0.0	0.0	0.0	0.0
42	0.0	0.0	0.0	0.0	0.0	0.0	0.0	0.0	92	0.0	0.0	0.0	0.0	0.0	0.0	0.0	0.0
43	0.0	0.0	0.0	0.0	0.0	0.0	0.0	0.0	93	0.3	0.0	0.0	0.0	0.0	0.0	0.0	0.0
44	0.0	0.0	0.0	0.0	0.0	0.0	0.0	0.0	94	0.0	0.0	0.0	0.0	0.0	0.0	0.0	0.0
45	0.0	0.0	0.0	0.0	0.0	0.0	0.0	0.0	95	0.0	0.0	0.0	0.0	0.0	0.0	0.0	0.0
46	NA	NA	NA	NA	NA	NA	NA	NA	96	0.0	0.3	0.0	0.0	0.0	0.0	0.0	0.0
47	0.0	0.0	0.0	0.0	0.0	0.0	0.0	0.0	97	NA	NA	NA	NA	NA	NA	NA	NA
48	0.0	0.0	0.0	0.0	0.0	0.0	0.0	0.0	98	NA	NA	NA	NA	NA	NA	NA	NA
49	0.0	0.0	0.0	0.0	0.0	0.0	0.0	0.0	99	0.0	0.0	0.0	0.0	0.0	0.0	0.0	0.0
50	0.0	0.0	0.0	0.0	0.0	0.0	0.0	0.0	100	0.0	0.0	0.0	1.6	0.0	0.0	0.0	0.0

